DOCTORAL DISSERTATION SERIES

TITLE INDUCED POLARIZATION: A METHOD OF GEOPHYSICAL PROSPECTING

AUTHOR DAVID FRANKLIN BLEIL

UNIVERSITY MICH. STATE COLLEGE DATE 1948

DEGREE PH. D. PUBLICATION NO. 989

INDUCED POLARIZATION: A METHOD OF GEOPHYSICAL PROSPECTING

By
David Franklin Bleil

A THESIS

Submitted to the School of Graduate Studies of Michigan State College of Agriculture and Applied Science in partial fulfillment of the requirements for the degree of

DOCTOR OF PHILOSOPHY

Department of Physics and Astronomy

1948

T A B L E O F C O N T E N T S

A. INTRODUCTION

1. Statement of Problem

Geophysical prospecting is the fascinating game of unraveling the subterraneous character of a region from clues supplied by measurements which can be made at the surface of the earth. These measurements determine the true or apparent physical properties of the region below. The physical properties of the earth most frequently studied are its elasticity, density, magnetic susceptibility and electrical resistivity. In general, the problem of determining what lies beneath the surface of the earth is so complex that measurements of one particular physical property alone cannot provide an unambiguous solution. Frequently however, information gathered from several related physical quantities may be pieced together into a reliable picture of the subsurface structure. It is axiomatic that the more independent physical quantities which are measured the more will be known about the nature of the structure below. Thus it becomes highly desirable to add to our list of measurable physical properties of earth materials. Induced polarization (IP) of the metallic minerals of the earth is one such additional physical quantity which may be used to contribute to the overall picture.

It has long been known that both the anode and cathode of an electrolytic cell become polarized upon the passage of a current. This polarization of the electrodes is generally regarded as a nuisance but it is an electrical property which, by its very existence, provides a useful tool for the detection of metallic minerals in the earth either in the form of solid ore bodies or as disseminated particles. The detection of electrically conducting minerals by this property, stripped of its many inherent difficulties (to be discussed later) consists essentially of the following procedure. The metallic mass M (Fig. 1) is surrounded by a rock matrix, the interstices of which are filled with an electrolyte. In general the more or less good electrical conductivity of a rock is due to the included electrolyte. The presence of the mass M will distort the current flow causing an increase or decrease of the current density in the body depending upon whether its resistivity is higher or lower than the

the matrix. The region where the current filaments enter the mass M corresponds to the cathode of an electrolytic cell and that region where they leave to the anode of the cell and the metal itself to the ordinary external circuit. A direct current, flowing from electrode A to electrode B, will polarize the mass M positive on the side where the current enters and negative where it leaves. If the current from A to B is interrupted the dipole on the mass M will dissipate itself by sending a current through the surrounding medium. The recorder R will indicate the ohmic drop between the points C and D due to this polarization current. In order to avoid measuring the ohmic drop due to the energizing current the switch S is not closed until the current circuit is interrupted.

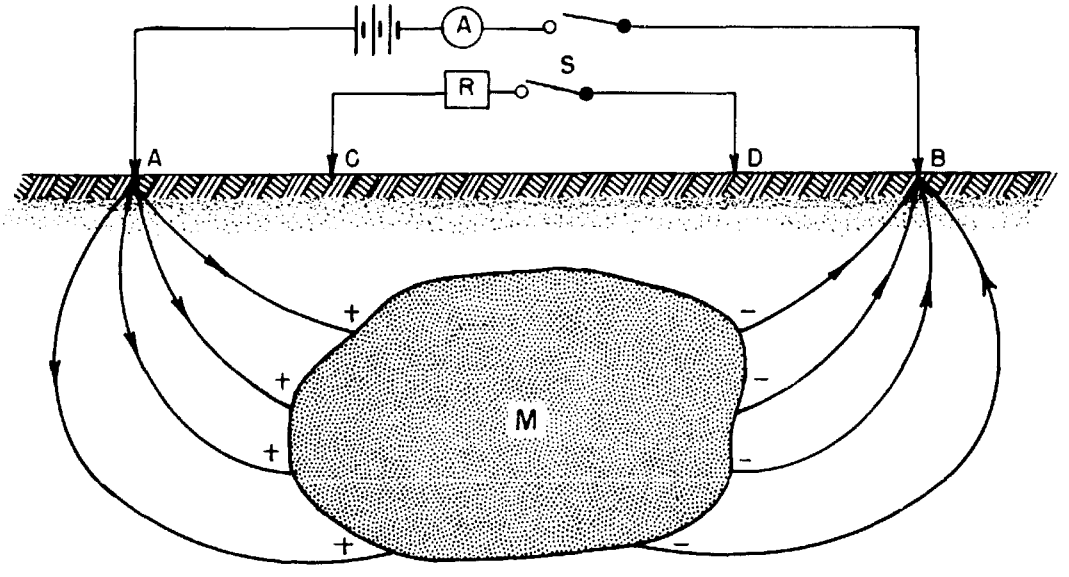

FIG. 1

NOTE: A vocabulary which is peculiar to the electrical methods of geophysical prospecting may be used profitably in the work to follow. Several terms which will be used frequently are here brought to the reader's attention. In all electrical methods where current is delivered directly to the ground a pair of current electrodes is required. Additionally a pair of potential electrodes is required. The manner of arranging the electrodes varies and the more popular systems have acquired names. When the current electrodes are widely separated and the potential is measured in the neighborhood of one current electrode the term "point

electrode" is applied to the system. More frequently the four or more electrodes are arranged in a straight line with some scheme of spacing employed. A very common spacing scheme is that of separating the four electrodes by an equal spacing "a". This system is referred to as the Wenner system. The method of measuring the resistivity employing a low frequency double commutator and the Wenner configuration is called the Gish-Rooney system.

This basic principle, although proposed as far back as 1912[1], has received little attention on the European Continent and practically no attention in this country. The definite lack of interest in the method probably stems from the confusion apparent in the literature and the cloud of mysticism which surrounds some of the earlier works. Heiland[2] has expressed a doubt that a new quantity had been measured by the method. It is the intent of this thesis to rectify some of the errors which have crept into the literature, remove some of the existing mystery and to bring out the advantages and limitations of the method with the hope that it will grow into a useful tool for geophysical prospecting.

2. Historical Development

A brief summary of the pertinent literature is outlined in this section in chronological order. Comments and criticisms relating to this published material will be reserved until they can be made in the light of the present investigation.

In the patent[1] granted to Schlumberger in 1912 there is mentioned, in one claim, the discovery of an induced polarization potential. However, it was not until his book[3] published in 1920 and later[4] revised in 1930, that he explained this new method of geophysical prospecting and gave a clear account of the basic principle of induced polarization. He was aware of the fact that the measured potentials decayed with time but nevertheless claimed to have measured them with an ordinary potentiometer. Schlumberger admitted that his experiments in the field were not successful and since the chapter on induced polarization remained unchanged when the book was revised in 1930 the difficulties he encountered apparently remained. Some of the conclusions he drew are included here for later reference:

a) that some deposits such as pyrite are spontaneously polarized and that the self-potentials so developed concealed the effect of induced polarization.

b) that the resistivity of the rock, surrounding the ore body, enters into the induced-polarization effect not more than to a secondary measure.

c) that there exists, in a region free of ore bodies, a "residual" polarization potential which disappears with time in much the same manner as the polarization of an ore body disappears.

d) that the effect of c) is observed when pure water is used in place of wet soil. (He attributed this volume polarization to a transport of ions creating a dissymetry between the regions surrounding the current electrodes.)

Schlumberger regarded observation a) as being highly interesting and may have abandoned his induced polarization studies in favor of spontaneous (self) polarization.

Müller[5] described apparatus which he claimed would measure "simultaneously" the activating potential and the oppositely directed polarization potential. A single pair of electrodes served both to send current into the ground and to measure the polarization potential. Pulsating unidirectional current was delivered to the electrodes by the secondary of a transformer in series with a vacuum tube rectifier. A galvanometer in series with another vacuum tube rectifier and a high resistance, all connected across the electrodes, measured the activating potential. A similar circuit connected across the same electrodes but with the rectifier reversed, measured the polarization potential. The deflections of both galvanometers were photographed on a common film. The method proposed by Müller was discussed in more detail by Weiss[6] under the name of the "Electrochemical Method".

Müller and Weiss were aware of Schlumberger's work but they chose to explain the cause of the polarization effect differently. They contended that the ore body came into equilibrium with the negative ions of the electrolyte by emitting positive ions and thus becoming negatively charged, all this long prior to passage of the energizing current. The energizing current was then supposed to upset this equilibrium causing a large current to flow simultaneously with and in the opposite direction to the energizing current. In addition, without making adequate explanation, they came to the conclusion that polarization effects are capable of being induced at "chemical" boundaries. The method of

measuring the effects has changed from time to time and the interpretation of the results[7] obtained has been entirely empirical. Their claims for the method are:

a) that the maximum polarization current flows simultaneously with the energizing current and in the opposite direction and, therefore, their apparatus will measure larger polarization effects than that of Schlumberger.

b) that, if one plots the measured polarization effects against the electrode separation, the "breaks" on the resulting curve are indicative of "chemical" boundaries. A one to one correspondence between depth and electrode separation is deduced.

c) that the "screening" effect which accompanies other ordinary electrical methods is absent in this method and, therefore, great depths of penetration are obtained with small amounts of expended power. (3000 to 6000 ft. for 1 to 2 watts).

An enlightening bit of the discussion which followed Weiss's paper is quoted in part, "Prof. A. O. Rankine confessed that, in spite of Mr. Weiss's description now, and of long talks he had had with him previously, the operation of the method he had been using remained a mystery to him, chiefly in relation to the measuring circuit."

The work of Müller and Weiss was criticized by Belluigi[8, 9] who pointed out that their greatest source of error arose from the deconcentration of their non-polarizable electrodes due to the energizing current passing through these electrodes. Belluigi modified, somewhat, the equipment of Müller and in particular used two pair of electrodes such that the energizing current did not pass through and deconcentrate his potential electrodes. His measurements, which were more refined but again used the same empirical interpretation of Weiss and Müller, showed that great depths are not likely to be revealed because of large near-surface effects.

A method of geophysical prospecting which measures the response of the earth to an electrical transient, called Eltran, was patented by Blau[10]. This method consists simply of applying a step pulse to the earth through a pair of electrodes and measuring the response of the earth to the step pulse across a second pair of electrodes. It is the complex impedance of the earth

which is measured and although polarization is not explicitly mentioned, it must have some effect on the capacitive reactance of the earth.

In a report[11] which discusses the measurements of resistivity when large electrode separations are employed it is pointed out that a finite time is required to establish steady state conditions. The rate of growth or decay of the potential, assumed to be exponential, has a time constant given by the expression

$$T = \frac{c\mu b^2}{\rho} \text{ seconds}$$

where $c = 2.32 \times 10^{-6}$ (dimensionless constant), $\mu = 1$, b = separation of the current electrodes in cm and ρ the resistivity in ohm-cm. Although the above formula was not developed in connection with Eltran, the constant given was obtained from measurements made on earth electrical transients, using similar electrode configurations and should, therefore, apply. Later, Hawley[12] observed that five years had elapsed after Blau's original disclosure, and that several companies had intensively investigated Eltran but no data had been published. It was his objective to study the effect and, with highly refined equipment and with corrections for the response of the instruments, he measured the transient response of the earth, both for currents and potentials, obtaining values which are not compatible with the equation above. The time constants measured for the potential decay were small, not exceeding 350 microseconds for a separation of the current electrodes of 12,000 ft. For distances which are near the upper limit of those anticipated for IP survey work, the time constant was about 150 microseconds.

The growth and development of apparatus, which in its final form is not too unlike in operation that described in this thesis, is traced by Potapenko[13,14] et al in a series of patents. Although the apparatus is well described, the explanation of the origin of the polarization effects is not clearly outlined. An analogy is drawn between the polarization effects at current carrying electrodes (first in an electrolyte and then in oil) and the polarization effects observed in the earth. They extend the analogy far enough to make the claim that the direct detection of oil may be accomplished. In the later patents they stress the idea that formation contacts are revealed by the measurements.

In addition to these patents there are several other American[15, 16] patents issued on geophysical prospecting methods which use induced polarization as the principle of operation. These methods are not capable of a detailed study of the polarization signal and are, therefore, not discussed. It is significant that, other than the patent disclosures cited in this section, the subject of induced polarization as applied to geophysical prospecting is not treated in the American literature.

B. LABORATORY EXPERIMENTS

1. Description of Apparatus

It did not appear possible to arrive at an intelligent approach to the problem of geophysical prospecting by induced polarization without first investigating the conflicting ideas contained in the literature. Experiments, therefore, were designed to study the existence of polarization, the "residual" volume polarization observed by Schlumberger, the large reversed currents of Müller and Weiss and the decay time of the polarization potential with particular reference to its relation to Eltran. All work of these early investigators had been conducted in the earth. The results of such experiments are always confused by the lack of exact knowledge of the state of mineralization, the concentration and amount of electrolyte present, the effective resistivity and the variation of all of these quantities both in the horizontal and vertical directions. In order to avoid the above complications the experiments were conducted in the laboratory where these factors were under the control of the experimenter. This part of the thesis deals with the results of these experiments.

To simulate earth conditions a wooden tank 6 ft. x 8 ft. x 3 ft. was filled with clean quartz sand. A second wooden tank 3 ft. x 5 ft. x 1 ft. was filled with water. At first the experiments were conducted in both the sand and water tanks. It soon became apparent that the same results were obtained in both tanks and because of the ease of operation the water was used almost to the exclusion of the sand tank. In both tanks the resistivity was adjusted by adding the proper amount of salt (NaCl) water. Therefore, the electrolyte in all these experiments was a solution of NaCl in concentrations which varied from 0 to 3.6% by weight.

The electrical circuit employed to record the data was essentially that shown schematically in Plate 1, and will be described here. The energizing current circuit consisted of the current electrodes CC', the resistor RC, the pulsing switch SP, reversing switch SR, control rheostat RH, batteries B, ammeter A and equivalent meter resistance RM. The ammeter was used to adjust the energizing current to a predetermined value. The meter was then replaced by its equivalent resistance RM to keep the circuit reactance entirely resistive. The current actually employed was shown by

PLATE I

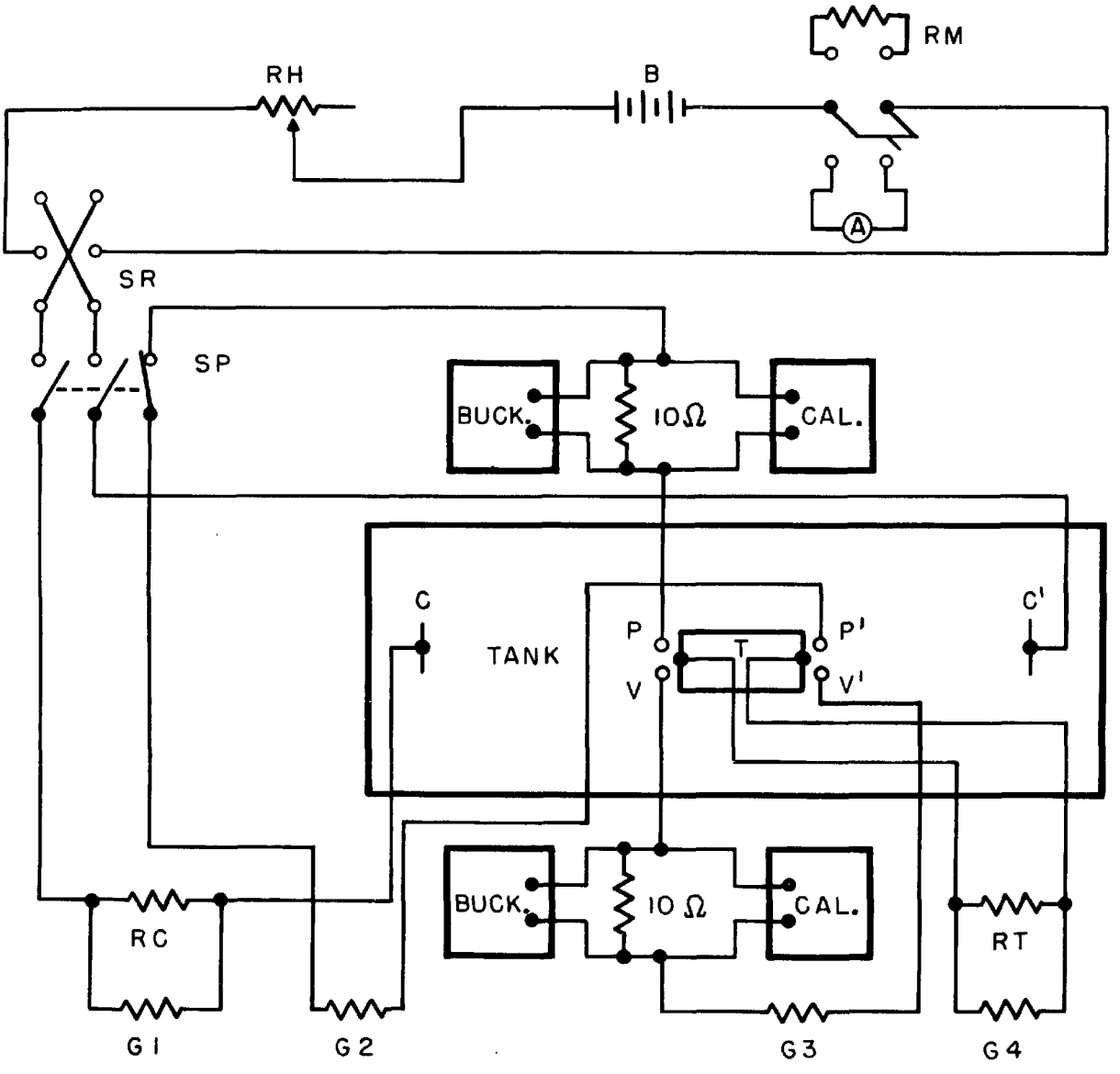

DIAGRAM SHOWING WATER TANK,
TARGET AND ELECTRICAL CIRCUIT

the galvanometer G1 which recorded the potential across RC. RC was generally a 1-ohm precision resistor. The recording element G2 was connected in series with the pulsing switch and a pair of ordinary Ag/AgCl electrodes RT', mounted in glass tubing, to form the circuit which measured the polarization potential. This circuit measured the potential which resulted from the induced polarization (IP), after the current had been interrupted. A second pair of electrode VV' were connected directly across the recording element G3 to indicate continuously the potential across the target space, which is referred to hereafter as the space potential. When the target T (described later) was used, it was inserted centrally between the electrodes TT' and RT' and was connected to the recording element G4 in parallel with RT. Except for one set of records, described in the section on resistivity, the resistor RT was a 1-ohm precision resistor. The inherent electrode potentials were never greater than 0.5 mv but frequently a steady difference of potential was produced when the target was immersed in the electrolyte. To null this difference of potential, a 10-ohm resistor was inserted in series with each potential circuit such that a current through the resistor provided a bucking voltage. The circuit, arranged to deliver current in either direction across the 10-ohm resistor and called the bucking circuit, is diagramed only as a block. A similar type of circuit was used to introduce known voltages into the potential circuits for calibration purposes.

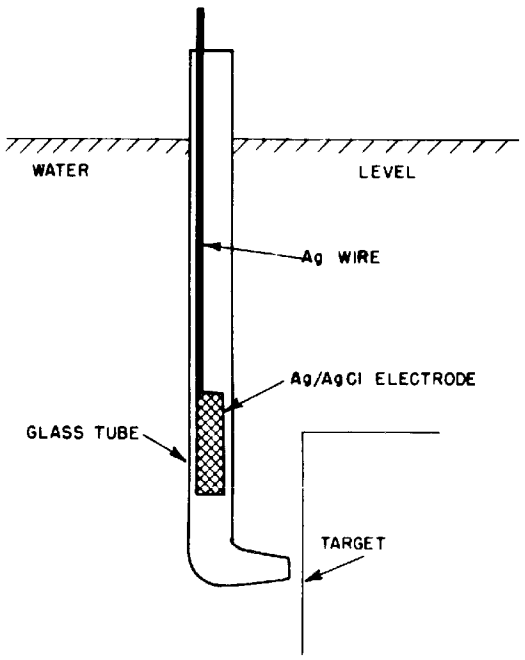

FIG. 2

Throughout the laboratory and field experiments special precautions were taken to shield the non-polarizable electrodes from the direct polarizing action of the energizing current. The method of mounting the Ag/AgCl electrodes, using glass tubing as a current shield, is shown in Figure 2.

A motor-driven car was used to open and close

alternately the polarization-potential circuit and both sides of the energizing circuit. The sequence of events executed by the mechanism was: 1) open the polarization-potential circuit, 2) close the current circuit, 3) open the current circuit and 4) close the potential circuit. The switching mechanism had to satisfy three requirements: a) that the current circuit was never completed while the potential switch was closed, b) that the closing of the potential circuit was delayed at least 5 milliseconds but not more than 50 milliseconds after the current circuit was interrupted, c) that the leakage resistance between the circuits remained higher than 50 x 10^3 ohms. In addition to meeting the above requirements, the mechanism permitted the use of a variety of time intervals for the current pulse. With this mechanism the "delay-time" interval (time between the opening of the current switch and the closing of the potential switch) was between 5 and 10 milliseconds.

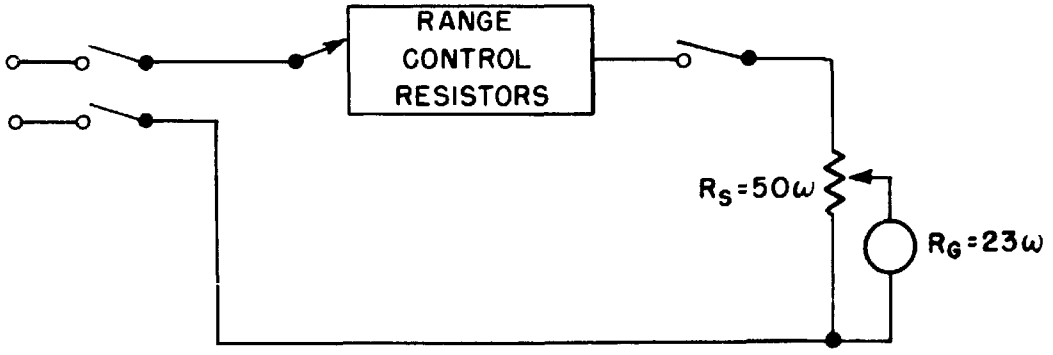

FIG. 3

Records were taken on an eight-element Shell oscillograph employing D'Arsonval-type galvanometers and photographic registration. The galvanometers have flat frequency response from 0 to 100 cps. Each galvanometer had a sensitivity of 0.[illegible] per cm deflection and could utilize the entire paper width of 10 cm. Because the galvanometer is a current reading instrument, care had to be exercised in matching the instrument impedance with the potential electrode resistance. The galvanometer circuit (Fig. 3) consisted of a variable shunt RS across the element and an adjustable range-control resistor. The range-control resistor allows two ranges, each increasing in steps which are multiples of 10. One range starts at 1 mv and extends to 100 v and the other covers the interval from 3 mv to 30 v. The instrument was always operated at or near critical damping. Timing lines were recorded on the photographic paper at 0.01 sec. and heavier

lines at 0.1 sec. intervals. The available paper speeds were 2.5, 5.0, 12.5 and 25.0 cm/sec.

A variety of polarizable bodies (targets) were investigated but one special body had a novel feature which was of considerable help in obtaining the data. The details of this target changed from time to time but it was essentially of the form shown in Plate 2. A plastic tube 20 cm long was machined to hold, at each end, a circular sheet-iron plate 1/16" thick and approximately 100 sq. cm in area. To the inside of the iron plates, wires were soldered and brought out through the center tube. The end plates were pressed into the tube and the whole cylinder was filled with a potting compound to keep out the water and to supply weight. The two wires leading out from the target were connected to the resistor RT (Plate 1).

The two end plates were, thereby, connected together electrically and the "target" became essentially a solid metallic body. The insulated lateral surface distorted somewhat the current distribution from that which would have been obtained if a solid body had been used. However, the fact that the current passing through the target (potential across RT) was measurable made this target a particularly desirable tool for the investigation of induced polarization.

A typical oscillogram obtained with the above equipment is shown in Plate 3. Trace 1 is a record of the energizing current, Trace 2 the decaying induced polarization potential measured by the electrodes PP', Trace 3 the potential, exterior to the target, across the target space measured by VV' and Trace 4 the current through the target.

The instruments described above were used to obtain the early data. At a later date however, many of the laboratory experiments were repeated with the equipment designed for the field investigations. This equipment is described later in Part D-1.

2. Existence of Induced Polarization

Before embarking upon a series of experiments concerning the factors which might influence induced polarization, it was considered wise to first establish the fact that polarization could be induced on a body. It is the purpose of this section to show the existence of induced polarization. However, before the full significance of any experimental evidence can be brought out, the procedure followed in obtaining the data needs

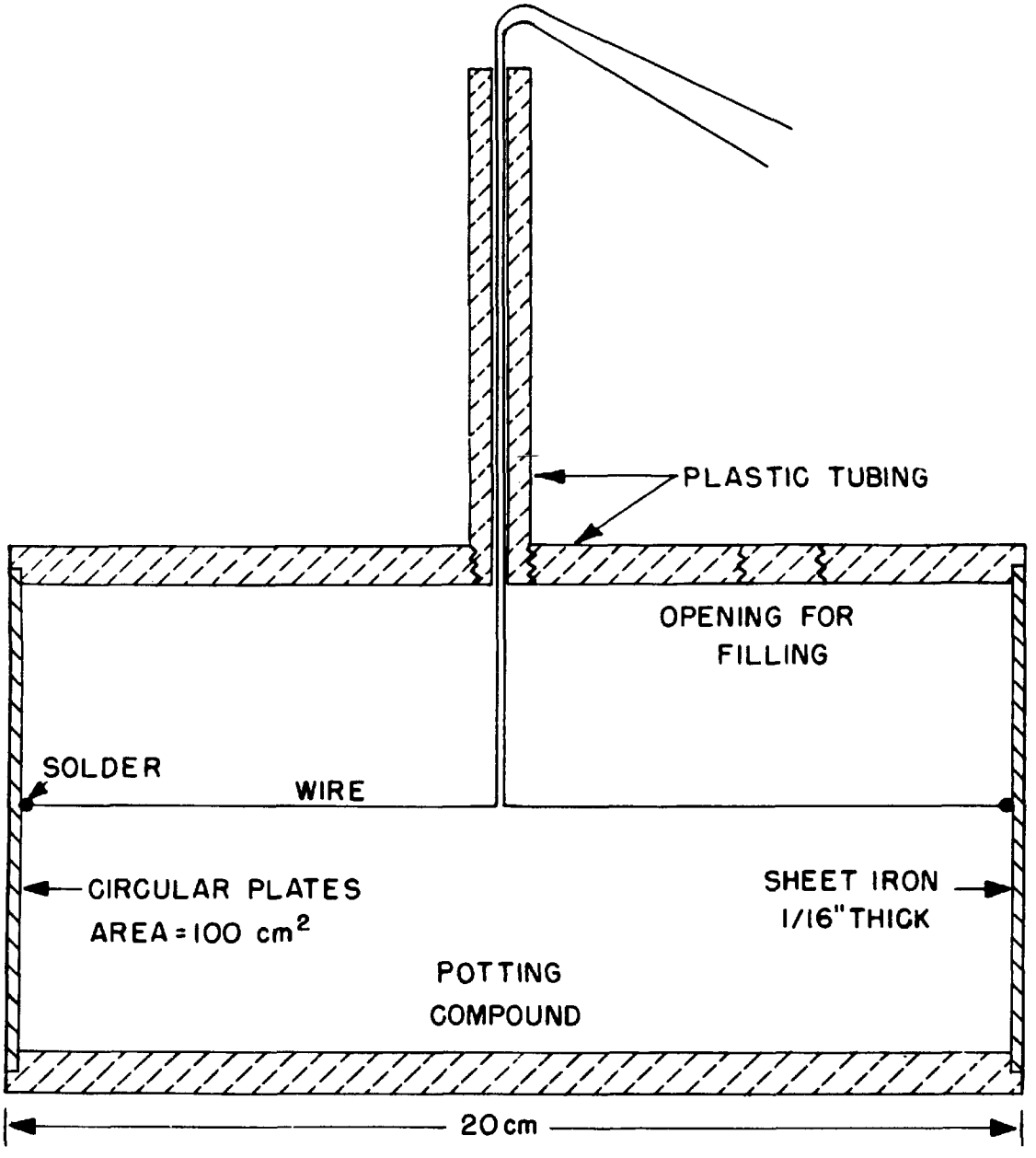
PLASTIC TUBING
OPENING FOR
FILLING
SOLDER
WIRE
CIRCULAR PLATES
AREA = 100 cm²
SHEET IRON
1/16" THICK
POTTING
COMPOUND
20 cm

TARGET

PLATE 3

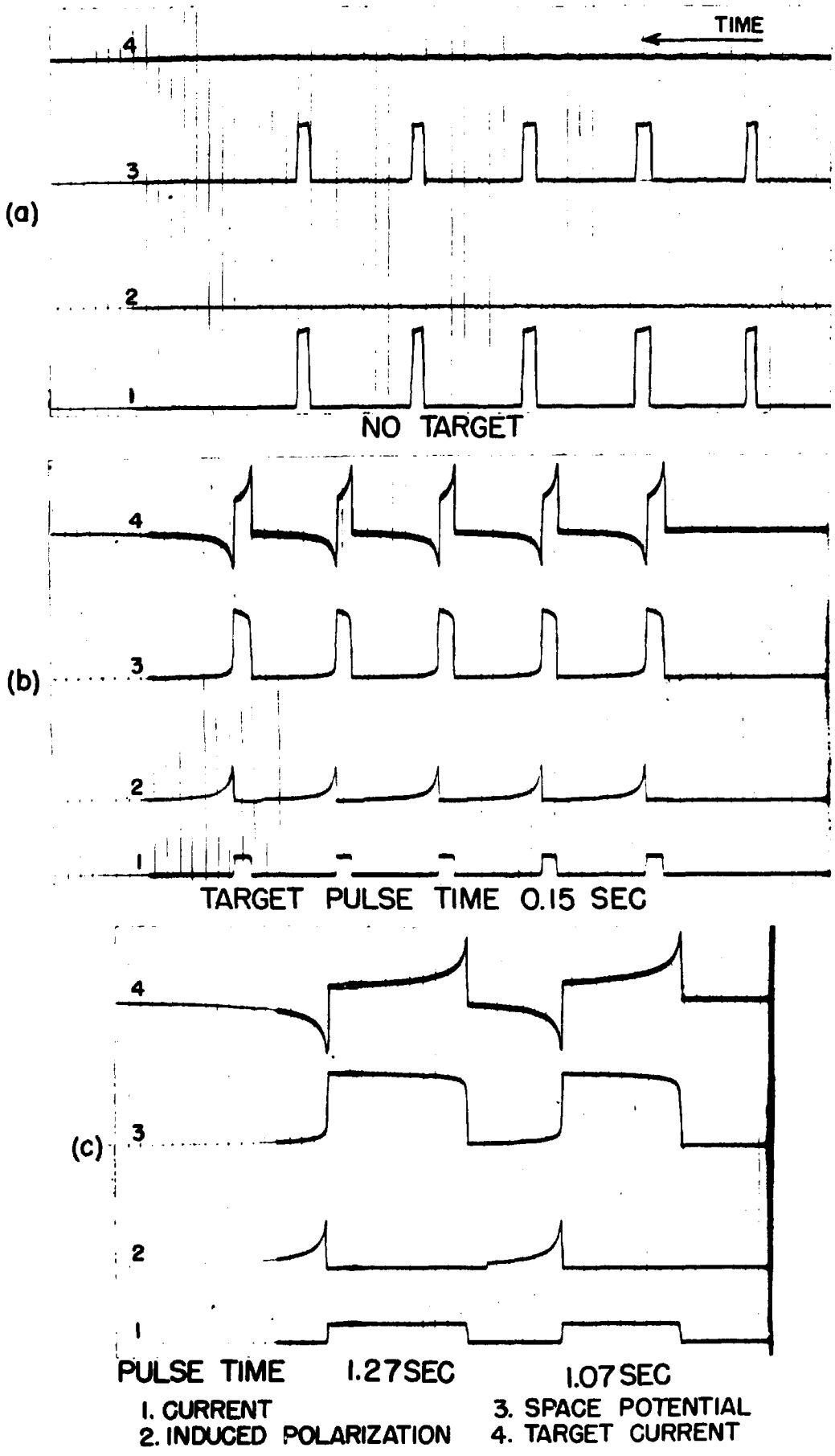
TIME
4
3
(a)
2
1
NO TARGET
4
3
(b)
2
1
TARGET PULSE TIME 0.15 SEC
4
3
(c)
2
1
PULSE TIME 1.27SEC 1.07SEC
1. CURRENT
2. INDUCED POLARIZATION
3. SPACE POTENTIAL
4. TARGET CURRENT

to be outlined. The instruments were arranged in the manner shown in Plate 1 and, with no target in the tank, several current pulses were delivered to the water through the electrodes CC'. The target was then inserted between the electrodes (PP' and VV') which previously had been located in the center of the tank and separated just enough to allow the target to slide between them. Current pulses were again delivered to the water. The traces obtained are shown in Plate 3 where (a) was obtained for the no-target run and (b) and (c) with the target in place. In (a), Trace 1 gives both the magnitude and the duration of the current pulse and Trace 3 shows the magnitude and shape of the potential across the target space. The sensitivity of the recorder element which produced Trace 2 was so adjusted that a potential of 25 μv would produce a deflection of 1 mm. However, no deflection of this element was obtained, even for a potential as large as 12 volts across the target space. The same results held when the medium employed was sand saturated with salt water. An interesting aside occurred when the first tank of sand was tested. Two rather large and well localized IP signals were obtained as the potential electrodes were moved about the surface. The signals were traced to two extraneous nails buried in the sand. After the nails had been removed a signal still persisted. The sand was then run over a magnetic chuck and a considerable amount of magnetic material was removed. After this treatment no signal was observed. All sand used from then on was passed over a magnetic chuck. It has not been possible to obtain a polarization potential which arises from clean quartz sand or water (salt or fresh). The situation, however, was greatly altered when a piece of metal was introduced between the electrodes. The results obtained when the target, with iron plates, was placed between the electrodes, are shown in (b) and (c). Examination of these records reveals that the shape of the energizing current pulse is essentially the same as that in the no-target case but the similarity of records ends there. The most significant feature of these (b and c) records is the decaying potential curves of Trace 2. They were measured by the electrodes PP' and the measurements were obtained entirely after the termination of the current pulse. These potentials arise from polarization induced at the target boundary. That these potentials are truly the results of polarization effects is further demonstrated by the record of the current which passes through the target (Trace 4). The faces of the target acted as electrodes (cathode and anode) at the initiation of the energizing pulse and current, therefore, passed through the

target. However, polarization at the target faces began and as a result the target current was decreased. The longer the pulse endured (c), the more the products of polarization developed, which resulted in a further decrease of the target current, but the current through the target was never reduced to zero. An equilibrium was established between the rate of formation and the escape of electromotively active material, which necessitated a small current to continue to flow through the target. When the energizing current was interrupted, the electrolytic cell, formed by the products of polarization, discharged itself through the surrounding medium. The discharge of these products is like the discharge of a battery where the surrounding medium plays the role of the electrolyte and the target that of the external circuit. The current delivered to the medium by the discharge of the products of polarization is shown as the reverse current through the target. A little reflection on shape of the space potential curve (Trace 3) gives added verification of the interpretation that the effects observed are due to polarization at the faces of the metal target.

3. Induced Polarization and the Energizing Potential

The procedure described above for obtaining data was followed for a variety of conditions, which produced oscillograms like those shown in Plate 3. These conditions were varied in such a manner as to facilitate a study of the IP potential as a function of the energizing current and the resistivity of the medium.

Although several metals were used as targets, the largest amount of data was obtained with targets of sheet iron. A discussion of the results obtained from measurements on other metals will be given later. No cleaning procedure was used on any of the metals other than to remove the excess grease.

The relationship of the induced polarization to the energizing current was studied by holding the resistivity, the target metal and target size constant and varying the energizing current. The energizing current was varied from 0.5 ma to 12 amp., the upper limit of current being determined by that value which produced arcing at the pulsing switch. For every sequence of runs made with the target in place, a corresponding set of runs was made with an identical setup except that the target had been removed. The target was next changed and all records were repeated. After the desired data at one resistivity was obtained,

the solution was altered and all records were re-run for the new value of resistivity. From these data several curves have been plotted and are described below.

Plate 4 shows the plot of the IP potential, the space potential for no-target and the space potential with-target in relationship to the energizing current. As it should be, (Ohm's law) the potential across the target space for no-target is a linear function of the driving current. The with-target space potential is larger than the value given by Ohm's law up to the cross-over point which is approximately 1.2 v. Beyond this it falls below that of the straight ohmic drop. It should be noted also that the IP potential remains linear with the energizing current up to 5.6 amperes at which value saturation begins. The current which produces the saturation of the IP curve is the same value which yields the cross-over of the potential curves. This suggests that the IP potentials might well be plotted as a function of the ohmic (no-target) potential. The curves shown in Plate 5a and 5b are curves of the IP potential plotted against the ohmic potential of the target space. The curves of 5b are merely scale enlargements of 5a in the neighborhood of the origin. Curve 1 was obtained by using tap water whose resistivity was 3630 ohm-cm. Salt water was used to obtain Curves 2, 3 and 4 where the resistivities were 820, 67 and 22.4 ohm-cms. respectively. Although the slope of each curve is different the curves have three common features, namely: 1) they pass through the origin (see 5b), and 2) they are linear to a saturation potential which appears to be approximately 1.2 v. From these curves it has been concluded that:

a) no threshold of energizing potential is required to establish polarization effects. Energizing potentials as small as 0.5 mv produced observable polarization potentials.

b) the induced polarization potential is a linear function of the ohmic (no-target) space potential up to a point beyond which saturation is approached. In place of the ohmic space potential, the potential gradient may be substituted because the abscissa, Plate 5, is proportional to the gradient.

c) a saturation of the polarization occurs which begins at approximately 1.2 v across the target space. (It is interesting to note, in this

PLATE 4

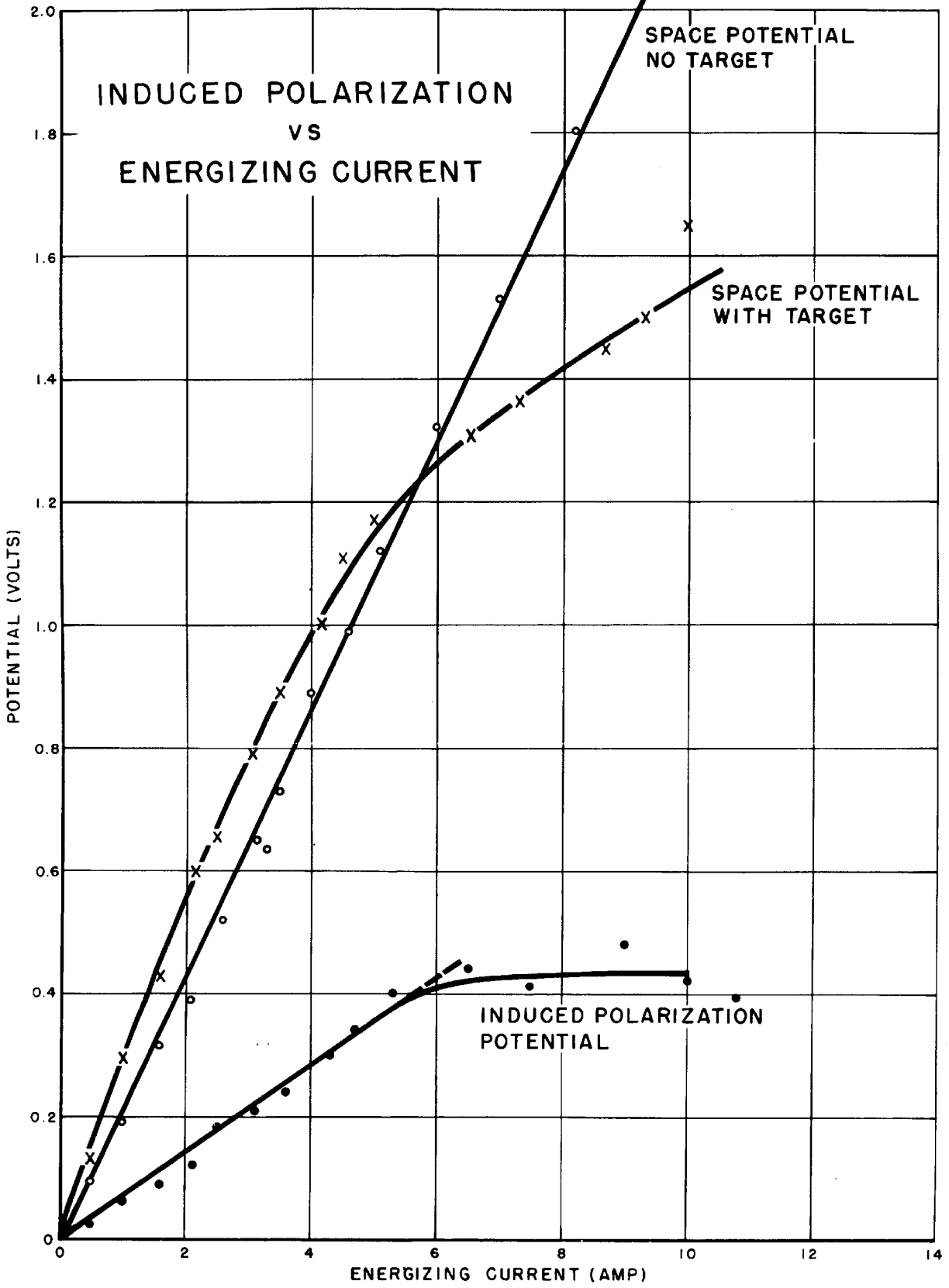
INDUCED POLARIZATION
VS
ENERGIZING CURRENT
SPACE POTENTIAL
NO TARGET
SPACE POTENTIAL
WITH TARGET
INDUCED POLARIZATION
POTENTIAL
POTENTIAL (VOLTS)
ENERGIZING CURRENT (AMP)
0
0.2
0.4
0.6
0.8
1.0
1.2
1.4
1.6
1.8
2.0
0
2
4
6
8
10
12
14

(a) INDUCED POLARIZATION POTENTIAL vs SPACE POTENTIAL (NO TARGET)

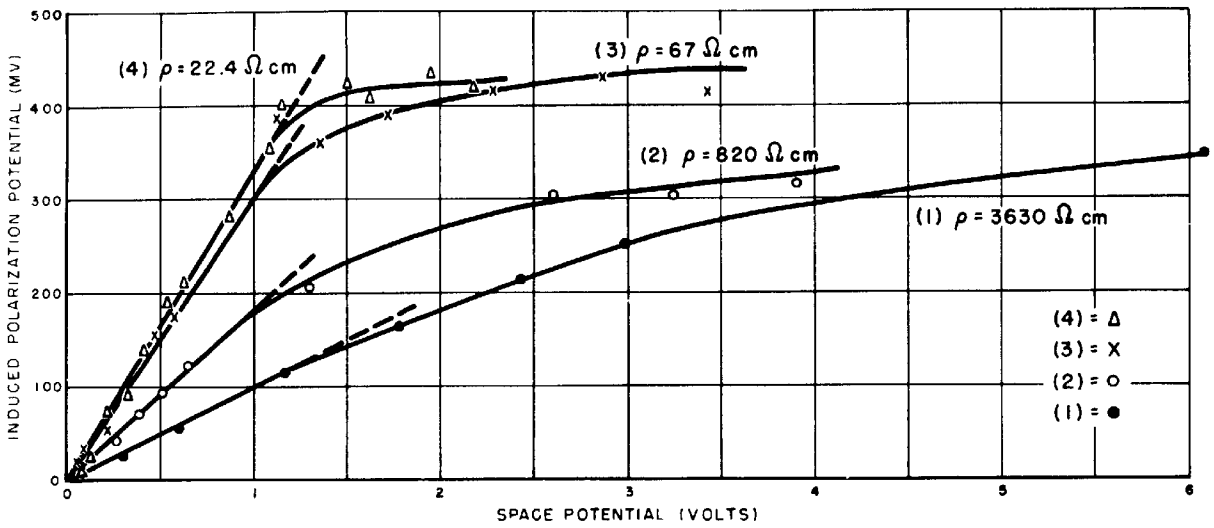

(b) INDUCED POLARIZATION POTENTIAL vs SPACE POTENTIAL (NO TARGET)

REGION NEAR ORIGIN AMPLIFIED

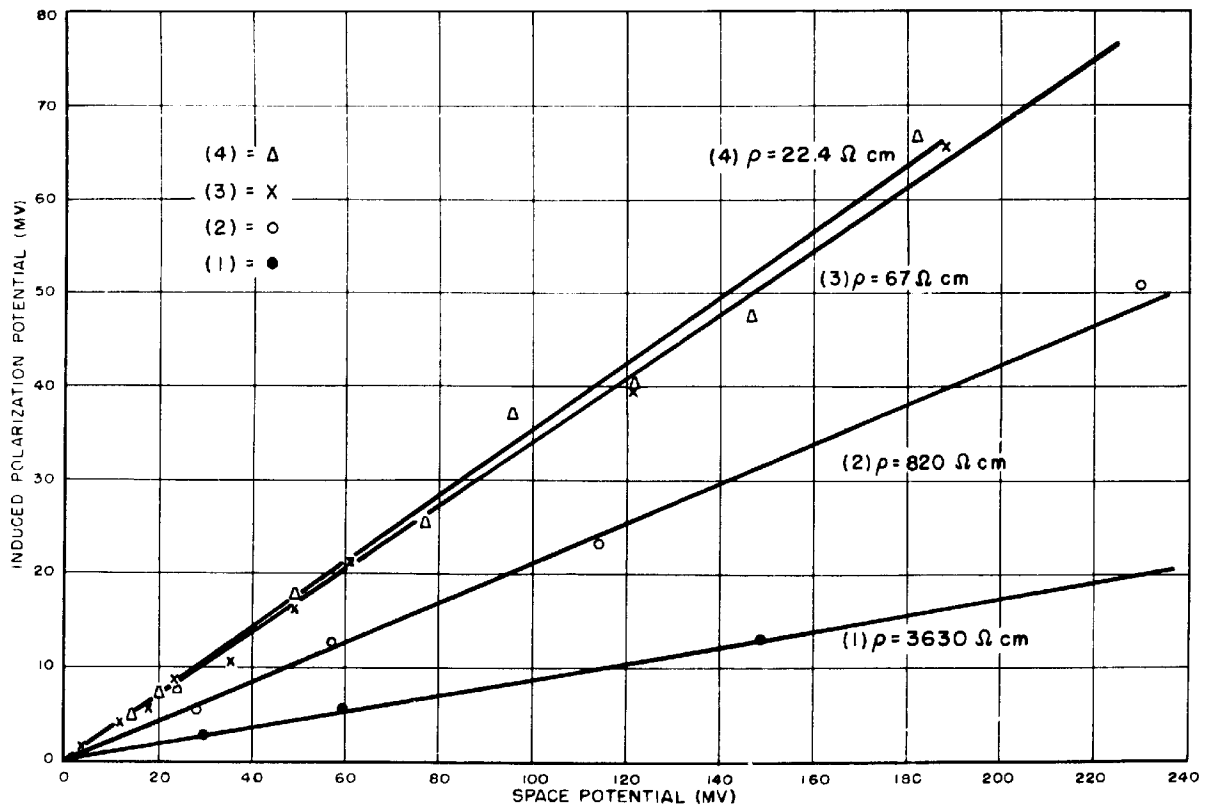

connection, that the theoretical value of the hydrogen-oxygen cell is 1.23 v. However, it is well known that the polarization of an electrode is influenced by the kind and concentration of the ions around it, the material of the electrode and its passivity. Therefore, a study of these factors is required before the full significance of the value 1.2 v is revealed.)

There is another saturation effect which is not observed in Plates 4 and 5 but can be seen in Plate 3. It is a saturation which depends on the length of the applied current pulse. If the pulse is short, a small potential is measured. As the duration of the pulse is increased the magnitude of the IP potential is increased until a saturation effect is obtained. The rate of approach of the saturation is a function of the resistivity of the electrolyte.

4. Induced Polarization and the Matrix Resistivity

The electrical discharge of the polarization is obviously through the surrounding medium. The rate of dissipation of the polarization potential must, therefore, depend upon the resistivity of the surrounding medium but the extent to which it depends upon resistivity or upon some other property of the electrolyte is not known. It is apparent that the growth of the IP effect depends upon the same factors. These two effects are discussed later.

It has been pointed out that the IP potential is a linear function of the potential gradient established. This will have a pronounced effect in prospecting and it will, therefore, require that the magnitude of both the resistivity and current density of the medium be known. The effect of resistivity is, for this reason, not of second order, as was believed by Schlumberger.

Up to this point little has been said about the current through the target. It has been measured and it is known that the polarization potential developed is proportional to the initial current through the target. However, it is well known that the current actually entering the target depends on the ratio of the target resistivity to the surrounding medium. It is difficult to arrange ratios of resistivities for the target and medium in the laboratory but one set of records has been obtained for which the target resistance RT has been varied. The results of those records are plotted in Plate 6.

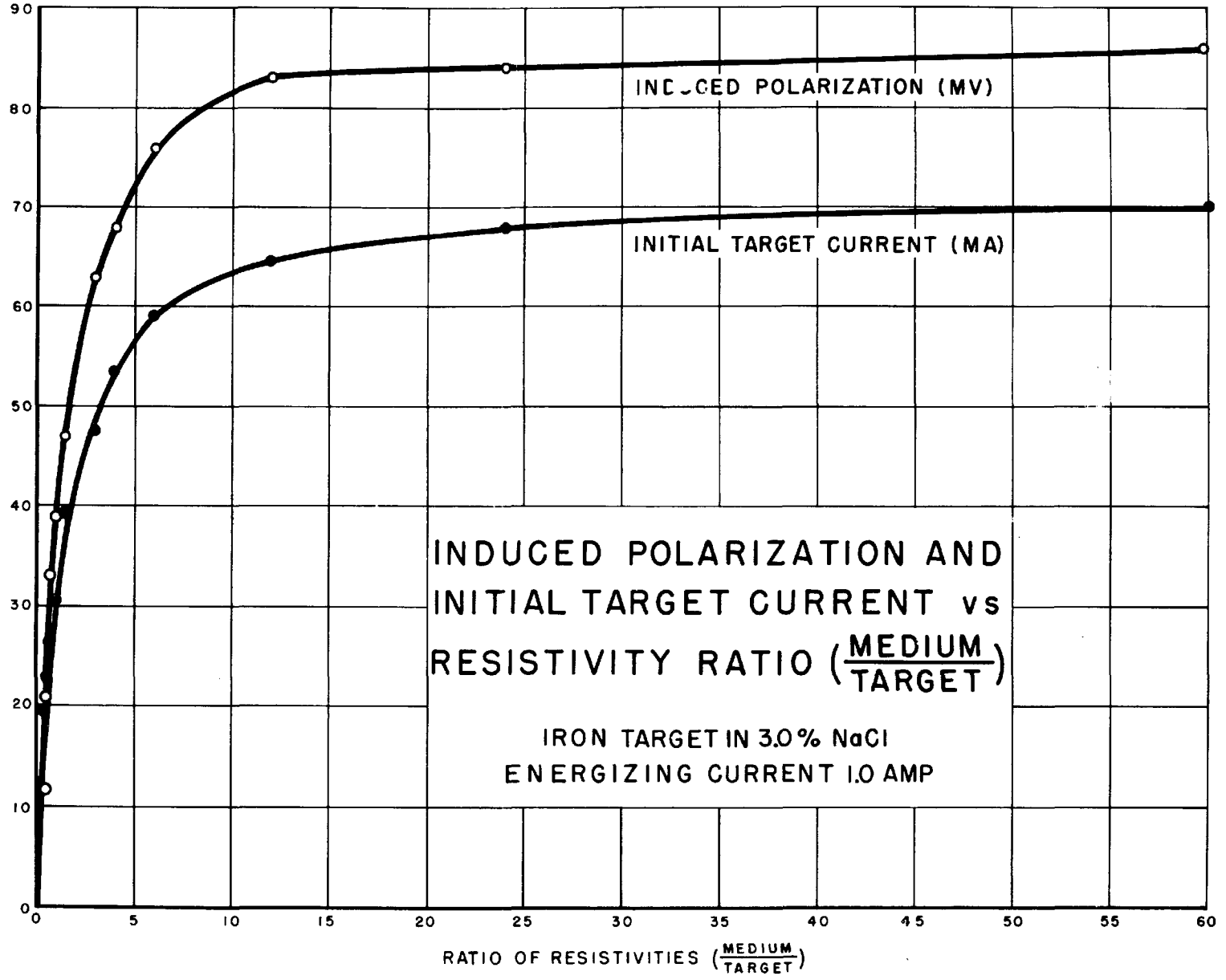
INDUCED POLARIZATION (MV)
INITIAL TARGET CURRENT (MA)
INDUCED POLARIZATION AND
INITIAL TARGET CURRENT vs
RESISTIVITY RATIO (MEDIUM/TARGET)
IRON TARGET IN 3.0% NaCl
ENERGIZING CURRENT 1.0 AMP
RATIO OF RESISTIVITIES (MEDIUM/TARGET)
0
10
20
30
40
50
60
70
80
90
0
5
10
15
20
25
30
35
40
45
50
55
60

PLATE 6

The initial current through the target and the induced polarization potential are plotted against the ratio of target resistivity to the resistivity of the medium. When the ratio of resistivities is zero, the current through the target and the polarization induced are also zero as is expected. A third saturation effect is to be seen on this plate. It appears that the maximum induced polarization potential will be developed across a mineral when its resistivity is one tenth of its surroundings. That is to say if a mineral, say serpentine for which $\rho = 2 \cdot 10^3$, is embedded in a matrix of resistivity 10 times this value, it will be strongly polarized, whereas if the matrix had an equivalent or lesser resistivity than the serpentine, that mineral would be only slightly polarized.

5. Decay Time of the Induced Polarization

In the preceding section it was pointed out that the dissipation rate of the polarization potential was a function of the resistivity and it was hinted that it may depend upon some other property of the electrolyte. Four decay curves are plotted in Plate 7a showing the decay as a function of time for media of resistivities 3630, 820, 67 and 22.4 ohm-cm. The ordinates of all the curves are in arbitrary units and have been matched at t = 80 milliseconds. This matching point was chosen because it was a convenient 2 mm after the zero time for a tape speed of 2.5 cm/sec. There is little difference in the decay rate of the three curves 2, 3, and 4. The fourth, (that for $\rho = 3630$ ohm-cm or tap water) however, decayed at a much slower rate than the others. The curves of the growth of the polarization potential follow the same type of behavior; i.e., the higher the resistivity, the longer is the time required to produce saturation. A knowledge of the growth curve is important in the determination of the required pulse time. The minimum pulse time is that which permits the polarization to reach saturation. A pulse time which is longer than the minimum is wasteful of the power supply.

One significant feature of the four curves of 7a is that they are definitely not exponential. If the polarizing charge upon the metallic mass discharges solely as an electric current through a resistive medium, the rate of decay would be proportional to the remaining charge and the decay curve would indeed have exponential form. Hence, it becomes apparent that some additional factor contributes to the rate of discharge of the polarization. Bowden and Rideal[17]

(a)

DECAY RATE OF POLARIZED IRON vs RESISTIVITY OF MEDIUM (SALT WATER)

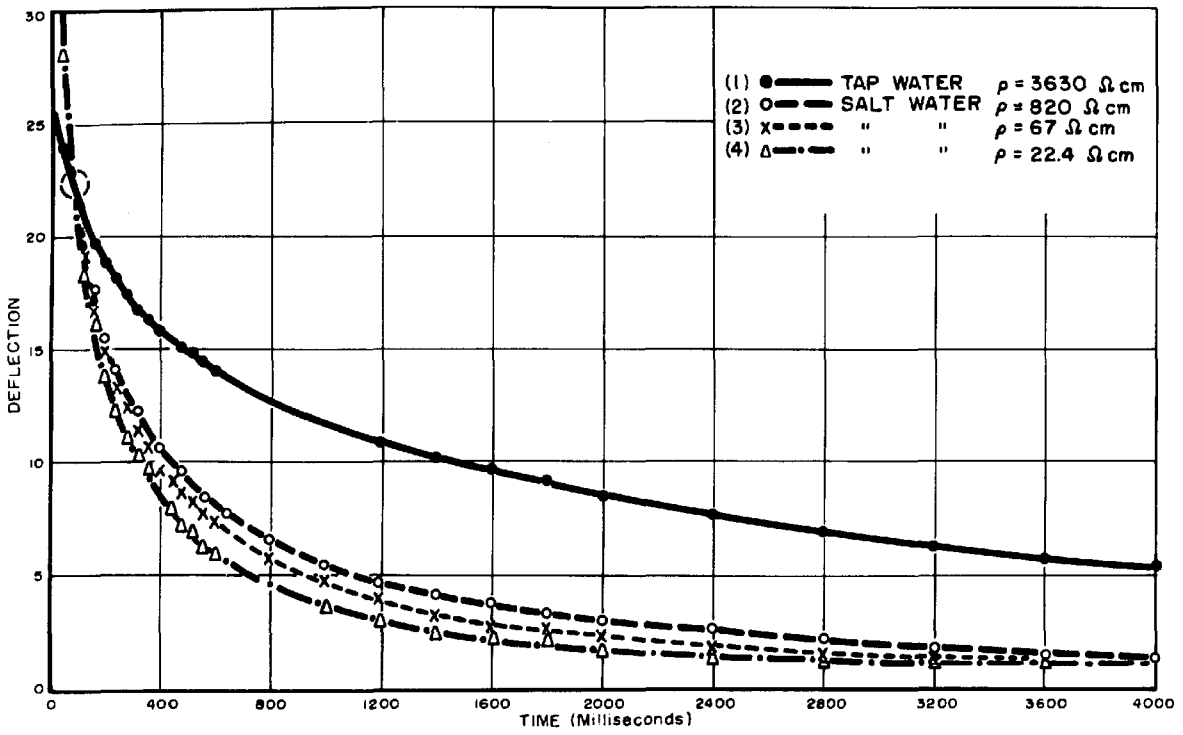

(b)

DECAY CURVES

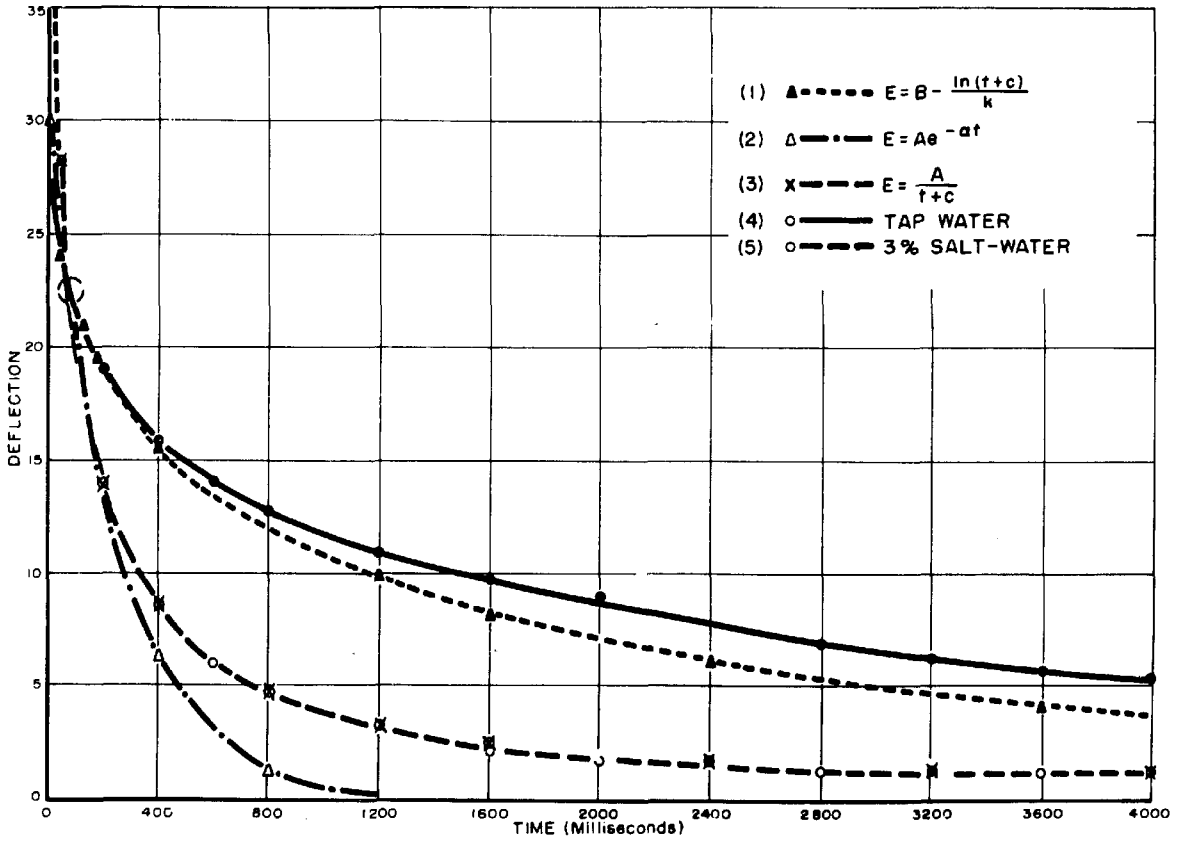

investigated the discharge of the polarization from the electrodes of an electrolytic cell. They found that the potential (E) exhibited by small quantities of electromotively active material deposited on an electrode is proportional to that quantity. "This quantity is very small indeed, the deposition of sufficient hydrogen to form only 1/3000th of an atomic layer raising the potential of the cathode 100 millivolts." They further found that the discharge rate on open circuit depends upon, among other things, the presence of oxygen in the electrolyte. An expression was obtained in which the rate of decrease of the polarization potential is directly proportional to e^{kE}. They pointed out that this was contrary to the rate of decay usually assumed (proportional to E^2) or that (proportional to E) proposed by Heyrovsky. The three equations are given in Table 1.

Table 1

	Rate of decay	Potential vs time	
a	$\frac{dE}{dt} = -Ae^{kE}$	$E = B - \frac{1}{k} \ln(t + c)$	Bowden and Rideal
b	$\frac{dE}{dt} = -kE^2$	$E = \frac{A}{(t + c)}$	Usually assumed
c	$\frac{dE}{dt} = -\alpha E$	$E = E_o e^{-\alpha t}$	Ordinary Exponential. Heyrovsky

According to Bowden and Rideal Equation a obtains only when the oxygen has been carefully excluded from the electrolyte. No effort was made in the laboratory to exclude the oxygen and the concentration of oxygen in the earth is known to be large. Therefore, the decay curves presented in this thesis should not follow Bowden's relation but should be more like the relations given by Equations b or c. However, still other conditions for which Equation b and c are valid were not met in the laboratory either. The theoretical equations, including Bowden's, represent the discharge of the active electrode material when no electric current flows through an external circuit. The electrodes formed by the target faces in the study of induced polarization were always connected, thus violating the no-current condition. If any agreement with the actual discharge curves shown in Plate 7a and either Equations a or b above obtains, it must then mean that the resistivity of

the medium is less important in determining the form of the rate of decay than the open circuit process of discharging the polarization products. A comparison of the curves resulting from the Equations a, b, and c and the actual decay curves for tap water and 3% salt water is shown in Plate 7b. Equation a is compared with the discharge curve for tap water and the fit has been forced at t = 80, 120, and 200 milliseconds. The agreement is not good but it was not expected to be. Both Curve 2 and 3 have been forced to fit the decay curve for iron in 3% salt water at t = 80 and 200 milliseconds respectively. The exponential (Curve 2) fits the actual curve (5) only at the two forced points. On the other hand, Curve 3 covered the decay curve over the entire range of the data available.

It is concluded that the decay of the induced polarization potential with time is not mainly governed by the resistivity of the surrounding medium because the decay curves are not exponential in form. It follows that variations in the resistivity of the earth from place to place can have little influence on the form of the decay curves obtained. On the other hand, the good agreement (in form) of the discharge curves obtained in the salt water tank and the curve calculated from Equation b is interpreted to mean that the primary factors which determine the shape of the discharge curve are the diffusion of the products of polarization into the electrolyte and chemical action between them. Although the composition of the electrolyte is expected to vary from one place to another the factors governing the discharge are not expected to vary appreciably. Hence, two discharge curves obtained at different places on the earth may be compared at corresponding values of time.

It seems appropriate at this time to compare the decay of the IP potentials with those of earth transient (Eltran) potentials. The curves shown in Plate 7 require at least 0.3 seconds to fall to 1/e of their original value. In order to compare the decay of these curves with the decay curves associated with Eltran it is necessary to choose one of the time constants (see Part A-2) reported in the literature. The formula, which arose from the resistivity studies, gives a time constant of several milliseconds when laboratory values are inserted into the equation. Remembering that the delay time introduced into the pulsing cycle was about 10 milliseconds, the magnitude of the transient to be expected upon closing of the potential switch may be calculated. Energizing potentials as large as 2.0 v were not uncommon and, therefore, a 2 millisecond time

constant would have given approximately a 14 millivolt residual signal in the tank for the no-target case. However, no signal as large as 5 microvolts was ever observed when the tank did not contain a polarizable object. Thus it appears that the results obtained by Hawley must be used and, therefore, with the time constants he reports, it is concluded that current electrode separations as large as 3000 ft. (more than is anticipated for field survey) may be employed without interference from Eltran potentials.

6. Behavior at Chemical Boundaries

It is the expressed belief of Müller, Weiss, Potapenko and others that a polarization potential can be induced at chemical boundaries. The term chemical boundary, although not defined, apparently refers to boundaries separating regions of chemically different electrolytes. It is further implied that a high correlation is expected between the chemical boundaries and formation boundaries. The mechanism of inducing a polarization at a boundary which does not have electrically conducting minerals on one side is not explainable in terms of the laboratory results so far described. Therefore, in order to investigate the effect produced at a chemical boundary, a cell made of plastic tubing 20 cm long and having an effective cross-sectional area of 20 cm^2 was filled with a concentrated solution of $CuSO_4$. The ends of the cell were closed with vegetable-paper diaphragms on to which a layer of bees wax had been condensed to reduce the rate of diffusion through the membrane. The cell containing the $CuSO_4$ was placed in the water tank in place of the target. The $CuSO_4$ target was first immersed in tap water and a series of records were made which showed the signal, the space potential across the target and the energizing current as the current was varied. Similar records were obtained for the target immersed in 0.1, 1.0 and 3.6% salt water. The $CuSO_4$ was removed from the target and in its place a 3% salt solution was added. A complete set of records was obtained for the NaCl target. Data were also obtained when this cell contained the same solution inside and out and also for a 1% salt solution inside surrounded by a 3% salt solution. No induced polarization potentials were observed for any of the solutions contained in the cell when immersed in a medium of low resistivity. Small potentials were observed for both the $CuSO_4$ and NaCl targets in tap water and still smaller potentials for the $CuSO_4$ cell in 0.1% salt water. The results obtained are shown in Plate 8a. A comparison of the largest potentials measured for the chemical cell; i.e., $CuSO_4$ in tap water,

(a)

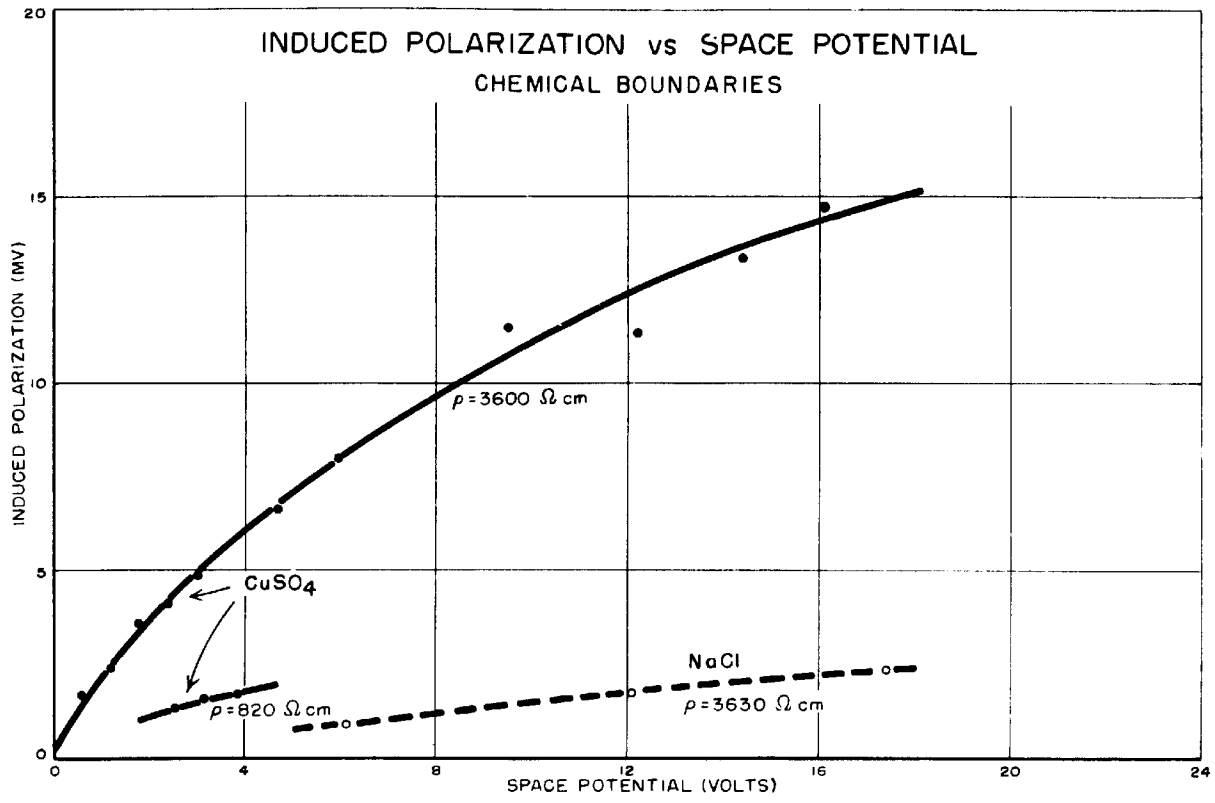
INDUCED POLARIZATION vs SPACE POTENTIAL
CHEMICAL BOUNDARIES
INDUCED POLARIZATION (MV)
SPACE POTENTIAL (VOLTS)
ρ = 3600 Ω cm
CuSO4
ρ = 820 Ω cm
NaCl
ρ = 3630 Ω cm
0
5
10
15
20
0
4
8
12
16
20
24

(b)

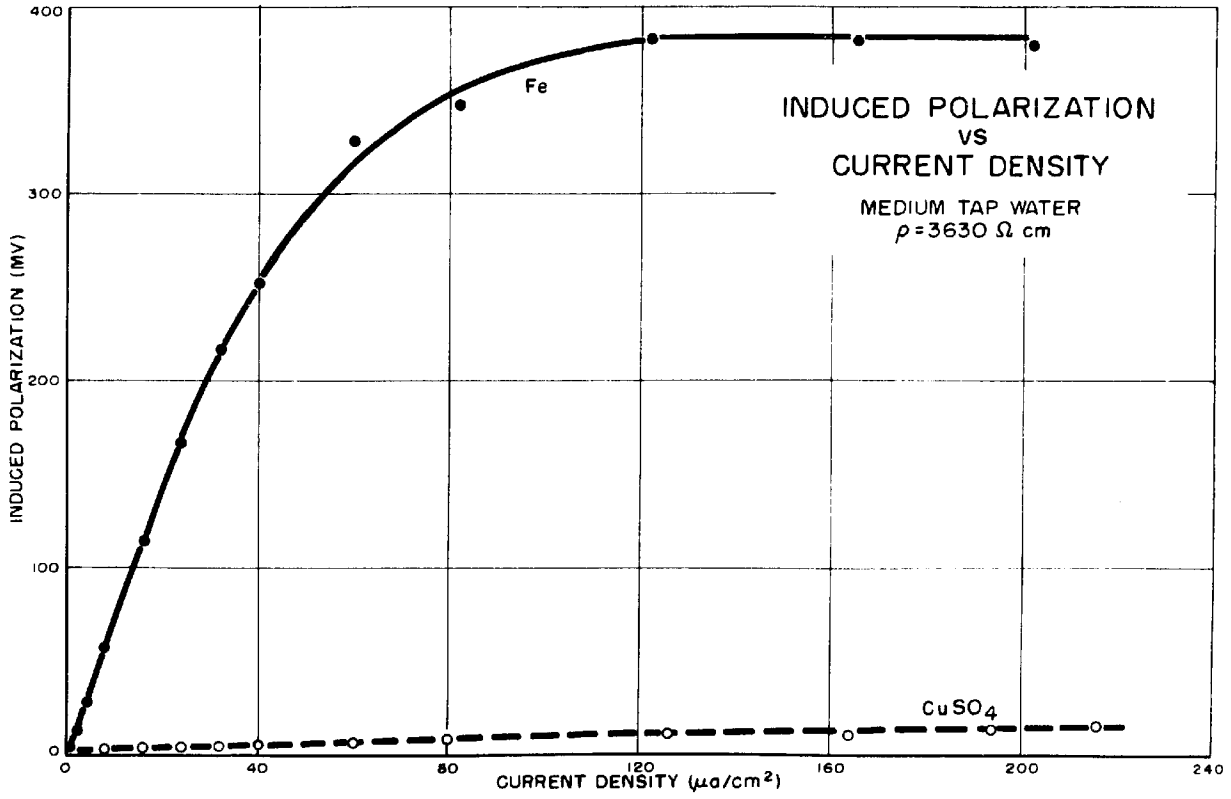
INDUCED POLARIZATION
VS
CURRENT DENSITY
MEDIUM TAP WATER
ρ = 3630 Ω cm
INDUCED POLARIZATION (MV)
CURRENT DENSITY (μa/cm²)
Fe
CuSO4
0
100
200
300
400
0
40
80
120
160
200
240

with the IP potentials for an iron target of the same dimensions, also in tap water, is made in Plate 8b. A potential which decays with time was observed at the non-metallic boundary separating two solutions, each containing different ions. This potential, whatever may be its origin, is seen from Plate 8b to be a second order effect in relation to the induced polarization potential of iron. It appears unlikely that Müller and Weiss could have observed an effect due to such a boundary at all and by no stretch of the imagination is its detection at 3000 feet a conceivable result.

7. Concerning Ionic Concentrations

Because no polarization was measured in either sand or water except when metal was introduced and because Schlumberger stated that an effect would appear because of the transport of ions producing a dissymmetry around the current electrodes, another experiment was designed to investigate this possibility. The apparatus employed was quite different from that already described and was designed to enhance the "dissymmetry" effect. A pair of current electrodes in the form of iron sheets 8 5/8 in. x 10 1/2 in. (same as previously used) were attached, as far apart as possible, to an axle in such a manner that they could be rotated in or out of the tank. Mounted at right angles to the current electrodes were a pair of nonpolarizable potential electrodes. These potential electrodes were so mounted on the axle that they entered the electrolyte almost immediately after the current electrodes departed. A commutator on the axle completed the current circuit the instant the current electrodes entered the electrolyte and broke the circuit when they left it. The potential electrodes were connected at all times to a Brown chopper-amplifier and an Esterline Angus recorder. The gain of the system was adjusted until 40 microvolts represented one small division (1/25 in.) on the recorder tape. The current electrodes were introduced into the electrolyte for a predetermined length of time. At the end of that time the axle was rotated rapidly, removing the current electrodes from the electrolyte (thus removing any possibility of measuring their polarization) and introducing the potential electrodes. In tap water and salt water (concentrations 0.1, 0.3 and 3.6%) a variety of potentials was applied for time intervals up to 1 minute without generating potentials measurable with the equipment used. It was concluded that an induced potential difference due to the dissymmetry of ion concentration arising from transport under the action of a current was either too small to measure or that it disappears too rapidly to be measured with the equipment

(a)

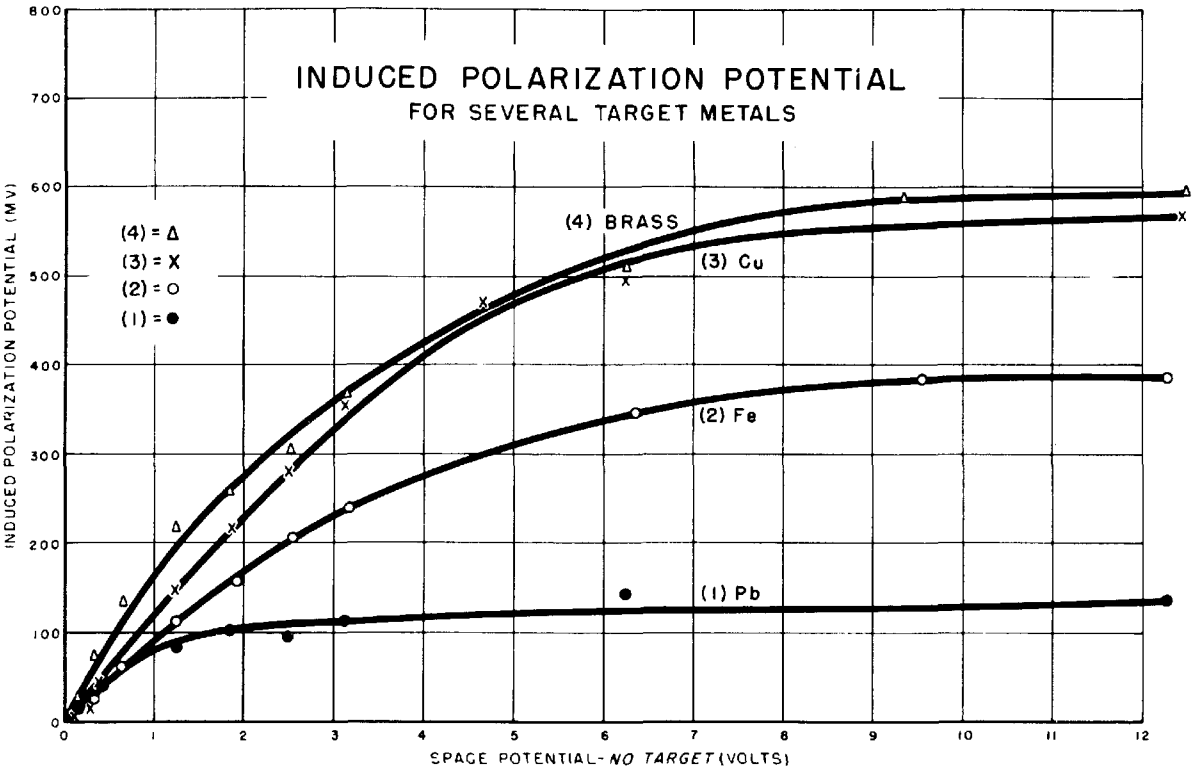
INDUCED POLARIZATION POTENTIAL
FOR SEVERAL TARGET METALS
(4) = Δ
(3) = X
(2) = O
(1) = ●
(4) BRASS
(3) Cu
(2) Fe
(1) Pb
INDUCED POLARIZATION POTENTIAL (MV)
SPACE POTENTIAL-NO TARGET (VOLTS)

(b)

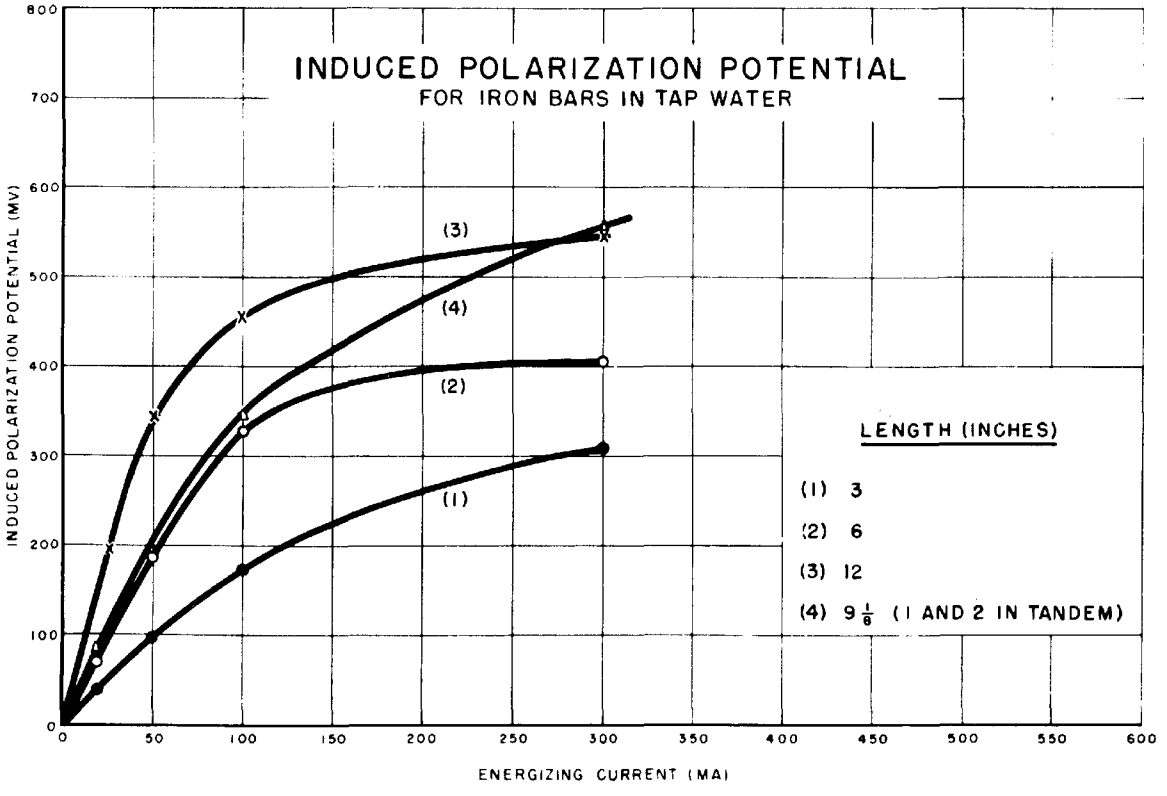
INDUCED POLARIZATION POTENTIAL
FOR IRON BARS IN TAP WATER
(3)
(4)
(2)
(1)
LENGTH (INCHES)
(1) 3
(2) 6
(3) 12
(4) 9 1/8 (1 AND 2 IN TANDEM)
INDUCED POLARIZATION POTENTIAL (MV)
ENERGIZING CURRENT (MA)

employed. The latter conclusion seems to be the more likely explanation in view of the relaxation time for salt water which Stratton[18] computes to be 2×10^{-10} seconds. Certainly the effect measured by Schlumberger, particularly with the instruments he used, was not that of an induced ionic concentration gradient. However, he reported potential measurements which decayed slowly and must, therefore, have arisen from some other cause, possibly a uniform dissemination of conducting mineral particles.

C. Other Factors Influencing the Polarization Signal

There are other factors such as temperature, ion concentration and the passivity of the metallic body which influence the polarization potential and are of particular interest to the physical chemist but have little bearing on the geophysical problem. One factor which is of importance in prospecting is the metal of which the ore body is composed. A study of the effect on the induced polarization produced by the target metal has been started but only a small amount of data has been obtained. A target, similar to that described in Part B-1 but of smaller diameter, was designed so that the target metal was readily interchangeable. With this target, end plates made of brass, lead, copper and iron were used to obtain curves of induced polarization as a function of the energizing (no-target) space potential. The curves obtained for the four metals, when the surrounding medium was tap water, are given in Plate 9a. Each metal investigated was found to be polarizable in tap and salt (NaCl) water. However, several irregularities have been observed, two of which may be seen in Plate 9a. The curve for the brass target is not as regular as the others and it departs from linearity near the origin. The knee of the curve for the lead target occurs at a potential less than 1.2 v. Two other curves (not shown) for the lead target in salt water (ρ = 820 and 67 Ω-cm respectively) did, however, show the knee of the curve to begin at 1.2 v. Several other departures from the curves obtained for iron have been observed but a discussion of the effects will be withheld until after further study has been made. For the problem at hand it is sufficient to say that the curves obtained for the metals investigated are essentially the same as those obtained when iron target-plates were used.

A piece of pyrrhotite from the Betty Baker mine (see Part D-4) and later a piece of magnetite "float" from Lebanon County, Pennsylvania (see Part D-5) were placed in the water tank and each subjected to polar-

izing currents. These clumps were too irregular to justify quantitative measurements, but they both gave signals which were comparable to those obtained with the iron target. A carbon rod was also inserted between the potential electrodes in place of the target and a large IP signal was observed. An induced polarization potential has been obtained for every metal investigated and also for a carbon rod. The magnitude of the measured potentials is comparable with those obtained with iron.

Another factor which can influence the polarization signal is the tandem effect of small disseminated particles. It was concluded, in Part B-3, that the induced polarization potential is proportional to the potential gradient. This means that the current density (and, therefore, energizing current) required to produce saturation is inversely proportional to the length of the mineral particle. That current which will saturate a particle of one length will not saturate a shorter one and, therefore, the polarization potential (at saturation) measured across two short particles in tandem will be greater than that across one particle of equivalent length. The induced polarization potential measured across several iron bars each of different length and across one combination of two bars in tandem is shown plotted in Plate 9b as a function of the energizing current in milliamperes. Curves 1, 2 and 3 were obtained for iron bars whose lengths were 3, 6 and 12 inches respectively. Curve 4 was obtained by placing the 3 and 6 inch bars in tandem separated by a 1/2 inch gap. The potential across the pair is approximately that to be expected for a 9 inch bar until saturation begins and then the potential across the combination exceeds that across the 12 inch bar. The potential across the combination will continue to increase until that current has been reached which will produce saturation across the shorter bar. This tandem effect will serve to emphasize the disseminated mineral, particularly if the particles are well aligned and not widely separated. An increase in the separation of the particles reduces the polarization potential measured across the combination. The induced polarization potential will, therefore, be sensitive to the percentage of polarizable mineral contained in the rock.

9. Other Tank Experiments

Several experiments, unrelated except for the fact that the medium in each case was sand wet with salt water, are described in this section and they conclude the laboratory experimentation.

a) A Zone of Disseminated Mineral

It was suggested in Part B-7 that the "residual" potential effect observed by Schlumberger might be explained by the induced polarization of electrically conducting minerals which are ore or less uniformly disseminated in the earth. The tandem effect discussed in Part B-8 adds weight to this hypothesis. In order to verify the assumption that a mineralized zone was able to account for the "residual" polarization a small volume of sand was mineralized and investigated. A volume of clean quartz sand, 11 x 6 x 5 inches, was mineralized by the addition of iron grit (sand-blasting shot) until the mineral content was approximately 10% by weight. The mixture was placed in a cloth bag and returned to the hole in the sand. The point electrode arrangement was used to measure the induced polarization potential. The return current electrode was in one corner of the sand tank and the reference potential electrode was in the diagonally opposite corner. The point current electrode and the probing potential electrode were kept 2.5 inches apart and were moved together along the opposite diagonal of the tank. The results obtained, shown in Plate 10a, prove that a zone of disseminated mineral can be polarized.

While the zone of disseminated mineral was in place, the IP potential was measured in various directions across the zone. A Wenner configuration of electrodes was used, for which "a" was 1½ inches and the center of the system was at the center of the zone. The line of electrodes was first oriented along the long dimension of the zone and then rotated to other positions which made angles of 30°, 60°, 90°, 120°, and 150° to that line respectively. The results from the six orientations of the line are shown plotted in the insert in Plate 10a and they are in good agreement with the predictions of Part C-3 concerning the ellipse of polarization.

b) Uniformly Mineralized Earth

The theoretical development of Part C-1 predicts that the induced polarization potential of a uniformly mineralized homogeneous earth under the influence of a point electrode falls off as 1/r. The conditions required are difficult to meet. They may be satisfied in the earth over a sufficiently large volume but there is no way to determine beforehand whether or not the conditions are satisfied at any given location. An attempt was made in the laboratory to check this

(a)

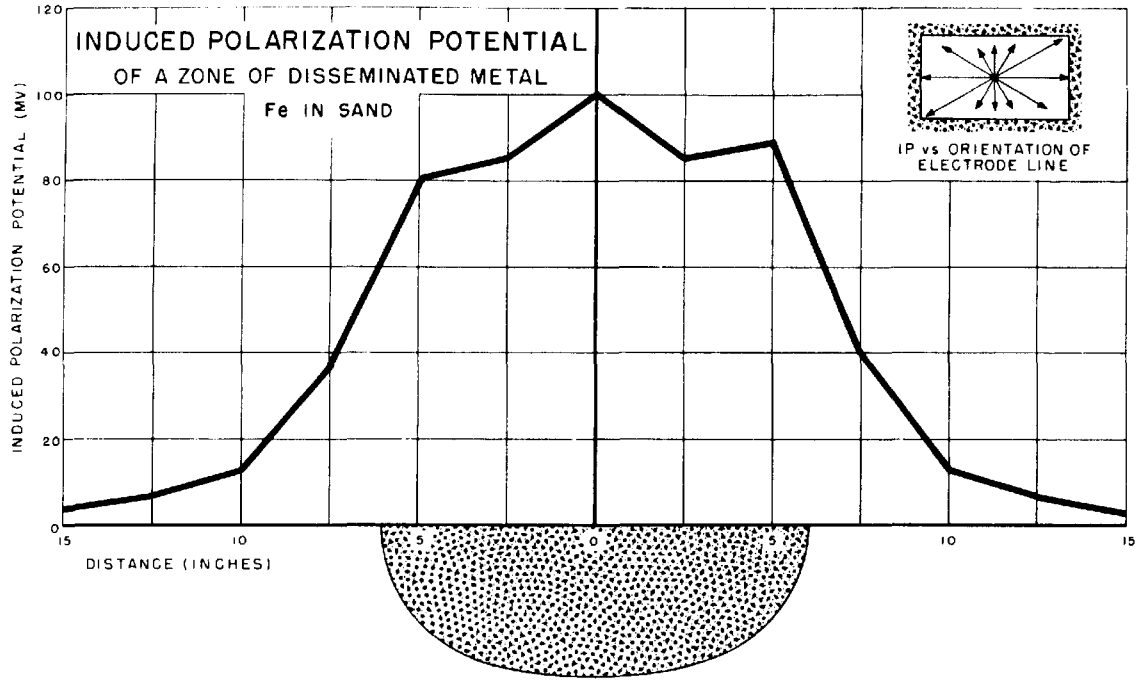
INDUCED POLARIZATION POTENTIAL
OF A ZONE OF DISSEMINATED METAL
Fe IN SAND
IP vs ORIENTATION OF ELECTRODE LINE
INDUCED POLARIZATION POTENTIAL (MV)
120
100
80
60
40
20
0
15
10
5
0
5
10
15
DISTANCE (INCHES)

(b)

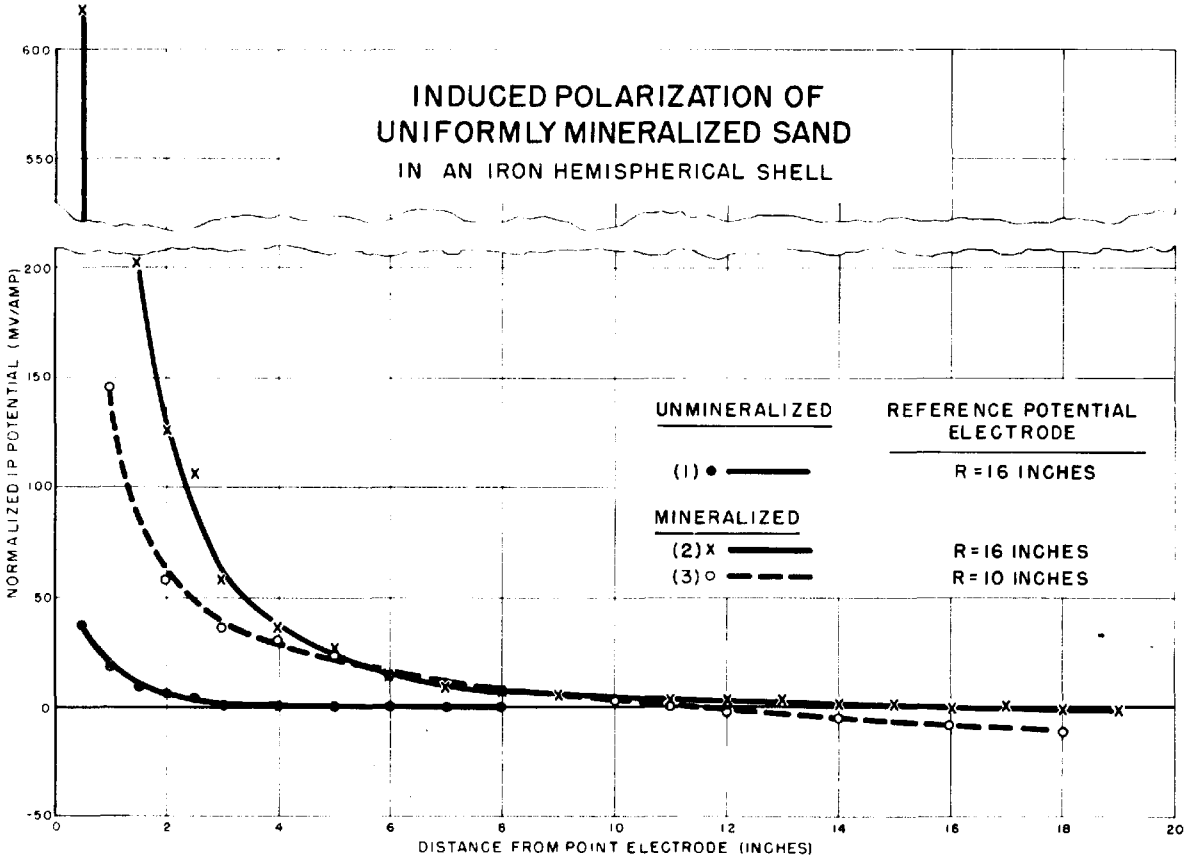
INDUCED POLARIZATION OF
UNIFORMLY MINERALIZED SAND
IN AN IRON HEMISPHERICAL SHELL
600
550
NORMALIZED IP POTENTIAL (MV/AMP)
200
150
100
50
0
-50
UNMINERALIZED
(1)
REFERENCE POTENTIAL ELECTRODE
R=16 INCHES
MINERALIZED
(2)
R=16 INCHES
(3)
R=10 INCHES
0
2
4
6
8
10
12
14
16
18
20
DISTANCE FROM POINT ELECTRODE (INCHES)

theoretical relation. A hemispherical shell 40.2 inches in diameter was filled with sand and wet with salt water. The point current electrode was a 1/8 inch iron rod which extended into the sand at the center of the air-sand plane. The hemisphere itself served as the return electrode and the two electrodes together provided a current density pattern which was essentially radial and yielded equipotential surfaces which were hemispheres, as required by the infinitely extended half-space. The reference potential electrode had to be at a finite distance from the point electrode because of the limited radius of the hemisphere. Its location, however, needed to be described only in terms of its distance from the center because the equipotential lines on the surface of the sand are circles. When the hemisphere contained only clean quartz sand and salt water a polarization potential, which fell off rapidly with distance from the current electrode, was measured. This background potential arises from a differential polarization of the current electrode. In order that a current of approximately 600 ma could be delivered to the sand, the rod had to be inserted nearly an inch into the sand and, therefore, contact of the current electrode with the sand was not a point but a cylinder. The background polarization potential was just measurable when the hemisphere was filled with tap water in place of sand.

The sand in the hemisphere was next mineralized to about 10% by weight by the addition of iron grit. Small batches of grit and sand were mixed by hand (in a wheelbarrow with a hoe) to attain a fairly uniform mixture. Water was added to the mixture until the water table was at the surface of the sand. The measured induced polarization potential is plotted in Plate 10b as a function of the position of the probing potential electrode from the center of the hemisphere. The relation of these results to the theory is discussed in Part C-1.

c) Induced Polarization Potential of a Buried Sphere

An attempt was made to obtain experimental verification of the theoretical results developed in Part C-2 for the potential of a buried sphere. The conditions required by the theory, in the development of the approximate formula, were never realized in the laboratory. One difficulty which thwarted every attempt at measurement was the size of the current electrode required. The largest iron sphere available at the time was only 3 inches in diameter. When that

sphere was buried to a depth of five times its radius, the current required to produce suitable potential measurements at the surface of the sand, was of the order of 1 ampere. The electrode area required to deliver one ampere was prohibitively large. A compromise was reached whereby the depth to the center of the sphere and the size of current electrode were both decreased until a measurable signal was obtained. The form of the measured potential distribution was in agreement with that predicted by the theory; i.e., the potential rose to a maximum over the sphere and then decreased and finally became negative as the distance from the point electrode was increased. The magnitude of the measured potential was, however, much greater than that predicted by the simplified expression (Equation 15) in Part C-2. The conditions required by the theory were not met and, therefore, no comparison of the experimental and theoretical results can be made which can check the validity of the theory.

10. Conclusions

The problem of establishing a potential by inducing electromotively active materials on the surface of a metallic object in an electrolyte has been investigated. The following facts have been established:

a) that a polarization potential can be induced on the surfaces of a metallic object in an electrolyte.

b) that the potential induced is a linear function of the potential gradient until a potential of 1.2 v has been established across the object. Beyond this potential a saturation effect begins.

c) that diffusion and chemical action of the products of polarization play the predominant role in the determination of the rate of growth and decay of the polarization potential.

d) that to a first approximation, only metallic or metallic-like objects are polarizable. The polarization of the cell containing $CuSO_4$ surrounded by tap water is an exception but it is a second order effect.

e) that metallic particles disseminated throughout an unpolarizable matrix are polarizable.

From these facts it is concluded:

a) that polarization products are induced on a boundary in an electrolyte only when there is a change in the mode of conduction; i.e., from ionic to electronic or vice versa.

b) that the charge density induced on the boundary is proportional to the current density crossing normal to the boundary and of such sign as to oppose the current which generates it.

c) that if a polarization is induced at all it is induced upon an electrically conducting mineral which is either in the form of a solid ore body or as a disseminated mineral.

d) that the current required to produce saturation will be greater for the disseminated mineral than for the solid ore. Further, that for a given energizing current the induced polarization potential of a mineralized zone will be smaller when the mineral is encased in a low resistive rock than in a higher resistive one on two accounts: 1) the potential gradient established across the mineral will be smaller and 2) the ratio of the resistivity of matrix to mineral will be decreased.

e) that the shape of the decay curves will be independent, as a first approximation, of the resistivity of the medium surrounding the mineral. The curves will, therefore, have a time constant which will always be approximately 0.25 sec.

It follows from the above conclusions that the "residual" polarization potential of Schlumberger arose from a more or less uniform distribution of electrically conductive minerals. The potentials which Potapenko claims to have measured probably had the same origin. None of the claims of Müller and Weiss are tenable in view of the above conclusions. They could not have measured anything other than the polarization of their own current electrodes which was many times greater than the effect they sought.

The conclusions which result from the laboratory experimentation establish some requirements on the procedure to be followed in the field and also on the method of reducing the data obtained. Measurements of the apparent resistivity will have to be taken in conjunction with the induced polarization data. The

resistivity factor must be removed from the measurements obtained in the field before such measurements are compared. Because of the linear relation between the energizing current and the induced potential the field measurements will have to be normalized to a given current. The form of the curve for the decay of the induced polarization potential requires an energizing-current pulse which is not less than 0.3 sec. duration in order to produce time-saturation for a given current. However, the pulse time does not have to exceed 0.5 sec. It appears from a consideration of the electrical transient effects that the delay time in the switching cycle may be as small as 10 milliseconds without interference from the rapidly decaying ohmic potential.

C. THEORETICAL DISCUSSION

It is not surprising that there have been no attempts at a theoretical development for the interpretation of induced polarization as applied to geophysical prospecting. The lack of understanding of the fundamental principles involved must have precluded any efforts along those lines. Certainly the usefulness of this prospecting method will be greatly enhanced as the theoretical interpretation is expanded. The results obtained from the laboratory investigations provide a beginning for a theoretical development. In this section three problems are discussed and mathematical relations are obtained for two of them.

The first problem (uniformly mineralized earth) is offered as an explanation of the "residual" potential observed by Schlumberger. In the second problem (the buried sphere) an ore body is represented by a sphere only because it simplifies the geometry. The solution obtained for the sphere is complete in an analytical sense but it is far from being satisfactory for computational purposes. The fundamental relation employed in the mathematical development was established in Part B-3; i.e., the induced polarization potential is proportional to the energizing potential gradient

$$P = c\rho i$$

In the earth the resistivity may well be a function of the three space coordinates. However, in the following work variations in the matrix resistivity are not treated analytically.

1. Uniformly Mineralized Earth

It was demonstrated in the laboratory (Part B-9) that a polarization potential can be induced into a region which contains disseminated metallic particles. Previous to that demonstration it had been shown that the sand itself is not polarizable and neither is water. It was then concluded that the "residual" effect (measured by Schlumberger and verified with the present equipment whenever used in the field) was the potential resulting from a uniform distribution of disseminated electrically-conducting mineral particles in the earth. Accordingly, assume the earth to be uniformly mineralized and of uniform resistivity. Under the action of

[illegible] energizing current from a point electrode at the origin, so Figure 4, an elementary volume δV at $\varphi(x,y,z)$ will become polarized. Let $\bar{P}$ be the polarization per unit volume where $\bar{P} = -\bar{J}$, $\bar{J}$ = current density at $\varphi(x,y,z)$ and $\bar{J} = \sigma \bar{E}$.

The potential at the point $S(x';y';z')$ on the surface of the earth due to the dipole $\bar{P}\,\delta v$ is

$$\delta\phi(x',y',z') = \frac{\bar{P}\cos\theta\,\delta v}{R^2}$$

and the total potential is the integral over the infinite half-space (V) bounded by the earth's surface and excluding the hemisphere Σ around the current electrode.

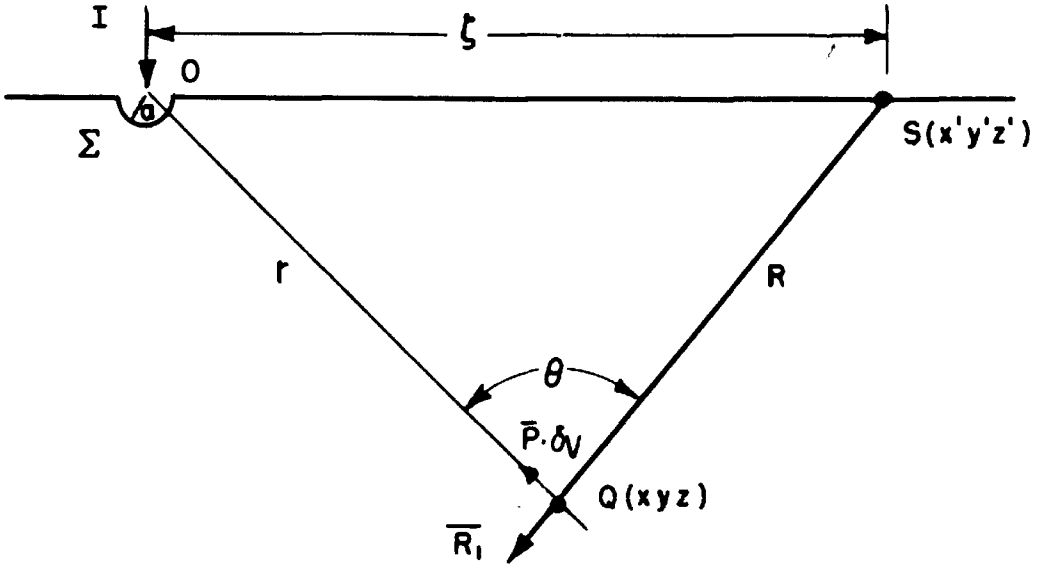

FIG. 4

[illegible] on

$$\phi(x',y',z') = \int_V \frac{\bar{P}\cos\theta\,dv}{R^2}$$

if $\bar{R}_2$ is a unit vector along R then

$$\frac{\bar{P}\cos\theta}{R^2} = -\bar{P}\cdot\left(\frac{\bar{R}_1}{R_2}\right)$$

but $$\frac{\bar{R}_1}{R^2} = -\nabla'\left(\frac{1}{R}\right)$$

where the prime indicates differentiation with respect to $x';y';z'$.

however $$\nabla\left(\frac{1}{R}\right) = -\nabla'\left(\frac{1}{R}\right)$$

by symmetry.

Therefore $$\phi(x',y',z') = -\int_V \bar{P}\cdot\nabla\left(\frac{1}{R}\right)dV$$

Applying Gauss' theorem

$$\phi(x',y',z') = \int_V \frac{\nabla\cdot P\,dV}{R} - \int_S \frac{P_n\,dS}{R}$$

but since $\bar{P} = -k\bar{i}$ and $\nabla\cdot\bar{i} = 0$

therefore $\nabla\cdot P = 0$

and $$\phi(x',y',z') = -\int_S \frac{P_n\,dS}{R}\ .$$

Now the normal component of $\bar{i}$ (and therefore of P) is everywhere zero on the surface of the earth except on the hemisphere Σ

where $$P_n = -ki_a = -\frac{kI}{2\pi a^2}\ .$$

However, the radius of the hemisphere can be chosen as small as we please and therefore R can be taken constant and equal to ζ over the integration which then gives

(1) $$\phi(x',y',z') = \frac{kI}{2\pi a^2\zeta}\int_\Sigma dS = \frac{kI}{\zeta}$$

From this it is seen that the induced polarization potential for the uniformly mineralized earth falls off like 1/r from a point energizing electrode.

An experiment, designed to test the 1/r relation for a uniformly mineralized earth, was described in Part B-9. The earth was simulated by an iron hemispherical shell filled with mineralized sand. The potentials measured are plotted, in Plate 10b, against the distance from the "point" current electrode at the center. Curve 1 represents the background obtained when the sand was unmineralized and that curve falls off more rapidly than Curve 2 or Curve 3. Both Curve 2 and Curve 3 decrease with distance at a rate which is like 1/r but departs from this relation close to the point electrode. As it has been pointed out, it was not possible to remove the reference potential electrode a great distance from the point electrode and, therefore, the effect of the nearby reference electrode has to be considered. The expression for the induced polarization potential which includes the effect of the nearby reference electrode is the difference of the two electrode potentials each considered with respect to the potential at infinity. The mathematical form of this expression is

$\Delta\phi\,(x',y',z') = \frac{kI}{r} - \frac{kI}{R}$ where r is the distance from the point electrode to the probing potential electrode and R is the corresponding distance to the reference potential electrode. If this expression is multiplied by r/I and the difference of potential is written as just ϕ the resultant equation

$$\phi\frac{r}{I} = -\frac{kr}{R} + k$$

becomes the slope-intercept form for a straight line when r/I is plotted as a function of r. The slope of the line is negative and equal k/R and obviously, the intercept is k. The data used to plot Curve 2 and Curve 3 in Plate 10b have been multiplied by r and replotted as Curve 1 and Curve 2 respectively in Plate 11. Neither curve appears to yield a straight line, particularly in the vicinity of the origin. On the other hand, the apparent curvature is different also in that it is concave for one and convex for the other. The departure of these curves from a linear relation is due to the influence of the current electrode which, considering the dimensions involved, was definitely not a point electrode. However, beyond the value r = 8 the two curves become reasonably straight. A straight line has been drawn through each set of data such that those points beyond r = 8 determine the line. The slope and the intercept of each line is different but it must be remembered that k is not necessarily constant because its value ($k = c\rho$) varies with the resistivity. The slope can be written

$$m = \frac{k}{R} = \frac{c\rho}{R}.$$

This equation is solved for c and its values, obtained from the two lines are equated; i.e.,

$$c = \frac{m_1 R_1}{\rho_1} = \frac{m_2 R_2}{\rho_2}.$$

For

Curve 1 $\quad R_1 = 16 \quad m_1 = \frac{.125}{15.4}$

and the corresponding values for

Curve 2 $\quad R_2 = 10 \quad m_2 = \frac{.250}{10.75}$

which gives

$$\rho_1/\rho_2 = .56$$

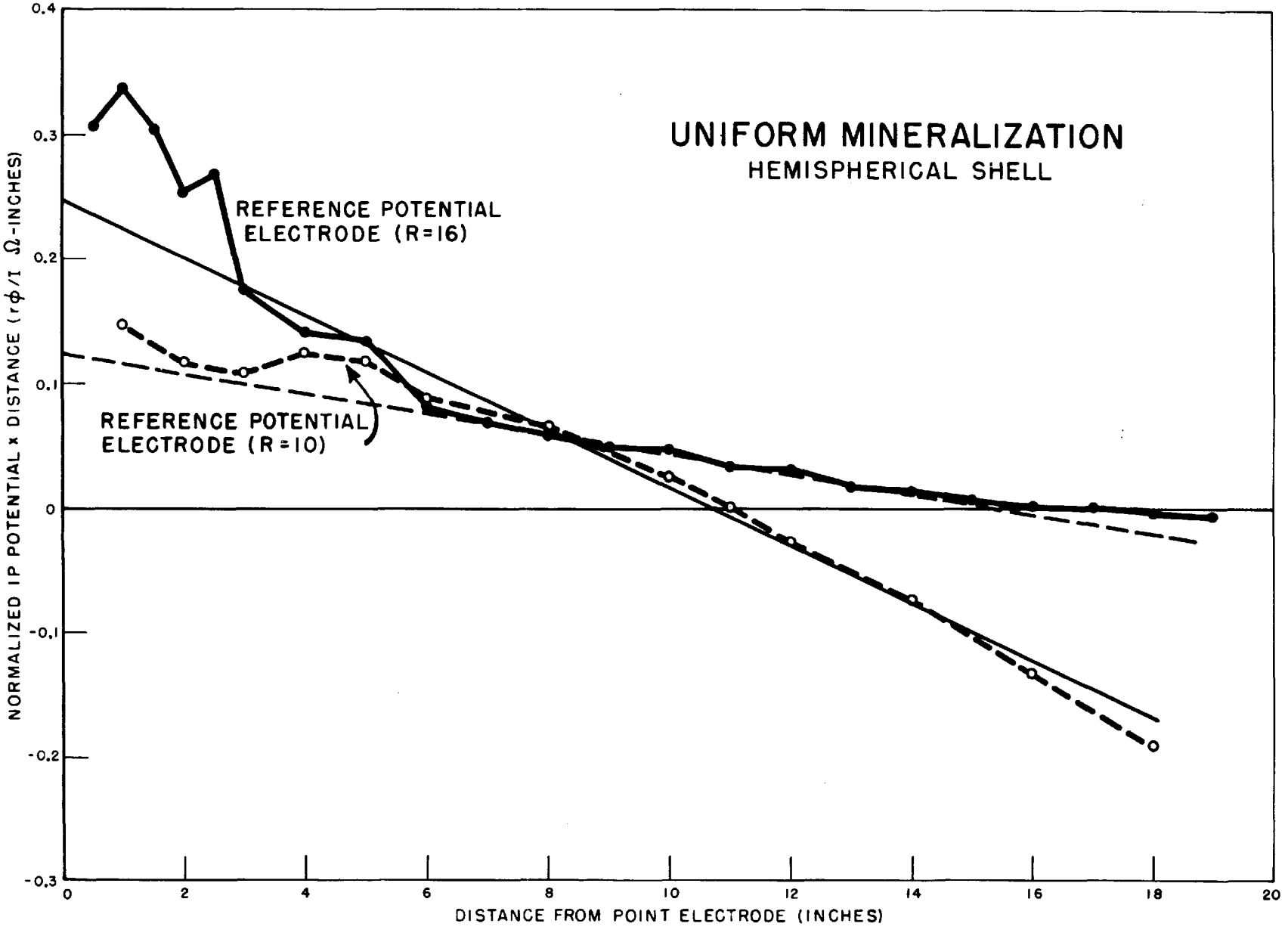
UNIFORM MINERALIZATION
HEMISPHERICAL SHELL
REFERENCE POTENTIAL ELECTRODE (R=16)
REFERENCE POTENTIAL ELECTRODE (R=10)
NORMALIZED IP POTENTIAL x DISTANCE (rφ/I Ω-INCHES)
DISTANCE FROM POINT ELECTRODE (INCHES)
0.4
0.3
0.2
0.1
0
-0.1
-0.2
-0.3
0
2
4
6
8
10
12
14
16
18
20

PLATE II

From the measured values of the ohmic potential and the current, the resistivity ratio has been computed and several values are tabulated:

r	6	8	12
ρ_1/ρ_2	0.58	0.63	0.49

Because the sand in the hemisphere is not uniformly mineralized, as the ratios of the resistivities indicate, the values obtained from the ratio of the slopes of the lines and the ratio of the resistivities are considered to be in good agreement and it is, therefore, concluded that the 1/r relation for the uniformly mineralized earth has been verified.

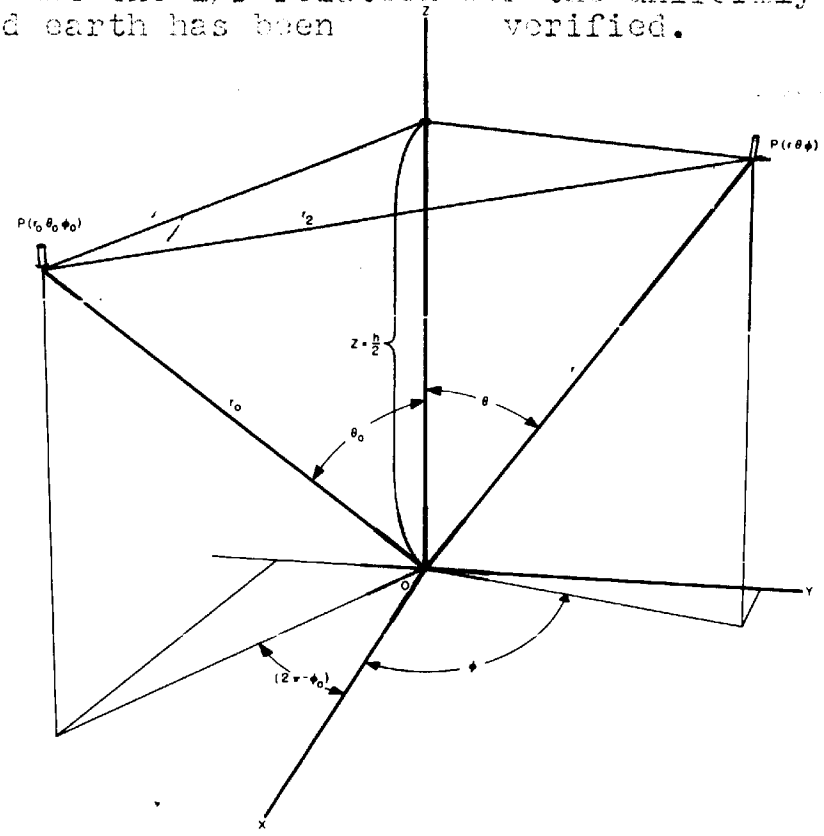

FIG. 5

2. Buried Sphere

There is little information at present to enable a quantitative determination of the depth or physical size and shape of an ore-body from the magnitude of the signals obtained. To serve as a guide in the interpretation, the potential of a buried sphere is calculated.

Consider a sphere of radius a and resistivity ρ_2 buried to a depth of z = h/2 in a homogeneous earth whose resistivity is ρ_1 (see Figure 5). Take the origin at the center of the sphere. A point-electrode, delivering a current I, is located at the point

$P(r_0, \theta_0, \varphi_0)$. The problem is to calculate the potential at the point $P(r, \theta, \varphi)$ due to the charge density σ resulting from induced polarization on the surface of the sphere. The charge density σ is generated by the sphere while the energizing current I is flowing through the outer electrode. The polarization potential is measured immediately after the energizing current has been interrupted and, therefore, the static potential produced by the current I at the point electrode is not to be considered.

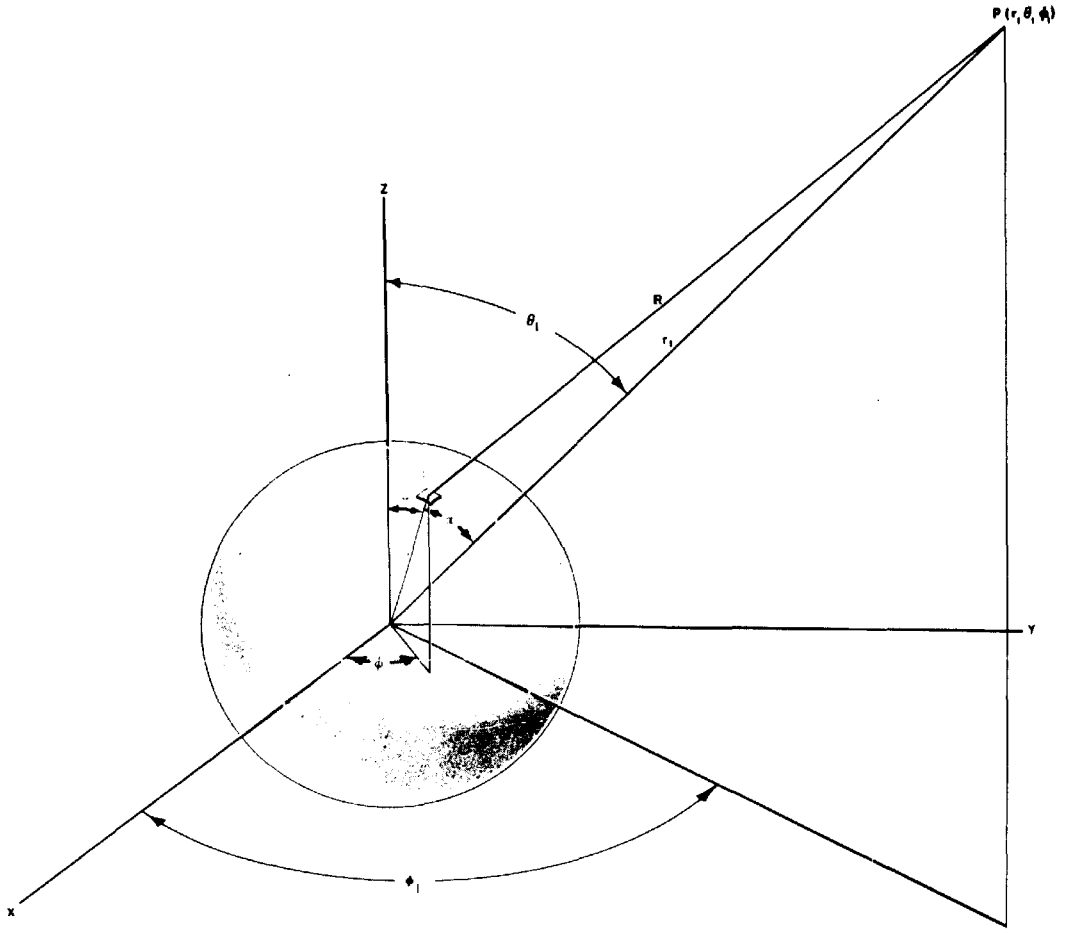

FIG. 6

The potential at any point $P(r, \theta, \varphi)$ due to a charge density σ on the sphere, (see Figure 6), is given by

$$(1) \quad \phi(r_1, \theta_1, \varphi_1) = \int_S \frac{\sigma \, dS}{R}$$

where R is the distance from the point P to the surface element dS on the sphere, and

$$dS = a^2 \sin\theta \, d\theta \, d\varphi,$$

$$R^2 = r_1^2 + a^2 - 2 r_1 a \cos\alpha,$$

and

$$\frac{1}{R} = \frac{1}{\left[r_1^2 + a^2 - 2 r_1 a \cos\alpha\right]^{\frac{1}{2}}},$$

Therefore,

$$\frac{1}{R} = \frac{1}{r_1} \sum_{n=0}^{\infty} \left(\frac{a}{r_1}\right)^n P_n(\cos\alpha) .$$

It is, however, better to have 1/R expressed in terms of θ instead of α. Therefore, expand the Legendre polynomial $P_n(\cos\alpha)$ in terms of θ. Form the biaxial expansion[19]

$$P_n(\cos\alpha) = \sum_{m=0}^{m=n} (2 - \delta_m^o) \frac{(n-m)!}{(n+m)!} P_n^m(\mu_1) P_n^m(\mu) \cos m(\varphi - \varphi_1)$$

where $\mu_1 = \cos\theta_1$, $\mu = \cos\theta$ and δ_i^j is the Kronecker delta, which gives

(2)
$$\frac{1}{R} = \frac{1}{r_1} \sum_{n=0}^{\infty} \left(\frac{a}{r_1}\right)^n \sum_{m=0}^{m=n} (2 - \delta_m^o) \frac{(n-m)!}{(n+m)!} P_n^m(\mu_1) P_n^m(\mu) \cos m(\varphi - \varphi_1)$$

$$= \frac{1}{r_1} \sum_{n=0}^{\infty} \left(\frac{a}{r_1}\right)^n {}_1L_n(\mu, \mu_1, \varphi, \varphi_1) .$$

The maximum (ϕ at t = 0) potential of polarization then is

(3)
$$\phi(r_1, \theta_1, \varphi_1) = \int_S \frac{\sigma}{r_1} \sum_{n=0}^{\infty} \left(\frac{a}{r_1}\right)^n {}_1L_n \, dS = \frac{1}{r_1} \sum_{n=0}^{\infty} \left(\frac{a}{r_1}\right)^n \int_S \sigma \, {}_1L_n \, dS$$

Now if σ were known the potential could be calculated. However, from the laboratory experiments it is known that σ results from a polarization-charge generated on the surface of the sphere while the current I is flowing.

It has been shown in Part B-4 that the induced polarization potential is proportional to the actual current density crossing the boundary. From Bowden's paper[17] it is known that the polarization potential is proportional to the surface charge density, therefore,

it follows that

(4) $\sigma = -\lambda i_a,$

where i_a is the normal component of the current density at the surface of the sphere. Now from Ohm's law

(4') $$\sigma = \frac{\lambda}{\rho_1}\left(\frac{\partial \Phi_E^\circ}{\partial r}\right)_{r=a} \qquad \text{because } i_r = -\frac{1}{\rho_1}\frac{\partial \Phi_E^\circ}{\partial r}$$

Here Φ_E° is the potential in the earth at any point outside the sphere resulting from the energizing current I, the sphere and the air-earth boundary.

The ohmic potential of a buried sphere was computed by Webb[20] and is given formally by

(5) $$\Phi_E^\circ = \frac{D}{r_o}\sum_{n=0}^{\infty}\left(\frac{r}{r_o}\right)^n {}_oL_n(\mu,\mu_o,\varphi,\varphi_o) + \sum_{n=0}^{\infty}\left(\frac{a}{r}\right)^{n+1} S_n(\mu,\varphi) + \sum_{n=0}^{\infty}\left(\frac{a}{r_1}\right)^{n+1} S_n(\mu',\varphi)$$

where

(6) $$ {}_oL_n(\mu,\mu_o,\varphi,\varphi_o) = \sum_{m=0}^{m=n}(2-\delta_m^\circ)\frac{(n-m)!}{(n+m)!}P_n^m(\mu_o)P_n^m(\mu)\cos m(\varphi-\varphi_o),$$

is a term which arises from the point-electrode alone,

$$D = \frac{\rho_1 I}{4\pi},$$

(7) $$S_n(\mu,\varphi) = \sum_{m=0}^{\infty}(A_{mn}\cos m\varphi + B_{mn}\sin m\varphi)P_n^m(\mu)$$

$$\text{and } \sum_{n=0}^{\infty}\left(\frac{a}{r_1}\right)^{n+1} S_n(\mu',\varphi) = \sum_{n=0}^{\infty}\left(\frac{r'}{a}\right)^n \sum_{m=0}^{\infty} P_n^m(\mu')\sum_{k=m}^{\infty} a_{mkn}(A_{mk}\cos m\varphi + B_{mk}\sin m\varphi),$$

$$\text{in which } a_{mkn} = \frac{(n+k)!}{(n+m)!(k-m)!}\left(\frac{a}{h}\right)^{n+k+1}.$$

(The coordinates r' and μ' refer to the image of the point P with respect to the center of the image sphere. Therefore, by symmetry the substitution of r and μ for r' and μ' respectively will lead to the potential at the point P with respect to the center of the real sphere). Now rewriting the potential to give

(8) $$\Phi_E^\circ = \frac{D}{r_o}\sum_{n=0}^{\infty}\left(\frac{r}{r_o}\right)^n {}_oL_n + \sum_{n=0}^{\infty}\left(\frac{a}{r}\right)^{n+1} S_n(\mu,\varphi) + \sum_{n=0}^{\infty}\left(\frac{r}{a}\right)^n \sum_{m=0}^{\infty} P_n^m(\mu')\sum a_{mkn}(A_{mk}\cos m\varphi + B_{mk}\sin m\varphi)$$

from which

$$(9)\left(\frac{\partial \Phi_E^o}{\partial r}\right)_{r=a} = \frac{D}{r_o}\sum_{n=o}^{\infty}\frac{n}{a}\left(\frac{a}{r_o}\right)^n {}_oL_n + \sum_{n=o}^{\infty} -\frac{(n+1)}{a} S_n(\mu,\varphi)$$
$$+\sum_{n=o}^{\infty}\frac{n}{a}\sum_{m=o}^{\infty} P_n^m(\mu)\sum_k a_{mkn}(A_{mk}\cos m\varphi + B_{mk}\sin m\varphi),$$

which gives the charge density from equation (4') to be

$$(10)\quad \sigma = \frac{\lambda}{\rho_1}\left[\frac{D}{r_o}\sum_{n=o}^{\infty}\left(\frac{n}{a}\right)\left(\frac{a}{r_o}\right)^n {}_oL_n - \sum_{n=o}^{\infty}\frac{n+1}{a} S_n(\mu,\varphi)\right.$$
$$\left.+\sum_{n=o}^{\infty}\frac{n}{a}\sum_{m=o}^{\infty} P_n^m \sum a_{mkn}(A_{mk}\cos m\varphi + B_{mk}\sin m\varphi)\right]$$

Substituting for σ into Equation (3) we get

$$\phi(r_1,\theta_1,\varphi_1) = \frac{1}{r_1}\sum_{n=o}^{\infty}\left(\frac{a}{r_1}\right)^n \int_S \frac{\lambda}{\rho_1}\left[\frac{D}{r_o}\sum_{n=o}^{\infty}\left(\frac{n}{a}\right)\left(\frac{a}{r_o}\right)^n {}_oL_n - \sum_{n=o}^{\infty}\frac{n+1}{a} S_n(\mu,\varphi)\right.$$
$$\left.+\sum_{n=o}^{\infty}\frac{n}{a}\sum_{m=o}^{\infty} P_n^m \sum a_{mkn}(A_{mk}\cos m\varphi + B_{mk}\sin m\varphi)\right] {}_1L_n a^2 \sin\theta\, d\theta\, d\varphi$$

The cross-product of the sums disappear because of the orthogonal properties of the zonal harmonics, leaving

$$(11)\quad \phi(r_1,\theta_1,\varphi_1) = \frac{\lambda}{a\rho_1 r_1}\sum_{n=o}^{\infty}\left(\frac{a}{r_1}\right)^n \left\{\int_o^{\pi}\int_o^{2\pi}\frac{D}{r_o} n\left(\frac{a}{r_o}\right)^n {}_oL_n \cdot {}_1L_n a^2 \sin\theta\, d\theta\, d\varphi\right.$$
$$-\int_o^{\pi}\int_o^{2\pi}(n+1)\, S_n(\mu,\varphi)\, {}_1L_n a^2 \sin\theta\, d\theta\, d\varphi$$
$$\left.+\int_o^{\pi}\int_o^{2\pi} n\sum_{m=o}^{\infty} P_n^m(\mu)\sum_k a_{mkn}(A_{mk}\cos m\varphi + B_{mk}\sin m\varphi)\right\}$$

Here there are three integrals to be evaluated:

(a) $$\int_{-1}^{1}\int_o^{2\pi} {}_1L_n \cdot {}_oL_n \, d\mu\, d\varphi$$

(b) $$\int_{-1}^{1}\int_o^{2\pi} {}_1L_n \cdot S_n \, d\mu\, d\varphi$$

(c) $$\int_{-1}^{1}\int_o^{2\pi} {}_1L_n \cdot \frac{\partial}{\partial r}\left(\frac{a}{r_1}\right)^{n+1} S_n'(\mu',\varphi)\, d\mu\, d\varphi$$

Now to evaluate (a) write

$$ {}_{1}L_n=\sum_{m=0}^{\infty} J_{mn} P_n^n(\mu)\cos m(\varphi-\varphi_1) \qquad {}_{0}L_n=\sum_{S=0}^{s=m} I_{sm} P_n^s \cos s(\varphi-\varphi_0) $$

where

$$ J_{mn}=(2-\delta_m^0)\frac{(n-m)!}{(n+m)!}P_n^m(\mu_1) $$

and

$$ I_{sn}=(2-\delta_s^0)\frac{(n-s)!}{(n+s)!}P_n^s(\mu_0) $$

However, the orthogonal properties require that s must equal n which then gives for (a)

$$ =\sum_{m=0}^{m=n}\int_{-1}^{1}\int_{0}^{2\pi} J_{mn}I_{mn}(P_n^m(\mu))^2\left[\cos^2 m\varphi(\cos m\varphi_0\cos m\varphi_1)\right. $$
$$ \left.+\sin^2 m\varphi(\sin m\varphi_0\sin m\varphi_1)+\sin m\varphi\cos m\varphi\sin(\varphi_0+\varphi_1)\right]d\varphi d\mu. $$

The first integration yields

$$ =\pi\sum_{m=0}^{m=n}\int_{-1}^{1} J_{mn}I_{mn}\left[P_n^m(\mu)\right]^2\cos m(\varphi_0-\varphi_1)d\mu=\pi\sum_{m=0}^{m=n} I_{mn}J_{mn}\cos m(\varphi_0-\varphi_1)\int_{-1}^{1}\left[P_n^m(\mu)\right]^2 d\mu $$

and the integral (a) becomes

$$ \int_{-1}^{1}\int_{0}^{2\pi} {}_{1}L_n\cdot{}_{0}L_n\,d\mu d\varphi=\pi\sum_{m=0}^{m=n} I_{mn}J_{mn}\cos(\varphi_0-\varphi_1)\gamma_{mn}. $$

In a similar manner the integral (b) becomes

$$ \int_{-1}^{1}\int_{0}^{2\pi} {}_{1}L_n\cdot S_n\,d\mu d\varphi=\sum_{m=0}^{m=n}\int_{-1}^{1}\int_{0}^{2\pi} J_{mn}\left[P_n^m(\mu)\right]^2\cos m(\varphi-\varphi_1)\left[A_{mn}\cos m\varphi\right. $$
$$ \left.+B_{mn}\sin m\varphi\right]d\varphi d\mu=\pi\sum_{m=0}^{m=n}(A_{mn}\cos\varphi_1 $$
$$ +B_{mn}\sin\varphi_1)J_{mn}\gamma_{mn}. $$

In a similar manner (c) becomes

$$ =n\int_{-1}^{1}\int_{0}^{2\pi} P_n^m(\mu)\Sigma a_{mkn}(A_{mk}\cos m\varphi+B_{mk}\sin m\varphi)\,{}_{1}L_n\,d\mu d\varphi $$
$$ =\frac{2n}{2n+1}(2-\delta_m^0)P_n^m(\mu_1)(\cos m\varphi_1\Sigma a_{mkn}A_{mk} $$
$$ +\sin m\varphi_1\Sigma a_{mkn}B_{mk}) $$

where

$$\alpha_n A_{mn} + {}'K_{mn}\left(\frac{a}{r_o}\right)^n = -\sum_k a_{mkn} A_{mk}$$

$$\alpha_n B_{mn} + {}^2K_{mn}\left(\frac{a}{r_o}\right)^n = -\sum_k a_{mkn} B_{mk}$$

(These expressions differ from those given by Webb[20], see Appendix I).

(12)

$$\alpha_n = \left[\frac{\beta+1}{\beta-1} + \frac{1}{n(\beta-1)}\right],\quad {}_2'K = \frac{D}{r_o}(2-\delta_m^o)\frac{(n-m)!}{(n+m)!}P_n^m(\mu_o)\begin{Bmatrix}\cos m\varphi_o\\ \sin m\varphi_o\end{Bmatrix}$$

$$\beta = \rho_1/\rho_2$$

which gives for integral (c)

$$\int_{-1}^{1'}\int_0^{2\pi} {}_1L_n \cdot \frac{\partial}{\partial r}\left(\frac{a}{r_1}\right)^{n+1} S_n'(\mu' d)\, d\mu\, d\varphi = -\frac{2n}{2n+1}(2-\delta_m^o)P_n^m(\mu_1)\left[\cos m\varphi_1\left(\alpha_n A_{mn} + {}'K_{mn}\left(\frac{a}{r_o}\right)^n + \sin m\varphi\left(\alpha_n B_{mn} + {}^2K_{mn}\left(\frac{a}{r_o}\right)^n\right)\right]\right.$$

Now substituting back into the equation for the induced polarization potential the equation becomes

(13)

$$\phi(r_1,\theta_1,\varphi_1) = \frac{\lambda I a}{2 r_o r_1}\sum_{n=1}^{\infty}\left(\frac{a^2}{r_o r_1}\right)^n \frac{n}{2n+1}\left[P_n(\mu_o)P_n(\mu_1)\right.$$

$$\left. + 4\sum_{m=1}^{m=n}\frac{(n-m)!}{(n+m)!}P_n^m(\mu_o)P_n^m(\mu_1)\cos m(\varphi_o-\varphi_1)\right]$$

$$-\frac{2\pi\lambda a}{\rho_1 r_1}\sum_{n=0}^{\infty}\left\{\frac{n+1}{2n+1}\left[A_{on}P_n(\mu_1) + 2\sum_{m=1}^{m=n}P_n^m(\mu_1)\left(A_{mn}\cos m\varphi_1\right.\right.\right.$$

$$\left.\left.\left. + B_{mn}\sin m\varphi_1\right)\right] + \frac{2n}{2n+1}\left(\left[\alpha_n A_{on} + {}'K_{on}\left(\frac{a}{r_o}\right)^n\right]P_n(\mu_1) + 2\sum_{m=1}^{m=n}P_n^m(\mu_1)\left[\left[\alpha_n A_{mn}\right.\right.\right.\right.$$

$$\left.\left.\left.\left. + {}'K_{mn}\left(\frac{a}{r_o}\right)^n\right]\cos m\varphi_1 + \left[\alpha_n B_{mn} + {}^2K_{mn}\left(\frac{a}{r_o}\right)^n\right]\sin m\varphi_1\right]\right)\right\}$$

The evaluation of the potential at the surface (Equation 13) requires the evaluation of the double infinite series (Equations 12). Webb[20] has demonstrated the existence of a solution but it is rather involved. The problem is complicated by the air-earth boundary which introduces an infinite but convergent series of images. A first approximation then is the problem of the buried sphere in a full space. The

solution of this problem is contained in the first two terms for the potential expressed by Equation (13) where the coefficients A_{mn} and B_{mn} are altered. A simpler form of the expression for the potential obtains if the z-axis (the azimuth) is the line joining the center of the sphere and the point electrode. With this change (see Appendix II) the potential becomes

$$(14)\quad \phi(r_1,\theta_1,\varphi_1)=\sum_{n=0}^{\infty}\frac{k\,I\,a^{2n+1}}{(r_0 r_1)^{n+1}}\frac{n}{2n+1}\left[1-(n-1)\beta_n\right]P_n(\cos\theta)$$

where $\beta_n=\dfrac{\rho_2-\rho_1}{n\rho_1+(n+1)\rho_2}$ and θ is the angle between r_0 and r_1.

Now if $\dfrac{\rho_1}{\rho_2}\geq 100$ the expression for ϕ further simplifies becoming

$$(15)\quad \phi(r_1,\theta_1,\varphi_1)=k\,I\sum_{n=0}^{\infty}\frac{a^{2n+1}}{(r_0 r_1)^{n+1}}P_n(\cos\theta)$$

3. Ellipse of Polarization

From the tank experiments it was shown that the charge density is proportional to the current density actually crossing normal to the boundary. The ability to detect a dipole by its potential depends on its moment; i.e., upon both the charge and the separation of the charge. The inclusion of the length factor then provides additional information. Imagine a lenticular body buried beneath the surface and a survey technique which employs a Wenner electrode configuration. Further assume that the current electrode separation is comparable with the longest dimension of the body. Then when the electrode line is in the direction of the longest dimension of the ore body, the maximum potential gradient is established across the ore body. This orientation not only produces the maximum charge density but also the greatest separation of the charges. Therefore, the dipole induced and also the potential measured at the surface will be greatest (on two accounts) along the longest direction

of the mass and smallest perpendicular to that direction. As the line of electrodes is rotated from a direction perpendicular to the long dimension of the body the signal will increase until the line of electrodes is along the longest direction. Further rotation will decrease the potential going through a minimum again. The values of potential obtained as a function of position will then generate an ellipse whose major axis is along the strike of the body. Verification of this effect was obtained over the magnetite deposit,(Plate 39) and in the laboratory (see insert in Plate 10a) over the mineralized zone.

4. Concerning the Interpretation of Measurements

The mathematical development carried out for the problem of the uniformly mineralized earth has succeeded in yielding an equation which enables an interpretation of the field measurements. The basic equation, which may be applied to any electrode configuration is Equation (1) Part C-1. However, Equation (1) can be rewritten, forgetting Figure 4, in more familar symbols by replacing $\int$ by r and introducing the resistivity back into the equation; then

$$\phi = \frac{c\rho I}{r}$$

Now if a four electrode array is used the IP potential difference measured across the potential electrodes is given by

$$\Delta\phi = c\rho I\left[\frac{1}{r_1} - \frac{1}{r_2} - \frac{1}{R_1} + \frac{1}{R_2}\right]$$

where the meaning of r and R is the usual one. For the Wenner configuration the equation reduces to

$$\phi_o = \frac{c\rho I}{a}$$

where ϕ_o represents the maximum difference in potential (at t = 0) across the potential electrodes. From the theory developed for the resistivity of a uniform, extended half-space it is known that for the Wenner configuration

$$\rho = 2\pi a \frac{V_o}{I_o}$$

Substituting for ρ in the equation for the induced polarization potential and solving for the value of c

(1) $$C = \frac{\phi_o I_o}{2\pi V_o I} = \frac{\phi_o}{2\pi V_o}$$

where the current flow I_o, which produced the ohmic potential V_o, is taken to be the same as the value of the energizing current I which produced the induced polarization potential ϕ_o. Substituting S for $2\pi c$ yields the expression

(2) $$S = \frac{\phi_o}{V_o} \quad \frac{mv}{volt}$$

The quantity S may be defined as the induced polarization susceptibility and regarded as a property of the volume under measurement. It is this quantity which is to be compared in a field survey. The ratio of these two potentials yields a dimensionless quantity but for convenience the values of ϕ_o have been expressed in millivolts whereas those of V_o are in volts. It is to point out the discrepancy in the magnitudes of the two quantities that the pseudo-dimensions millivolt/volt have been appended to the susceptibility constant S.

The graphical portrayal of the polarization susceptibility of an area will depend upon the manner of applying the electrode configuration to the area. In general there are two applications for any given electrode configuration. In the first of these the electrode separation is maintained fixed and the whole configuration is moved from point to point along a traverse. The process is repeated for each traverse selected until the area has been covered. Any one configuration of the electrodes in this system is called a station. If the values of S obtained at the various stations are plotted at the points representing the center of those stations, a curve of the polarization susceptibility along each traverse is obtained. From these curves an areal susceptibility map may be constructed. The second application holds the center of the electrode configuration fixed and the electrode separation is varied. The measurements obtained come from larger and larger volumes of earth as the electrode separation is expanded; hence, this application is called vertical profiling. The values of S so obtained are plotted against the electrode separation. At the present time insufficient data have been obtained to establish an exact correlation between the depth and the electrode separation.

The apparatus described in Part D-1 could not, unfortunately, always measure both ϕ_o and V_o for the same current. In such a case it becomes necessary to return to Equation 1 of this section. One intentional feature in the design of the field apparatus which precludes the direct application of Equation 2 or 1 is the delay time in the switching cycle. There is a choice available in the manner of handling the data in connection with the IP potential at zero time. A workable method would be to displace the zero on the IP decay curve by a fixed time interval from the true zero, treat the IP potential at that point as the ϕ_o and compute S from it. A second and perhaps more desirable method is to extrapolate back to zero time. It should be pointed out that extrapolation is justified on the grounds that two properties of the curve are used (i.e., magnitude and rate of decay) provided that the curves fit a fixed form. From a study of the decay curves obtained in the field it was found that their form fits the E^2 relation for the rate of decay acceptably well and the values of ϕ_o will be obtained from the equation

$$\phi = \frac{A}{t + c}$$

where ϕ, the difference of potential measured at the surface of the earth, has replaced the electrode potential E used in the equations of Part B-5.

D. FIELD SURVEY RESULTS

1. Description of Field Instruments

A large amount of laboratory experimentation had been completed before the first field trip was undertaken. An attempt was made at the beginning of the field work to adapt the laboratory measuring equipment to satisfy field requirements. The Shell oscillograph is a rather cumbersome field instrument but it has in its favor the small amounts of power required to operate the galvanometer lamps. However, with it the results of field work remained unknown until the photographic record had been developed. The serious limitation on the use of the instrument imposed by bad impedance matching between the electrodes and the galvanometer element added to the inconvenience of developing paper in the field. The resistance offered by the potential electrodes varied widely as the electrodes were moved from place to place. Coupled with the variable electrode resistance was the frequent need to operate the instrument on a range where its resistance was many times less than that of the electrodes. Under this condition an appreciable amount of current could flow, temporarily polarizing the potential electrodes. Difficulties were also encountered with the mechanical pulsing switch. The operation of that switch had been excellent in the laboratory but failed in the field because it did not satisfy the requirement of high insulation resistance between the current and potential circuits, particularly in the extremely high relative humidity encountered in the Washington, D. C. area. An entirely new assemblage of equipment was prepared. This equipment was used throughout all the field work and is described now. Plates 12a, 12b and 12A, 12B are photographs of the equipment and Plate 13 shows its arrangement in block diagram form.

The first concern in the design of the pulsing switch was to maintain the leakage resistance adequately high (in excess of one megohm). The simplest solution to the problem was to physically separate the current and potential switches which was easily accomplished by a system of three relays. The switching circuit is shown schematically in Plate 14. The relay L1 is the master relay and its normal position is that which completes the L2 coil circuit. When the switch S1 has been closed for a sufficient time to charge the condenser C the switching circuit is armed. A pulse is obtained

FIELD EQUIPMENT

a

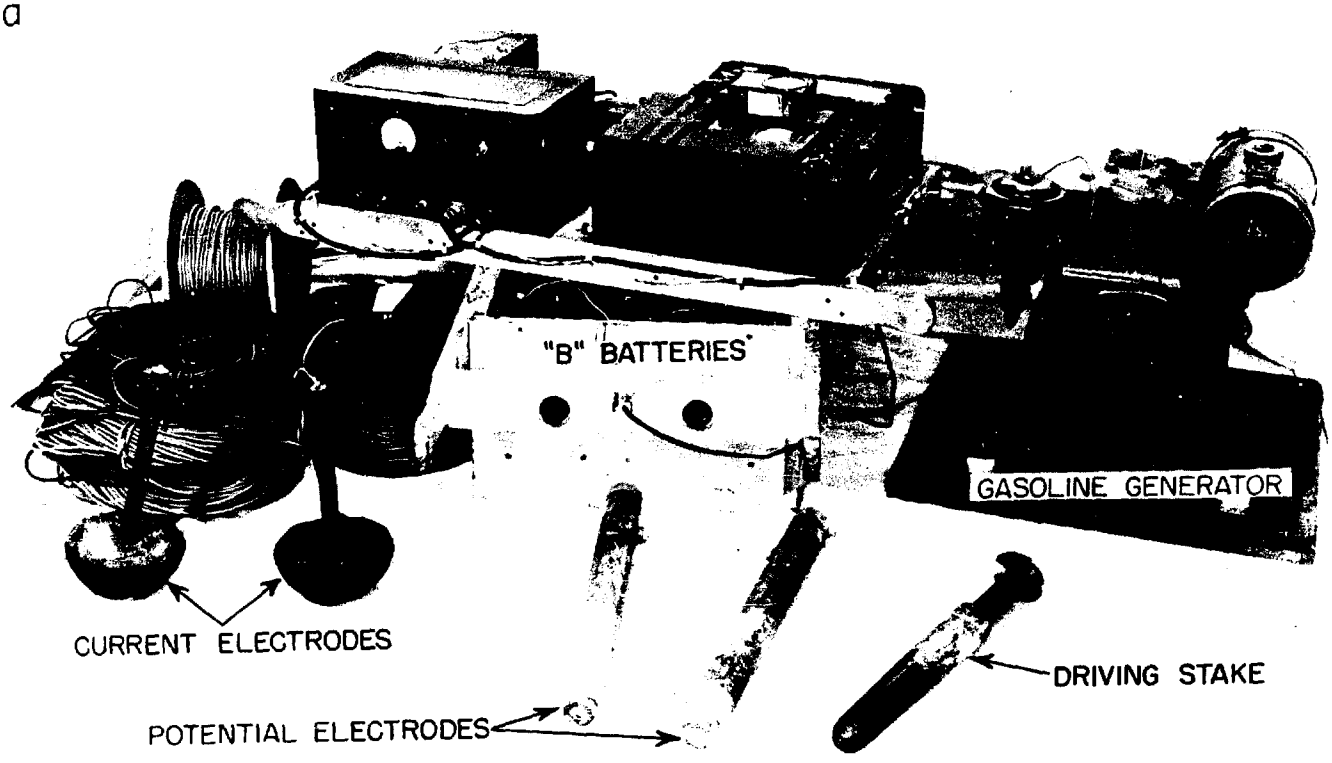

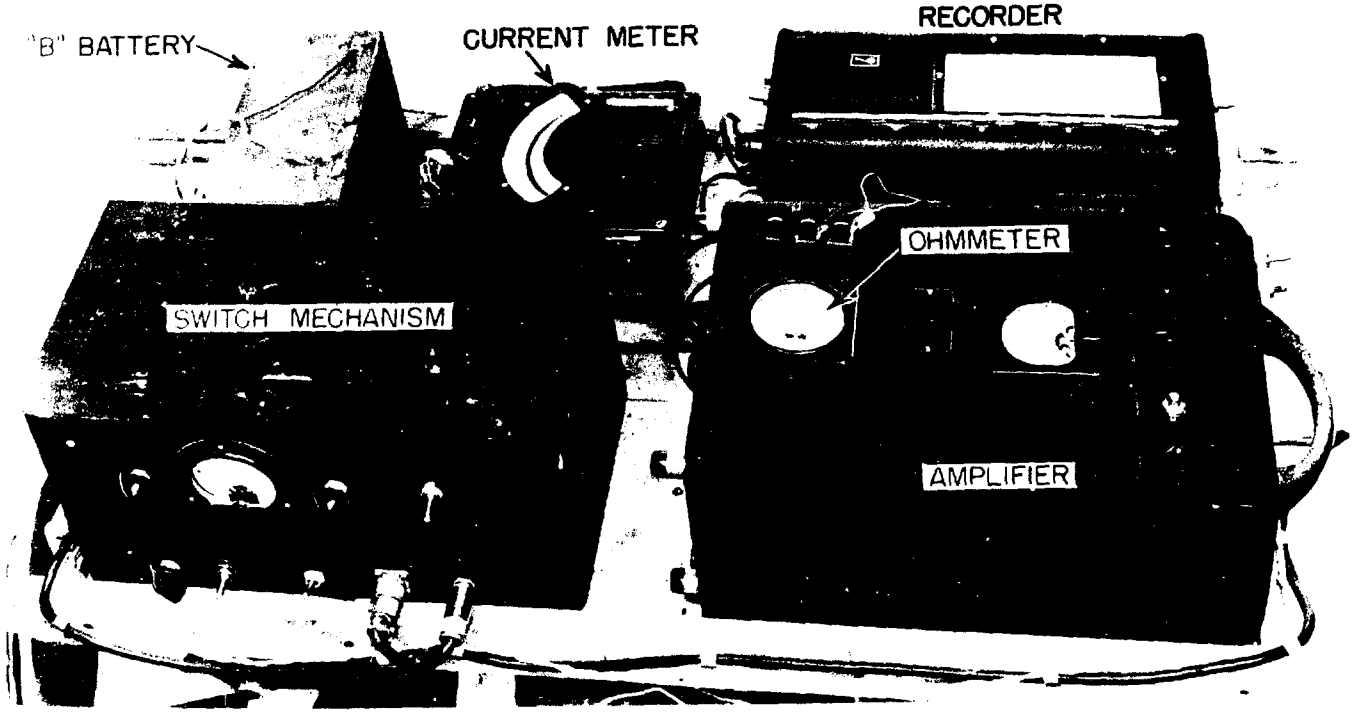

PLATE 12A

PLATE 12B

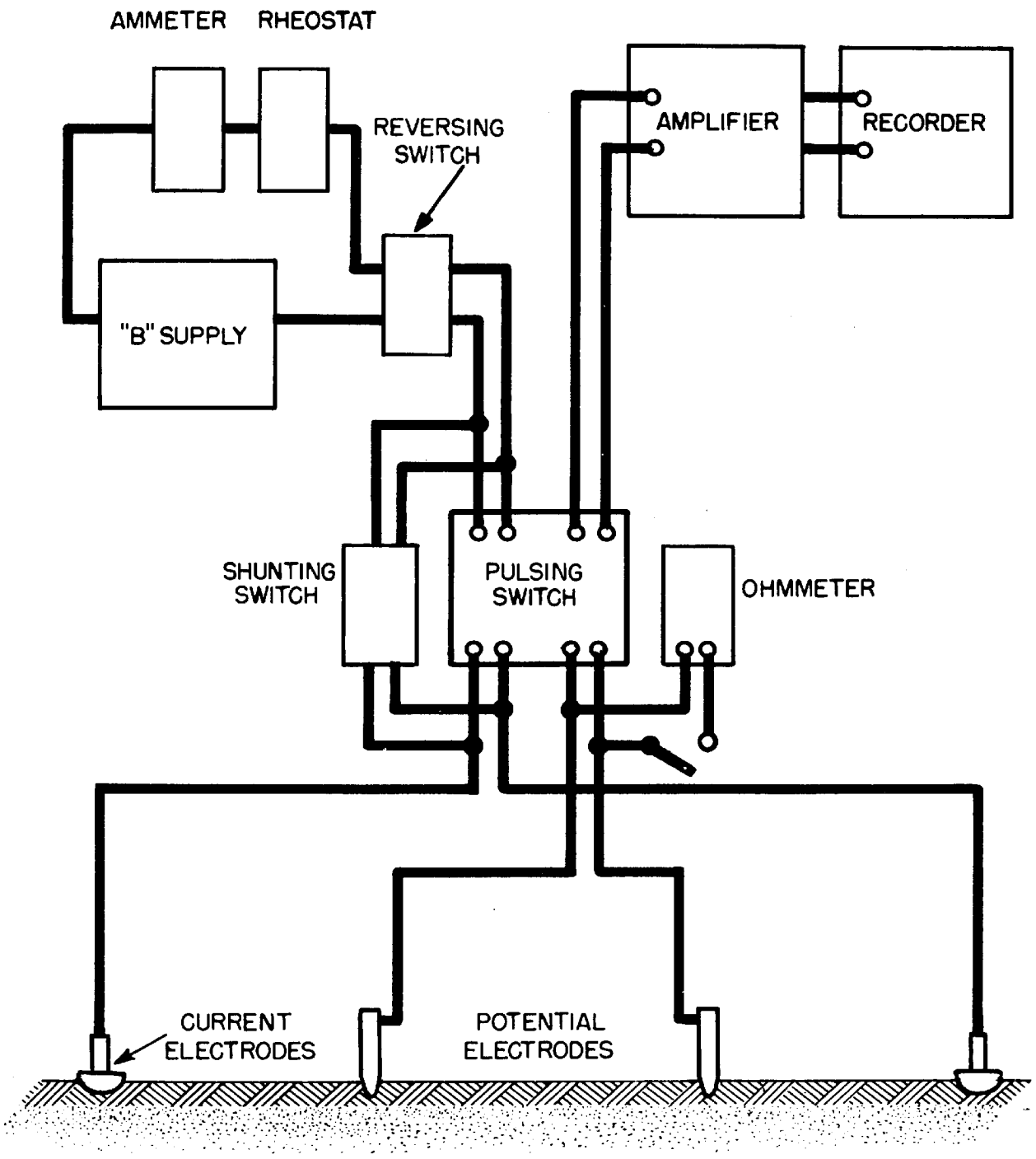

BLOCK DIAGRAM

OF FIELD EQUIPMENT

by momentarily closing switch S2 which discharges the condenser through a 10-ohm resistor. The condenser then accepts current through the coil of relay L1 breaking the L2 relay coil circuit which effects the opening of the potential electrode circuit. Further, the closing of the contacts of the L1 relay completes the circuit through the coil of the relay L3 closing its contacts and thereby sending a pulse of current through the ground. As the condenser becomes charged the current through the coil of L1 decreases until the clapper can not be held to the magnet. When the L1 contacts open the current through the L3 coil is interrupted to terminate the current pulse. When the clapper of L1 has returned to its normal position the current again flows through the coil of L2 closing that relay and completing the switching cycle. The cycle may be repeated at will by momentarily closing the switch S2. The duration of the pulse is controlled by the time constant of the condenser circuit and may be altered by changing its circuit resistance (selector switch S3). The time intervals of the various stages of the pulsing cycle depend upon the magnitude and duration of the current through the relays. The time intervals are, therefore, controlled by the resistors in these circuits. A heavy duty 45v "B" battery serves to power the three relay circuits. The circuit constants employed provided an energizing current pulse time which was approximately 1.45 seconds. The time interval between the opening of the current switch and the closing of the potential switch (delay time) varied in length from 12 milliseconds to 50 milliseconds with the average, for ten or more observations, of about 25 milliseconds. The variations found in the closing time of the potential switch is one of the undesirable features which should be removed in any redesign of the equipment.

It has been shown (Part B-4) that a knowledge of the apparent resistivity is required in conjunction with the induced polarization data. In order to make the resistivity measurements the ohmic potential must be measured while the energizing current flows. Since the pulsing mechanism was designed to avoid closing the potential circuit during the current pulse a toggle switch S7 had to be used to shunt the current relay contacts. With the shunting switch S7 and the reversing switch S8 current could be delivered to the ground in either direction which enabled records of the ohmic potential and the current to be obtained simultaneously. From these measurements the so-called dc apparent resistivity is computed.

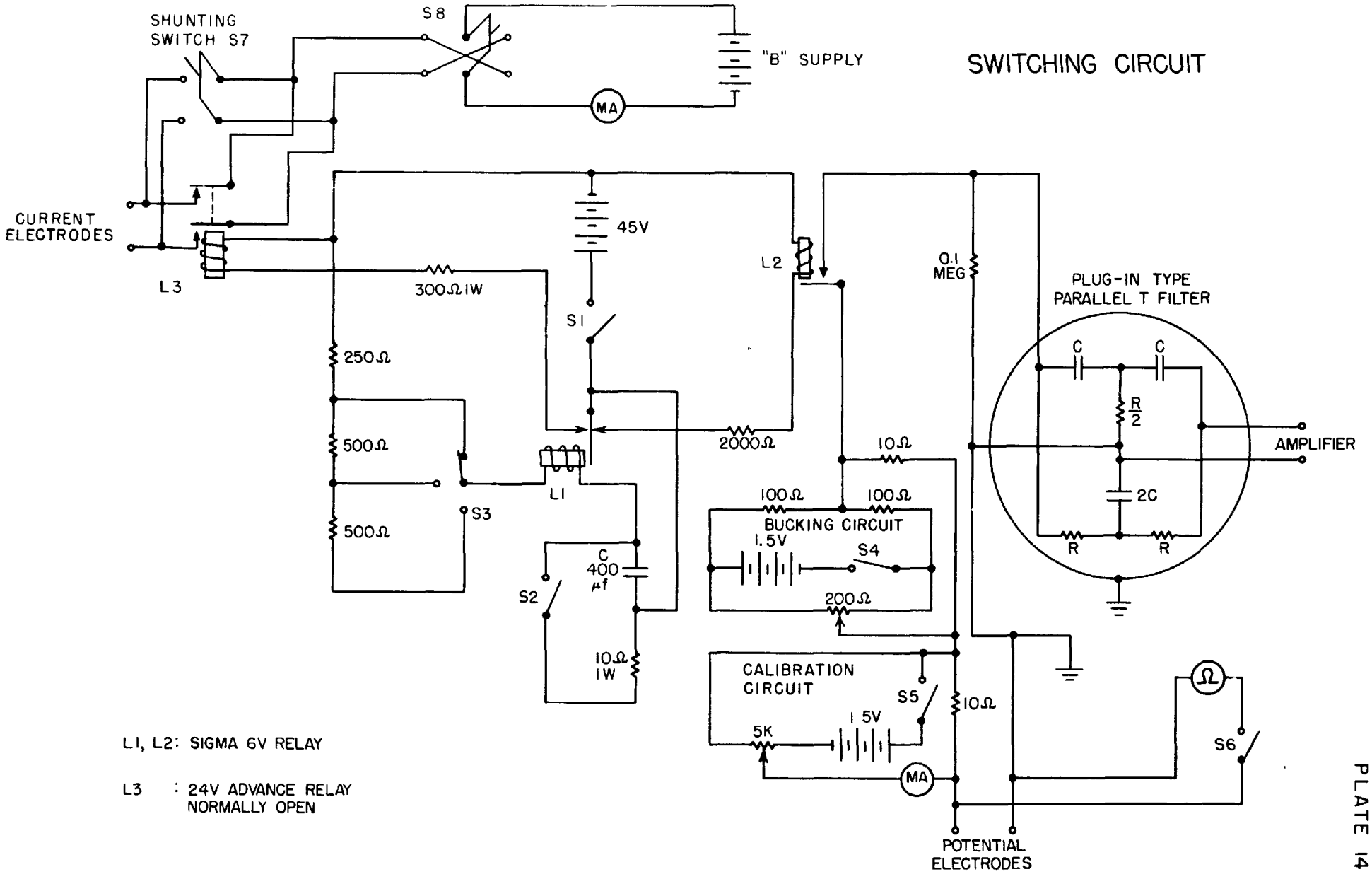
SWITCHING CIRCUIT
SHUNTING SWITCH S7
S8
"B" SUPPLY
MA
CURRENT ELECTRODES
L3
300Ω 1W
45V
S1
250Ω
500Ω
500Ω
S3
L1
L2
0.1 MEG
2000Ω
10Ω
PLUG-IN TYPE PARALLEL T FILTER
C
C
R/2
2C
R
R
AMPLIFIER
100Ω
100Ω
BUCKING CIRCUIT
1.5V
S4
200Ω
S2
C 400 μf
10Ω 1W
CALIBRATION CIRCUIT
S5
10Ω
1.5V
5K
MA
Ω
S6
POTENTIAL ELECTRODES
L1, L2: SIGMA 6V RELAY
L3 : 24V ADVANCE RELAY NORMALLY OPEN
PLATE 14

The recording equipment employed was a commercially available Brush dc amplifier and magnetic pen-motor recorder. The 3 inch pen is driven by a D'Arsonval type galvanometer element which moves in the field of a permanent magnet. The amplifier and recorder combined have an essentially flat frequency response from zero to 100 cps. The amplifier always operates at its maximum gain which is about 1000. Sensitivity control is accomplished by a potential divider at the grid of the input stage. It is arranged to divide incoming signals into ranges which are multiples of 10 and further permits continuous control within each range. The power required for the amplifier and recorder combined is 185 watts at 110v, 60 cps. A large size 500-watt gasoline driven ac generator was used in spite of its weight because the regulation of smaller units was poor, which resulted in a considerable drift of the pen.

The input impedance of the amplifier is 10 megohms which is safely higher than the maximum (5000 ohms) potential electrode resistance tolerated. Because of the high input impedance of the amplifier, difficulties were encountered whenever the input circuit was opened. The grid of the first tube alternately "looked" into very low and very high impedances. To combat this a 0.1 megohm resistor was placed across the input to the amplifier shielding it from the action of the input switch but not without the loss of some signal. Very early in the field measurements it was discovered that on occasion man-made disturbances were of sufficient amplitude to mask the polarization effect. In the vicinity of Beltsville, Maryland an electrified railroad two and one half miles away was the source of 25 cps background which at times produced potential gradients as large as a 30 μv/meter. The 60 cps power lines were a constant source of interference. The magnitude of the disturbances depended upon the proximity to the power line, the resistance of the potential electrodes and their separation. A filter was used to minimize these spurious potentials. The predominant background varied in frequency from one locality to another and, therefore, several different filters were required. Connections were provided ahead of the amplifier for plug-in type filters. Resistance-capacitance filters of the "parallel-T" type (shown schematically on the drawing of the switching circuit) were used. The 60 cps rejector was required more often than any other and rarely was there an area where no filter was needed. A typical attenuation curve for one of these filters is shown in Figure 7. The use of the filter further decreased the signal arriving at the amplifier. The insertion losses introduced by the

0.1-megohm shielding resister and the filter reduced the incoming signal about 50%. However, the distortion introduced by the filters was found to be insignificant for exponentially decaying transients whose time constants were comparable to those of the IP signals.

A calibration circuit, similar to that described in Part B-1 was used to inject known dc voltages into the potential circuit. A similar circuit was employed to supply a bucking voltage to neutralize any steady potentials encountered in the earth. The ohmmeter across the input circuit was used to check the resistance of the potential electrodes for each set-up. However, the readings were used only to avoid instrumentation difficulties.

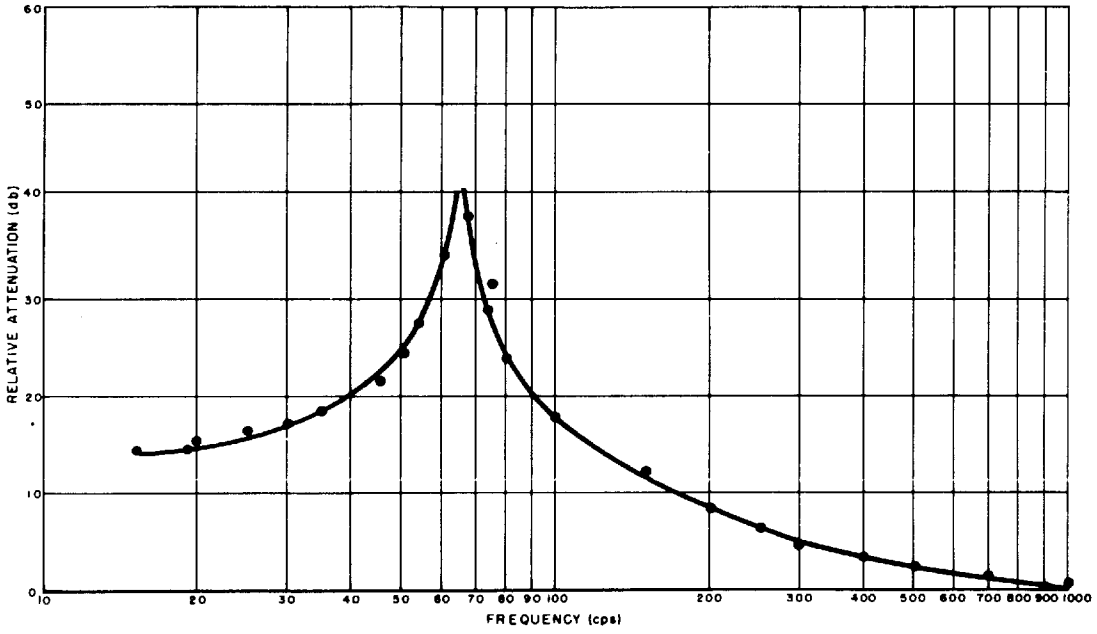

FIG. 7

It was not always possible to determine, from the recorder tape showing the IP signal, when the current pulse had ended. A knowledge of when the current pulse ended was required because of the variation of the closing time of the potential circuit relay 12. The Brush recorder had an additional pen which was used to register the onset and termination of the current pulse.

The current electrodes were sheet iron hemispheres, 6 inches in diameter and filled with lead to provide a good pressure contact to the ground. The hemispherical form was chosen to avoid the possibility of forming long dipoles by differential polarization (see Part B-4)

of the power electrode itself. It proved, however, to be an unnecessary precaution whenever the electrode separation was 10 ft. or greater. Short iron rods 6 inches long and 7/8 inch in diameter were used for the longer separations and the results obtained were the same as those obtained with the hemispheres. The potential electrodes were the standard Cu/CuSO4 type except that shielding from the direct action of the energizing current, a precaution mentioned earlier, was provided. A special electrode housing, Figure 8, consisting of a cylindrical plastic tube with a plastic well-point nose was designed. The Cu electrode was always shielded from the energizing current even when the electrode housing had to be driven into the ground to reach moist soil. Glazed pots have also been used successfully when placed flat upon the earth. The glaze should be ground off the bottom of the pot only and the electrode should extend just a short distance into the cup. The high inherent resistance of the porous pot with such a small unglazed area is undesirable but this electrode is extremely convenient.

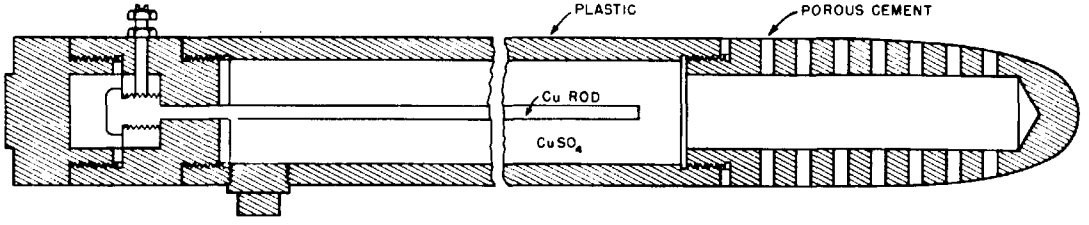

FIG. 8

The apparatus which has been described was designed originally as preliminary equipment. It was tested on an abandoned airfield located on the properties of the U. S. Agricultural Research Center, Beltsville, Maryland. A detailed knowledge of the geology of the area was not available. The testing, therefore, was confined to the operational characteristics of the equipment. After the equipment had performed satisfactorily for some time it was decided that further testing of the equipment required a region where the geology was better known. The problem of locating a suitable area, where there existed sharp boundaries separating zones of good electrical conducting minerals from poor conductors, was turned over to the U. S. Geological Survey of the Department of Interior. A list of more than ten possible areas in Fairfax County, Virginia was immediately supplied. Only two of these were investigated.

2. Measurements Over an Amphibolite Dike

About 14 miles out of Washington, D. C. along Route 7, Fairfax County, Virginia an amphibolite (meta basalt) dike is exposed in a road cut. The dike comes up through a knoll of Wissahickon (mica schist) a little off the center of the knoll, dipping to the east at an angle of about 60° with its strike roughly N 20°E. The dike is about 50 feet wide on the north side of the road and nearly 60 feet wide on the south. The topography, other than the knoll at the road cut, fails to reveal the dike.

This dike was chosen as the object of the first investigation. Two traverses parallel to the road were made. The term traverse in all of the following work will mean a line along which measurements are made. Measurements, for which the electrode separation remains constant, made along any traverse are referred to as a run. When the electrode spacing is increased during the set of measurements with the same center maintained for all spacings, the name vertical or depth profile is used to describe the measurements. Unless otherwise indicated the distance moved along the traverse from station to station in a given run is to be taken as being equal to the electrode separation. The first run over Traverse 1 used a Wenner configuration for which the electrode separation "a" was equal to 20 feet. At each station several current pulses were delivered to the earth in each direction and the resulting IP potential was recorded. A section of recorder tape showing a typical signature is given in Plate 15. The paper speed for this record was 2.5 cm/sec. With the paper speed reduced the resistivity data was next obtained. Six dc resistivity measurements were made; the polarity being reversed between successive measurements. Fourteen stations were taken along the first traverse. For Run 2 the electrode spacing was increased to 50 feet and the first traverse was again covered. A second traverse, parallel to the first and 50 feet away was run using only a 50-foot separation.

The measurements obtained from this preliminary investigation over the dike were treated in the manner outlined in Part C-4 using Equation 2 to compute S. However, in order to bring out the effect of the various factors involved in reducing the data several preliminary curves obtained from Run 1, Traverse 1 have been plotted. In Plate 16a a comparison is made between the resis-

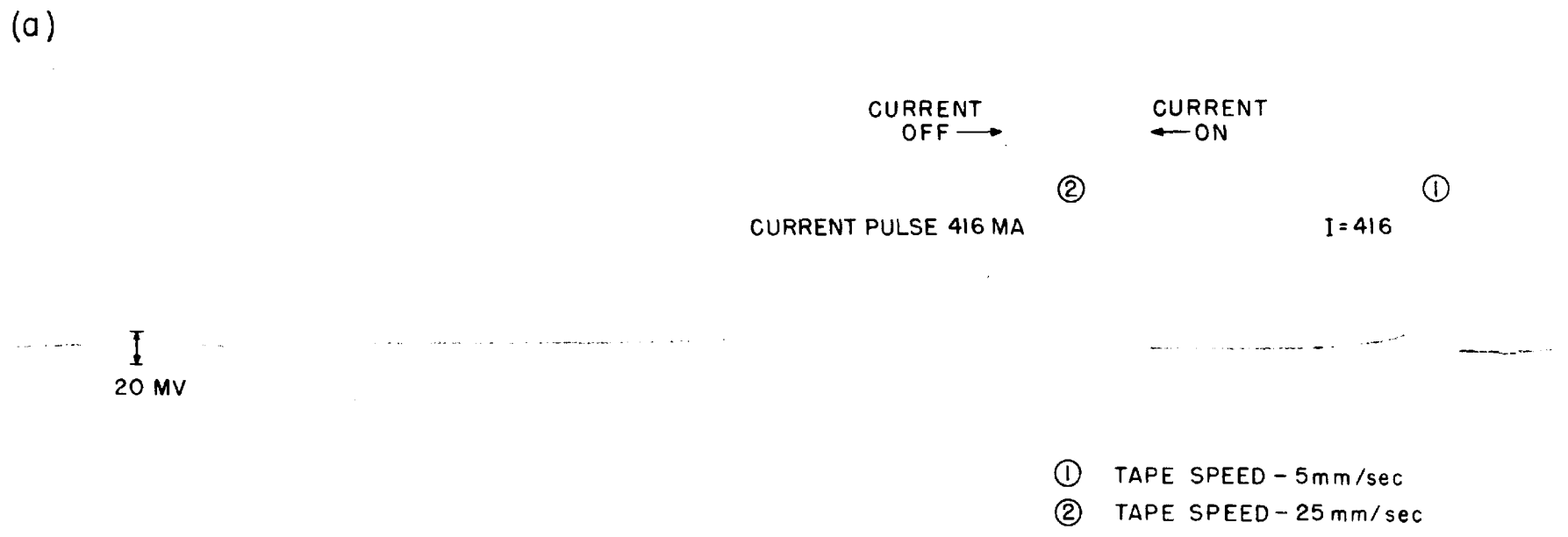

TYPICAL SIGNATURE

(a) INDUCED POLARIZATION POTENTIAL

(b) RESISTIVITY

PLATE 15

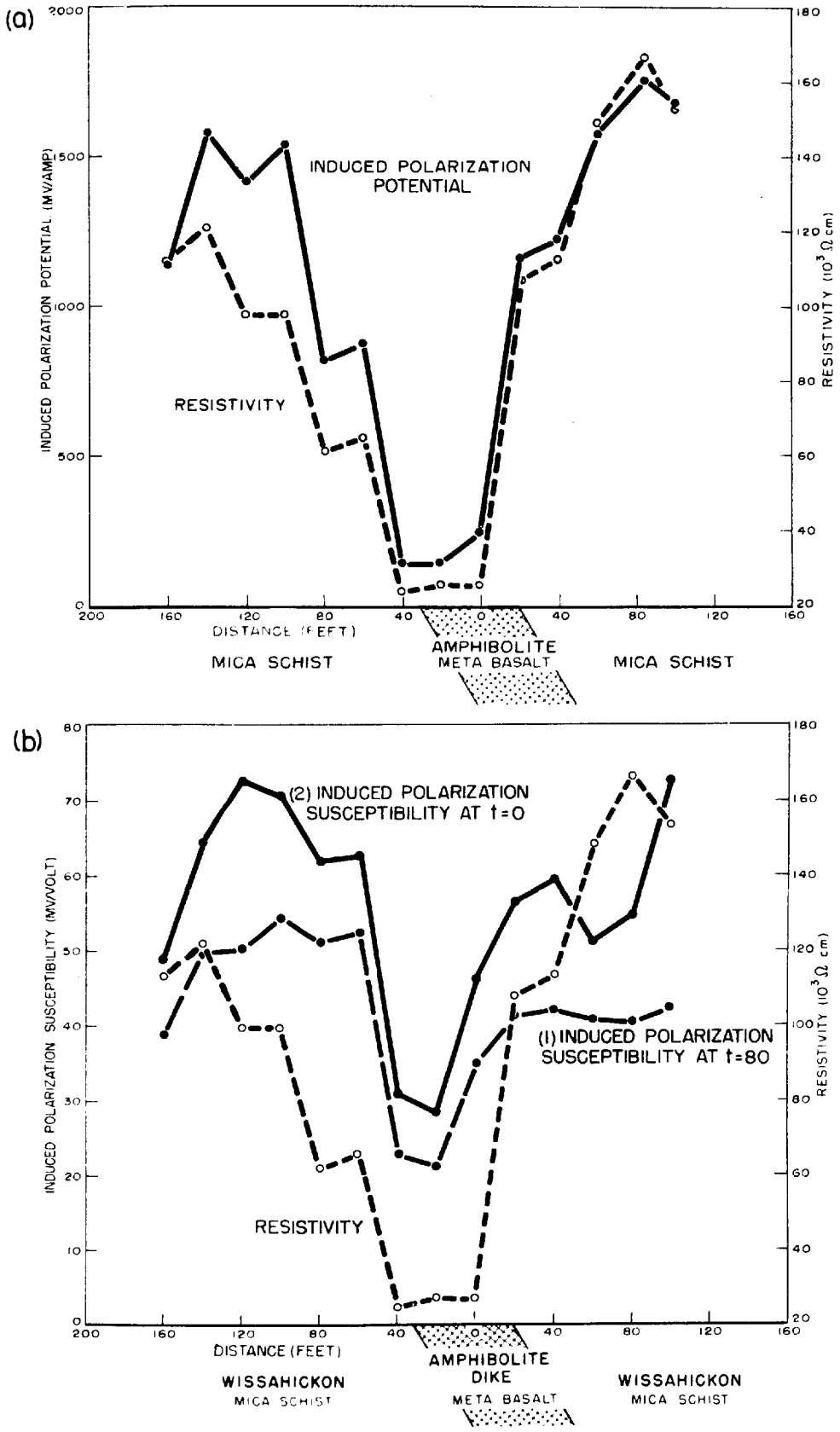

INDUCED POLARIZATION POTENTIAL AND RESISTIVITY vs DISTANCE

AMPHIBOLITE DIKE

tivity and the induced polarization potential (measured at t = 80 milliseconds and normalized for the current). Just as the theory predicts, there is good correlation between the IP potential and the resistivity. The effect of removing the resistivity factor (computing the ratio ϕ/ρ_o) is shown as Curve 1 in Plate 16b. The good correlation between the curves of induced polarization and resistivity no longer persists. Curve 2 in Plate 16b shows the effect of extrapolation of back to zero time. Comparing Curves 1 and 2 in Plate 16b it is seen that the shape of the curves, for this run, has not greatly changed because of the extrapolation process. This is not always the case. From this point on, the plotted curves are curves of the induced polarization susceptibility S computed for ϕ extrapolated back to zero. Values of S for Run 2 of Traverse 1 and Run 1 of Traverse 2 are shown with the corresponding values of resistivity on Plate 17.

It had been expected that the high polarization readings would appear over the dike. In an effort to learn more about the two rocks, a sample of the mica schist was taken from an area approximately 100 feet northwest of the dike and a sample of the dike material was taken from the center of the dike. Both samples were dug from the road cut and from holes deep enough to give fresh material. The samples were ground to pass a 100 mesh sieve and then passed over a magnetic chuck. It was surprising to find that the mica schist examined contained 3.3% magnetite whereas the amphibolite contained only 0.36%. The amount of nonmagnetic conducting mineral which may have been present is not known. The dike material contained a large amount of moisture and it was hygroscopic. It had to be dried repeatedly in order to pass it through the sieve. An electron diffraction pattern of the dike material[21] matched that given for Nontronite ($FeOSiO_2 \cdot 2H_2O$). It was concluded that the low resistivity of the dike material was due to electrolytic conduction rather than electronic conduction. This is reasonable in view of the large amount of moisture contained in it because of its hygroscopic nature. (The zone under measurement was well above the water table). The higher polarization potentials measured over the mica schist are interpreted to be due to the higher concentration of magnetite. The results of this preliminary investigation were reviewed with members of the Geophysics Section of the USGS. The opinion of the group was that more supporting data were required. As a result two more traverses, parallel

INDUCED POLARIZATION SURVEY
AMPHIBOLITE DIKE
HORIZONTAL TRAVERSE
ELECTRODE SEPARATION 50 FT

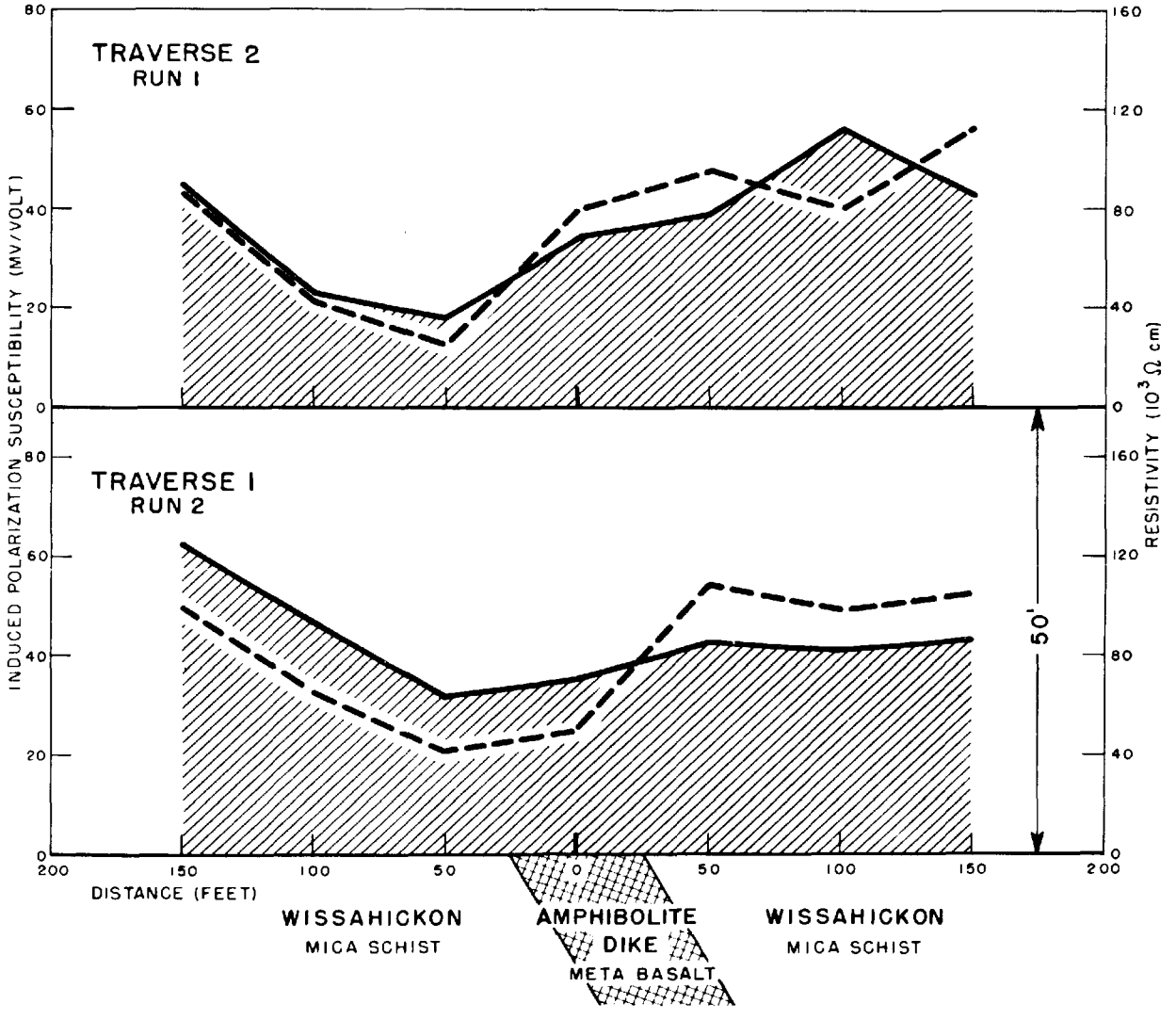

to the first but displaced to the north 175 feet and 350 feet respectively were run. The electrode separation used was again 20 feet. In addition to these induced polarization data, all the traverses were remeasured for resistivity, employing the Gish-Rooney system, and vertical magnetic field readings were taken over the first three traverses. The resistivity as measured by the Gish-Rooney and the dc methods were in good agreement. All of the resistivity values plotted for the amphibolite survey are those obtained by the Gish-Rooney system. The magnetometer data for the first three traverses have been plotted in Plate 18. Plate 19 is arranged to display the general area of the survey, the portion of the dike which is visible as well as the induced polarization susceptibility and resistivity data for Traverses 1 (Run 1), 3 and 4.

The induced polarization susceptibility and the resistivity both fail to definitely reveal the existence of the dike beyond the second traverse. The magnetometer data do not indicate any large magnetic anomalies other than the one on Traverse 1 which occurs off the dike on its northwest side. These observations force the conclusion that the dike tapers out and disappears on the north side of the road. Its existence beyond Traverse 2 is questionable in terms of the results of any of the three methods. Unfortunately, the magnetometer data for Traverse 4 have not been obtained. One physical feature of the area is brought to the support of this conclusion. The dike is wider where it is exposed on the south side of the road cut than on the north side. If straight lines are drawn across the road lining up with the exposed edges of the dike they converge in the neighborhood of the third traverse; i.e., the one 175 feet north of the first traverse.

The conclusions drawn from the amphibolite survey are: 1) that disseminated conducting minerals may yield rather large values of polarization susceptibilities and 2) that bodies which are good conductors by virtue of the electrolyte present rather than the conducting minerals are not polarizable.

3. Measurements Across a Manassas Sandstone and Wissahickon Fault

The correlation of the polarization susceptibility with the magnetite analysis obtained on Traverse 1 suggested that the method might be used to detect faults

VERTICAL MAGNETIC FIELD SURVEY
AMPHIBOLITE DIKE

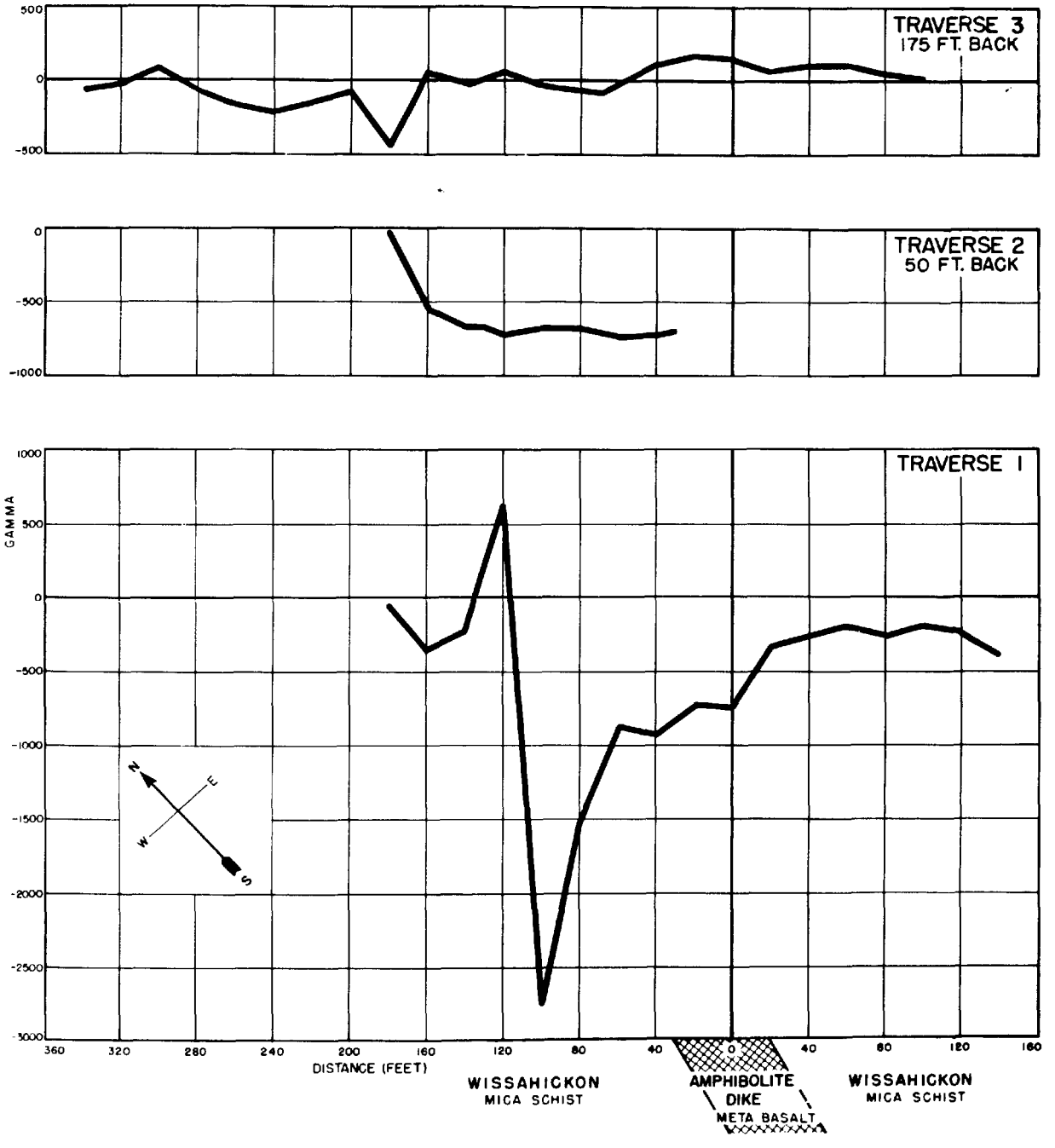

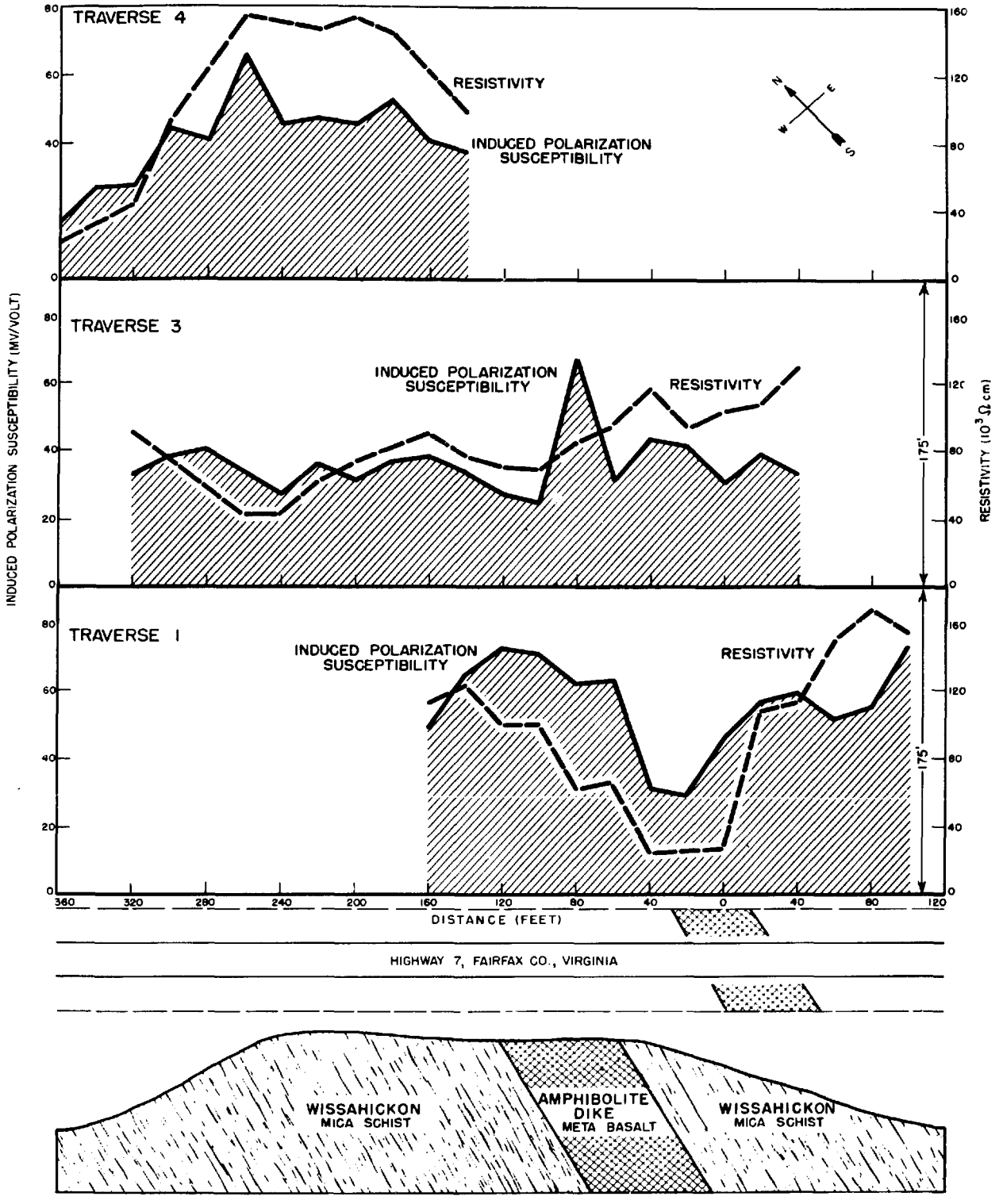

INDUCED POLARIZATION SURVEY

AMPHIBOLITE DIKE

IN WISSAHICKON

ALONG HIGHWAY 7, FAIRFAX CO., VIRGINIA

where the change in resistivity is not pronounced and where a change in the amount of conducting minerals occurs. It was believed that a fault of this type exists near Manassas, Virginia where the Missahickon, known to contain variable amounts of magnetite, has pushed up against the Manassas Sandstone. The fault (see Plate 20) is exposed along the Buck Hall road about 1 1/2 miles east of Manassas. (Plate 20 is a composition of a portion of the U. S. Army Engineers map of the Quantico Quadrangle and a portion of the USGS map of the Fairfax Quadrangle. The two maps did not quite coincide, therefore, several roads have been "faked" in to provide continuity. The line of the fault was located by Hilton.[22]) The area selected for the measurements was a gently sloping corn field. Induced polarization and resistivity measurements were made along three traverses roughly perpendicular to the fault and each 200 feet apart. A Wenner system of electrodes in which "a" was equal to 20 feet was again employed. Samples of earth were taken from the road cut at 25, 50, 75, 100 and 150 feet in each direction from the exposed fault. The material gathered, approximately 5 pounds per sample, was ground to pass a 100 mesh sieve. The magnetic materials were separated from all but the sandstone sample at 75 feet which met with an accident and was completely lost.

The measured values of the IP susceptibility, the resistivity in ohm-cm and the results of the magnetic mineral analysis are shown plotted in Plate 21. The resistivity data show a definite correlation from traverse to traverse. The change from low to high resistivity is along the probable strike. There is little correlation from traverse to traverse in the IP susceptibility curves. One relative high is maintained in the center of the three traverses. The very high peak of Traverse 1 diminishes until at Traverse 3 it has disappeared whereas a slight hint of a peak on the other side of the center of Traverse 1 grows as one progresses back to Traverse 3. From the mineral analysis it must be concluded that there is more variation in the magnetic mineral content within either the sandstone or mica schist than there is from one to the other. The magnetic materials which entered into the determination of the percentages shown contained a substantial amount of weakly magnetic mineral which was not identified.

It is concluded from this survey that the IP susceptibility measurements do not locate this fault because a sufficient change in the conducting mineral

PLATE 20

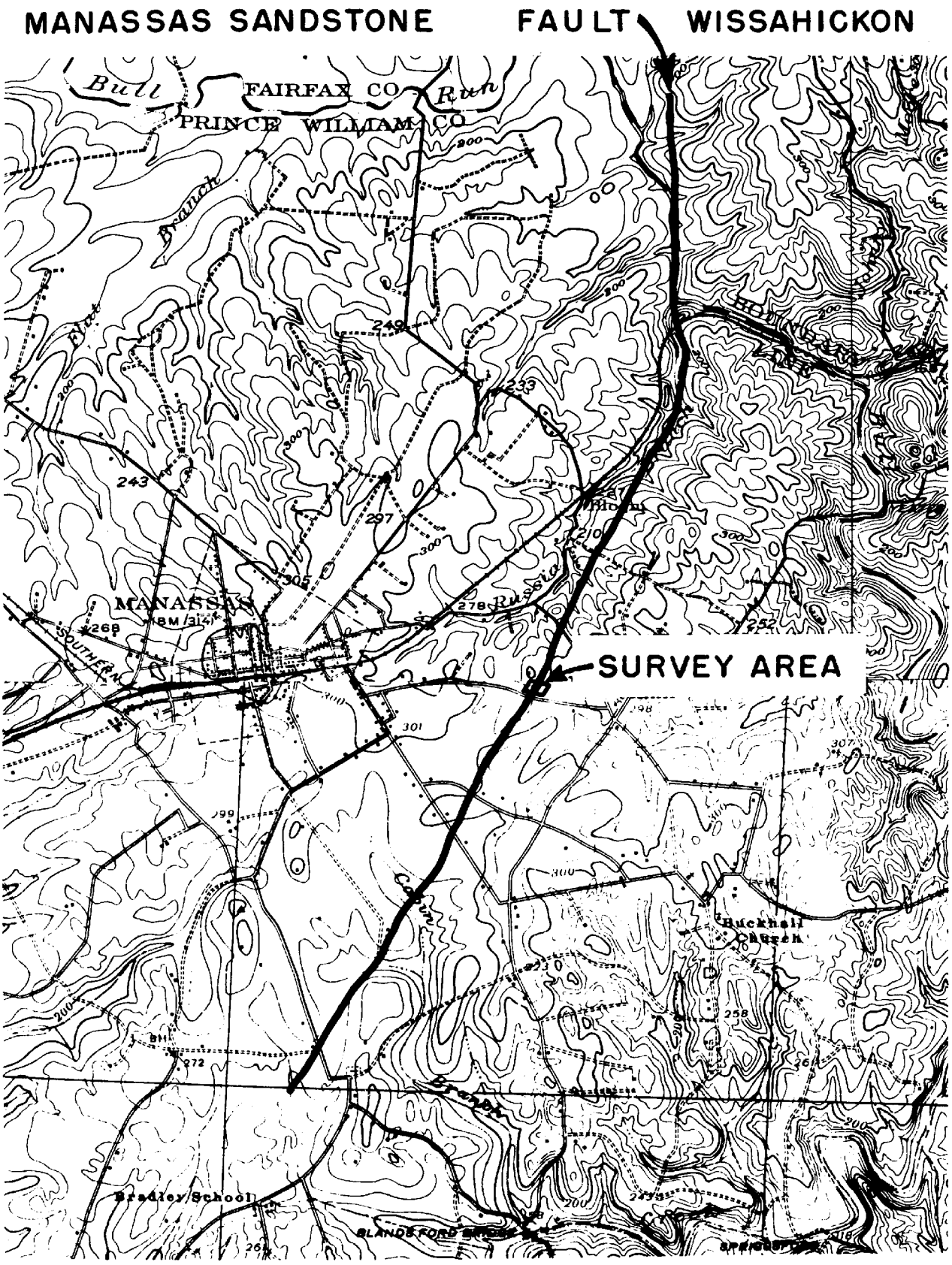
MANASSAS SANDSTONE
FAULT
WISSAHICKON
Bull Run
FAIRFAX CO.
PRINCE WILLIAM CO.
Broad Run
MANASSAS
BM 314
SURVEY AREA
Russia
Bradley School
Buckhall Church
Broad Run

PLATE 21

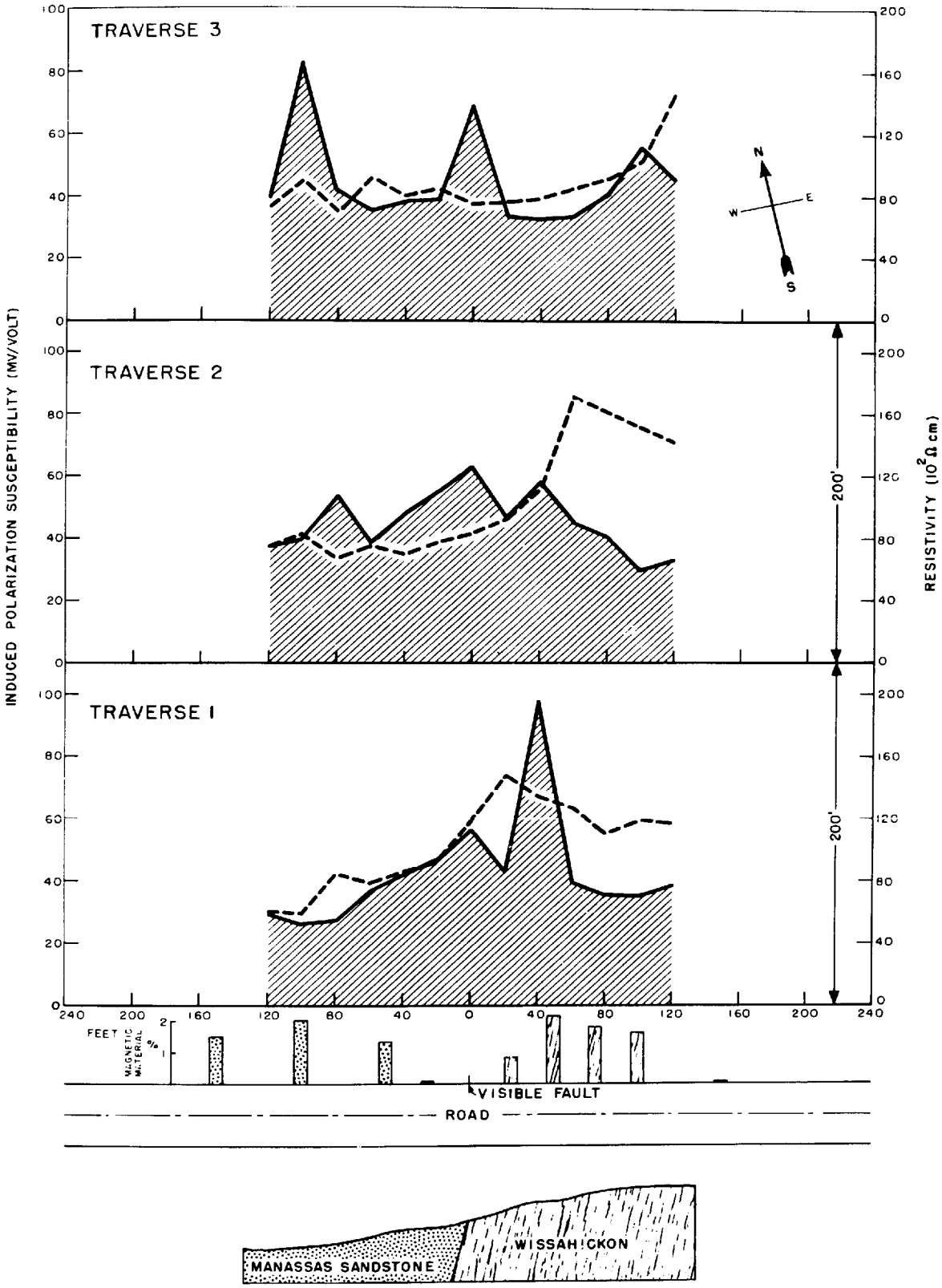

INDUCED POLARIZATION SURVEY

MANASSAS SANDSTONE-WISSAHICKON FAULT

MANASSAS, VIRGINIA

content from one formation to the other does not exist. This conclusion is supported by the magnetic mineral analysis.

4. Measurements Over a Pyrrhotite Outcrop

The results obtained from the amphibolite dike and the Manassas Sandstone surveys are inconclusive and confused because of a lack of knowledge concerning the variation in the concentration of disseminated minerals. In order to avoid this confusion, measurements should be made over an area where the mineralized zone is definitely known to exist in quantities which approach those of an ore body. Information about two ore bodies, not far from Washington, D. C., was obtained through USGS. The first of these is described as the Gossan Lead[23], Carroll County, Virginia. Plate 22 is a photograph of a map (furnished by USGS) showing the Gossan Lead which extends for 17 miles from near Galax, Virginia to the vicinity of Sylvatus, Virginia. The Gossan Lead consists of a series of elongated sulphide ore bodies of which the primary ore is pyrrhotite. The mineralized zone is incased in the pre-Cambrian Lynchburg gneiss. The ore in the Cranberry segment outcrops (see [1] in Plate 22) along U. S. Highway 52 near Hillsville, Virginia for a distance of approximately 200 feet. The background in the photograph of the instruments in Plates 12A and 12B (supplied by H. C. Spicer) is the outcropped pyrrhotite along U. S. Highway 52. The "float" found along the outcrop was rather massive pyrrhotite. (When a piece of ore with freshly exposed faces was connected to the leads of an ohmmeter, the meter read zero on the 1-ohm scale).

Two traverses were run across this outcrop; one along the shoulder of the road and the second one parallel to the first, 20 feet NE of the road and about 12 feet above the road level. The second traverse ran only across the west contact of the mineralized zone because the hillside was steep, covered with the dump of an old pit and heavily overgrown. A Wenner system for which "a" was 20 feet was used to obtain the data of Traverse 1 Run 1 and Traverse 2 Run 1. The results of these two runs, plotted in Plate 23, show the induced polarization susceptibility increasing to a maximum as the contact is approached from the side of the country rock. Once the contact is crossed the polarization susceptibility appears to fall to zero. However, it is really the induced polarization potential which has fallen to zero (or at least below the lower limit of

UNITED STATES DEPARTMENT OF THE INTERIOR
GEOLOGICAL SURVEY

STRATEGIC MINERALS INVESTIGATIONS
PRELIMINARY MAPS

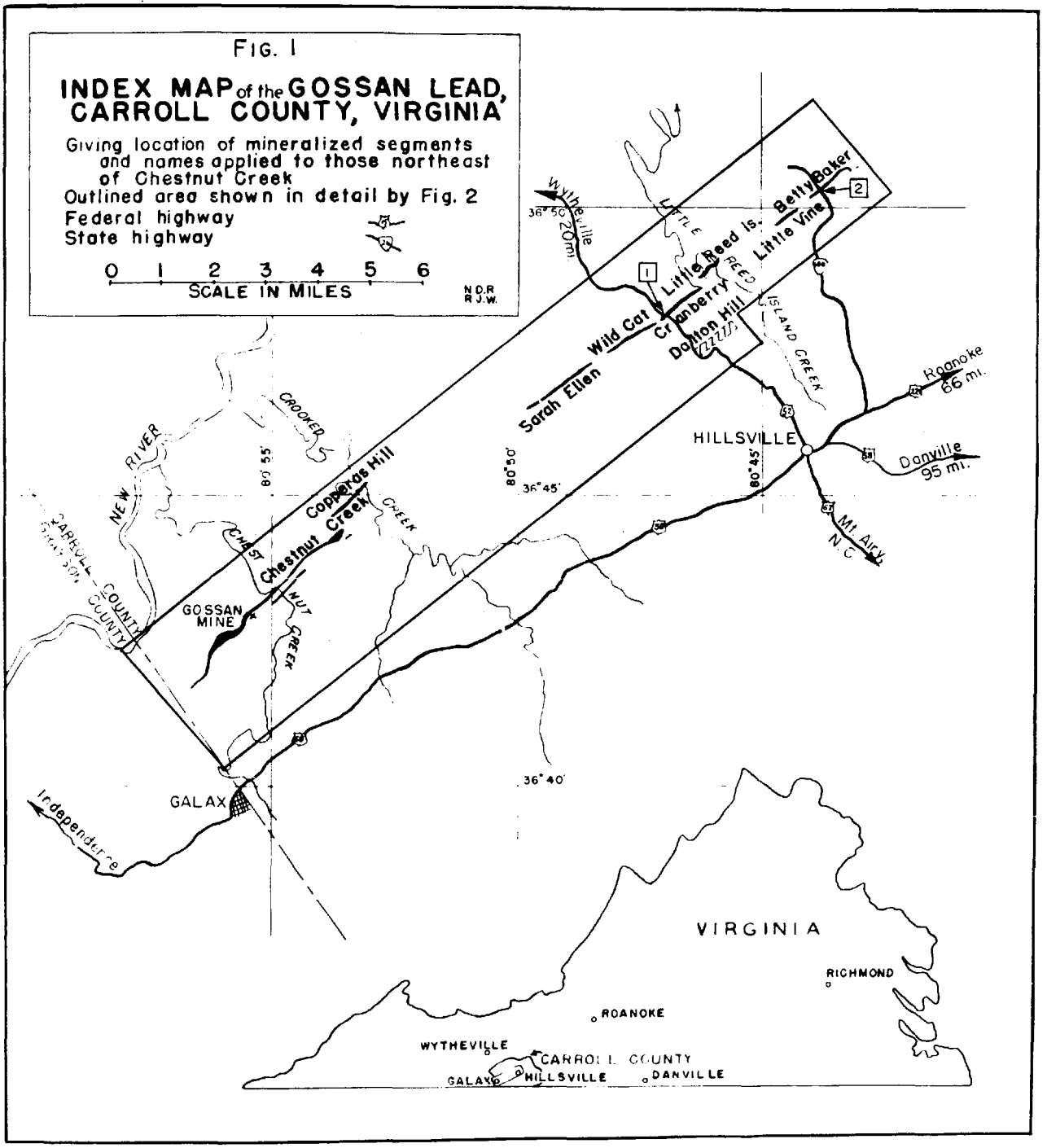

PLATE 23

INDUCED POLARIZATION SURVEY

PYRRHOTITE

CRANBERRY SEGMENT

ALONG U.S. HIGHWAY 52, HILLSVILLE, VIRGINIA

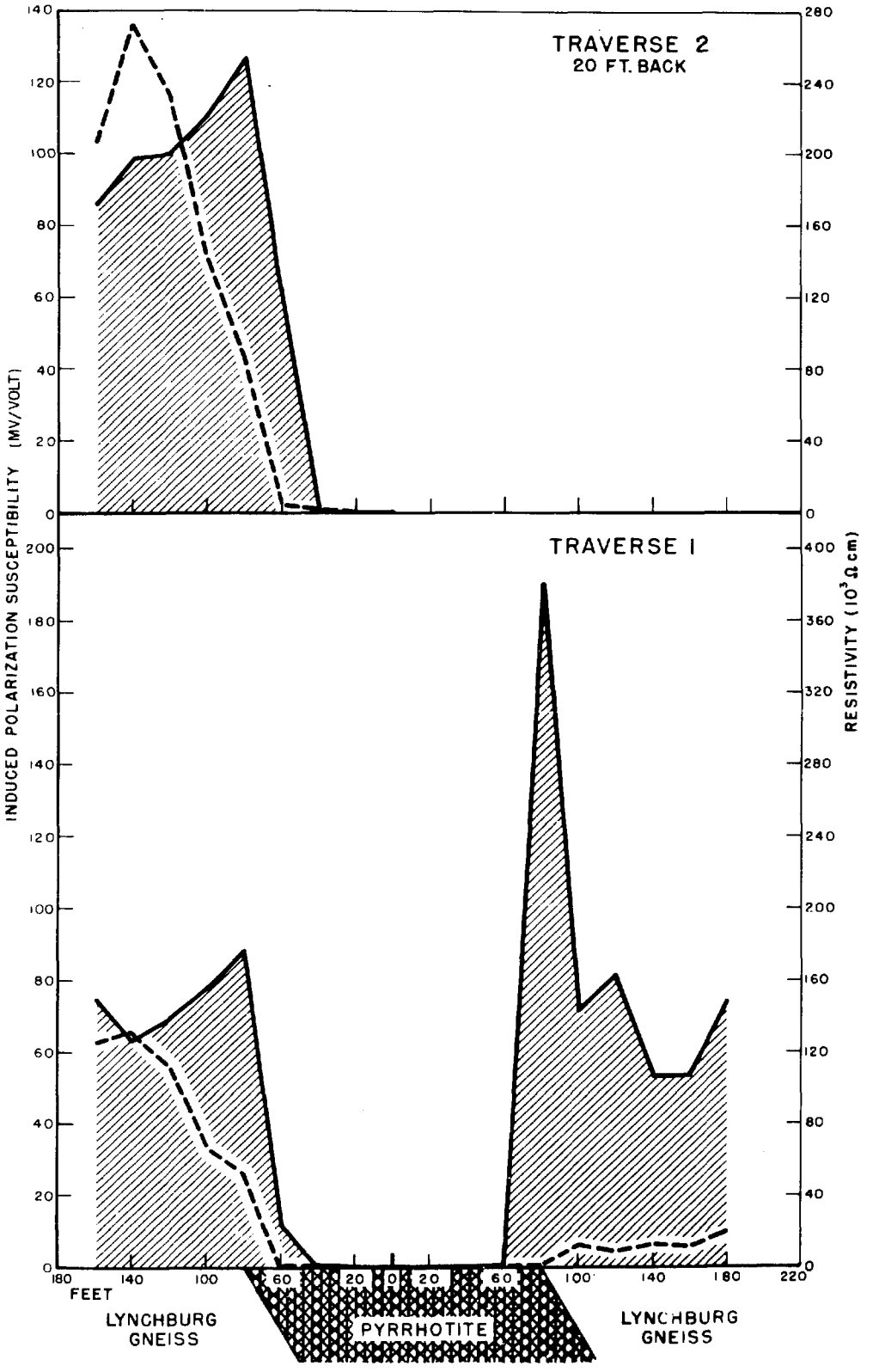

the instrument sensitivity). The fact that this potential falls to zero should make the susceptibility also zero except for the fact that the ohmic potential also falls to zero over the pyrrhotite zone. The susceptibility is the ratio of these two potentials and is, therefore, indeterminate over the mineralized zone. The zero value of the induced polarization potential is in excellent agreement with the established result (Part B-10) which states that the polarization potential is proportional to the potential gradient. Here the current was increased to 1.0 ampere, the separation of the potential electrodes was 20 feet but the resistivity was zero as far as the field instruments were concerned and, therefore, the potential gradient and consequently the induced polarization potential remained zero.

It has long been known that pyrrhotite displays self ("spontaneous") polarization and because Schlumberger[3] stated that the "spontaneous" polarization of an ore body would conceal the induced polarization potential, measurements of the self potential were made. The reference electrode was located 220 feet west of the center of the ore body and the potential difference between it and the probe electrode was recorded as the probe electrode was moved across the ore body in 20 foot intervals. These data are plotted in Plate 24 along with readings of the vertical magnetic field measurements taken along the same traverse. The ore body is definitely spontaneously polarized but the self potentials do not influence the induced polarization potential. The energizing current was pulsed in both directions but no change in the magnitude of the induced polarization potential was observed. It was necessary, however, to use large bucking potentials to keep the recorder pen in the center of the paper. There is a self-potential "well" at each interface of the pyrrhotite and an additional one just west of the center of the ore. An inclusion of mica schist is visible in the road cut which corresponds in position to the extra "well" in the self potential curve. A small increase in both the induced polarization potential and the resistivity (both too small to appear in Plate 23) were observed at the same location. The extent of the inclusion is not known.

A vertical profile was run over Traverse 1 starting with an electrode separation of 400 feet and decreasing the separation 100 feet at a time until the potential electrodes were 100 feet apart. The center of the

VERTICAL MAGNETIC FIELD AND SELF POTENTIAL MEASUREMENTS

PYRRHOTITE

CRANBERRY SEGMENT

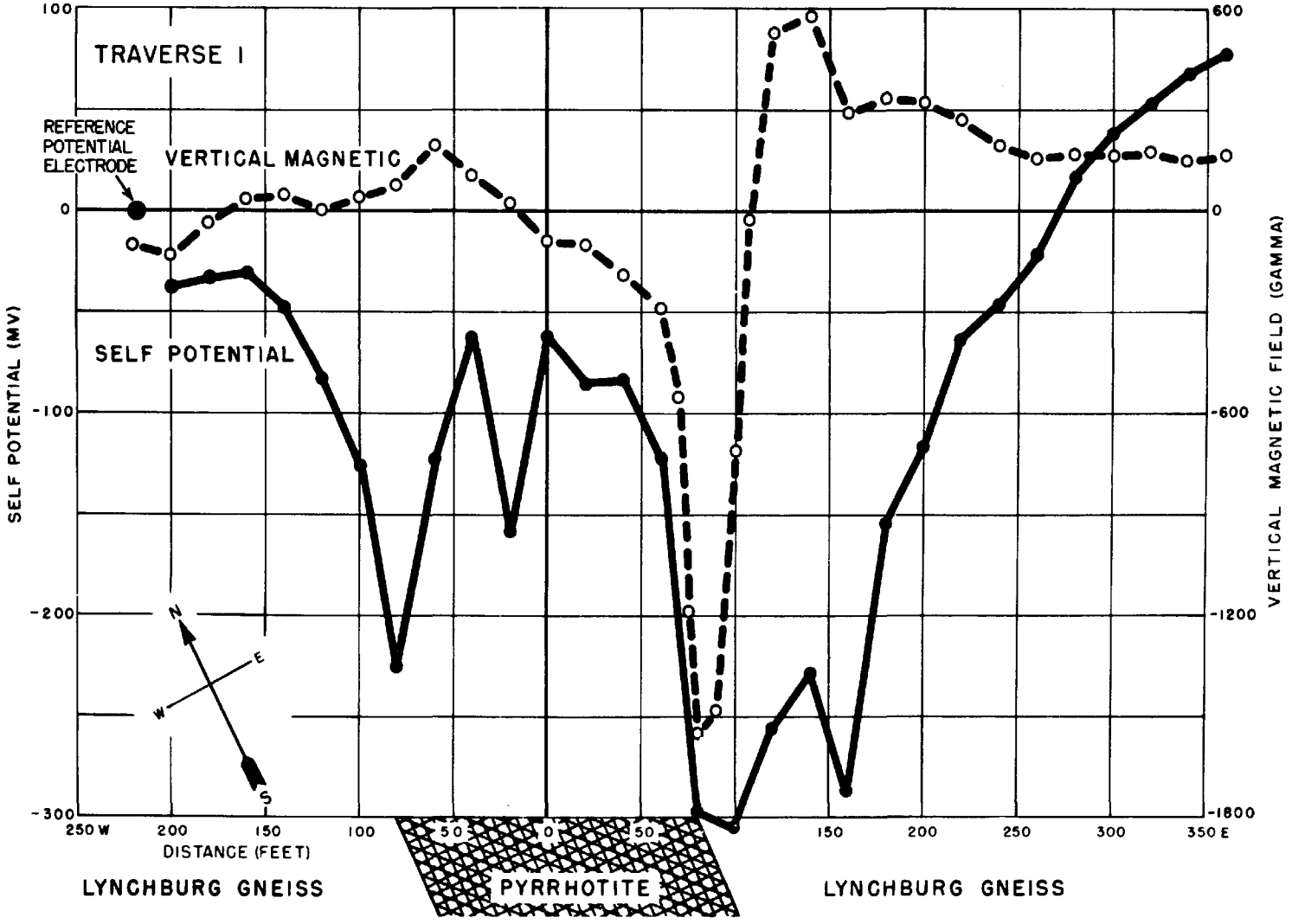

PLATE 24

system was the center of the ore body. Thus when the potential electrodes were 100 feet apart they were inside the zone whereas at 200 feet they were outside. The results, shown in Plate 25b, are consistent with those already obtained. Inside of the zone the resistivity is zero and so is the IP potential and outside the zone they are both greater than zero. Unfortunately, the measurements were not extended far enough outward to determine the maximum susceptibility value.

Several other electrode configurations were tried in an effort to obtain a measurable polarization signal when the electrodes were all within the mineralized zone but the resistivity was just too low. The potential electrodes were maintained at a 20 foot separation from the current electrodes (either on the inside or the outside of the current electrodes) and the system was expanded. As long as the electrodes were sufficiently removed from the mineralized zone so that a potential gradient was established (resistivity no longer zero) a polarization signal was measured. Nine combinations of the four electrodes are shown in Plate 25a along with the IP susceptibility and resistivity measured at each position.

The pyrrhotite outcrop in the Cranberry segment had little or no cover along either Traverse 1 or 2. The potential electrodes were in direct contact with the ore and since it was such a good conductor the potential across the electrodes remained zero for all applied currents. It was decided to investigate another portion of the Gossan Lead where the ore was sufficiently massive to provide low resistivity but where the cover was rather thick. A site, indicated by [2] in Plate 22, near the outcrop of the Betty Baker mine was selected. An expanding electrode system was employed which had its center located approximately 350 feet N 65° E of DDH 1 (Bureau of Mines Project 2902). The line of electrodes ran N 70° E and the strike of the Betty Baker was approximately N 42° E. The vertical depth of the ore of DDH 1 is from 196 feet to 207.8 feet, which gives a thickness of ore of 11.8 feet. The dip in this area is about 47°. It was originally planned that the line of electrodes would parallel the strike. However, because the area is heavily overgrown the electrode line had to make an angle of about 39° to the strike. This meant that at one end of the line both the current and potential electrodes were nearer to the ore than the electrodes at the other end were and the situation became worse as the electrode array was expanded. Because

THE EFFECT OF ELECTRODE CONFIGURATION ON INDUCED POLARIZATION SUSCEPTIBILITY

PYRRHOTITE CRANBERRY SEGMENT

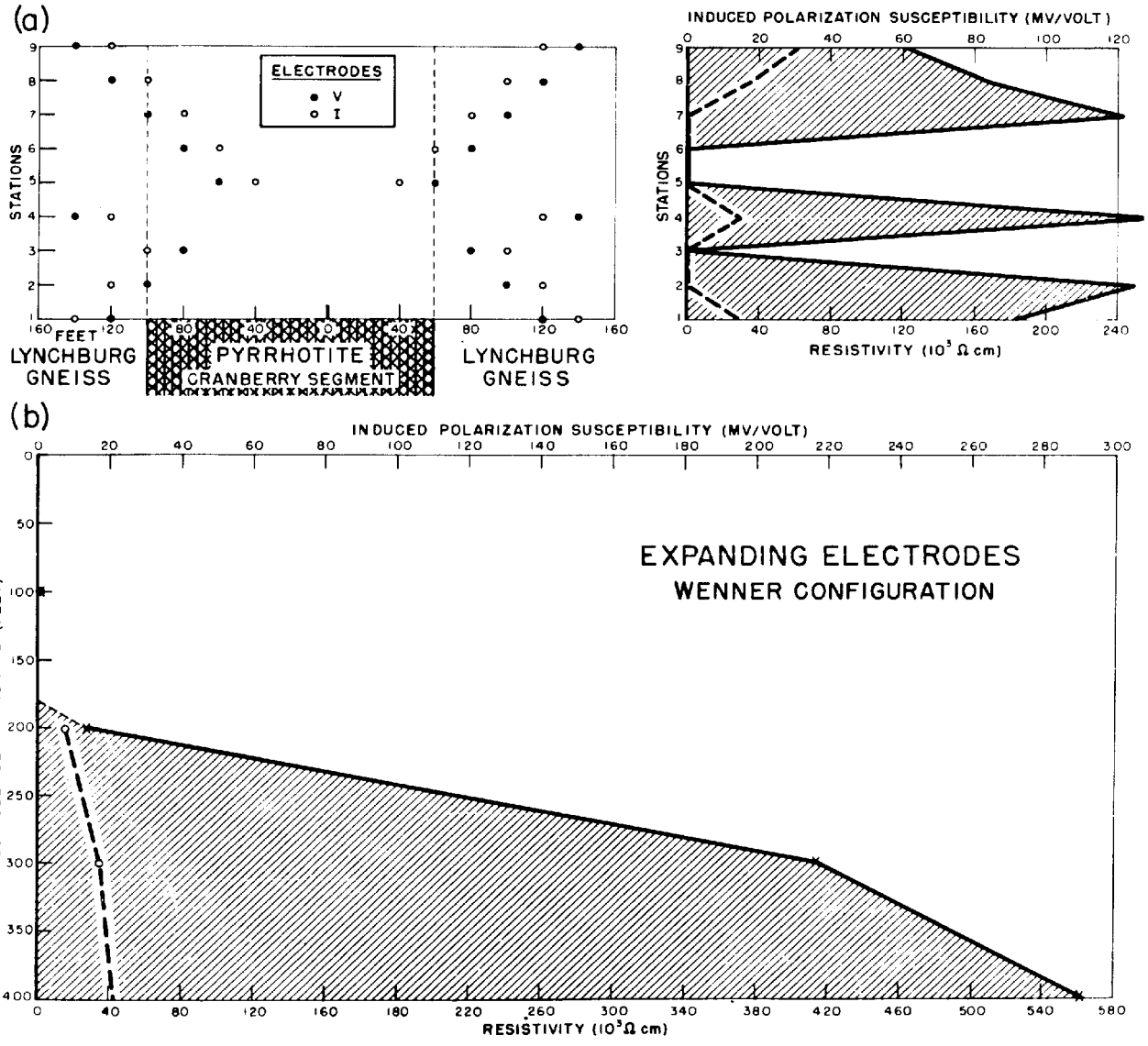

the several electrodes changed their positions with respect to the ore this type of a survey may not be used to discover experimentally the relation between the electrode separation and the depth of influence. The data obtained from the vertical profile over the Betty Baker mine has been portrayed in the usual manner in Plate 26. There appears to be a one-to one correlation between the depth to the ore and the electrode separation. At the 150 foot separation there is a sharp break in the curve. The vertical depth to the ore is 196 feet which places the shortest distance from the surface to the ore at about 150 feet. An appreciable amount of current will flow through the ore body for electrode separations greater than 150 feet. However, the break in the curve indicates a decrease in the polarization susceptibility. As an explanation of this inverse effect it is suggested that the overburden is highly mineralized and, as it can be seen in Plate 26, has a high resistivity. Therefore, a large potential gradient is developed and all minerals contained in the overburden which have resistivities of 20 x 10^3 ohm-cm or less will be polarized. As a result, a high value of induced polarization susceptibility is measured. As the electrode array is expanded, more current reaches the ore body which, because of its low resistivity, robs the upper region of its share of the current and decreases the potential gradient. The saturation effect prevents the ore from becoming as highly polarized as the disseminated mineral which is also closer to the surface and as a result the polarization susceptibility decreases. As the electrode system expands still further, a larger volume of the overburden is traversed by the current which again increases the polarization susceptibility.

It was mentioned earlier (Part D-2) that the extrapolation back to zero time occasionally introduced changes in the polarization susceptibility curve. The curve obtained for values of ϕ at 80 milliseconds is compared in Plate 26 to the curve for ϕ_o and the changes introduced are apparent.

5. Measurements Over a Magnetite Ore Body

Information about a second ore body was obtained through USGS. The ore, wedged between a limestone and diabase contact, was one of the many small magnetite deposits found in Lebanon County, Pennsylvania. Fortunately, the area had been explored and the data from six diamond-drill holes (DDH) were available. The projection onto the horizontal plane of the probable limit of

VERTICAL PROFILE
BETTY BAKER MINE

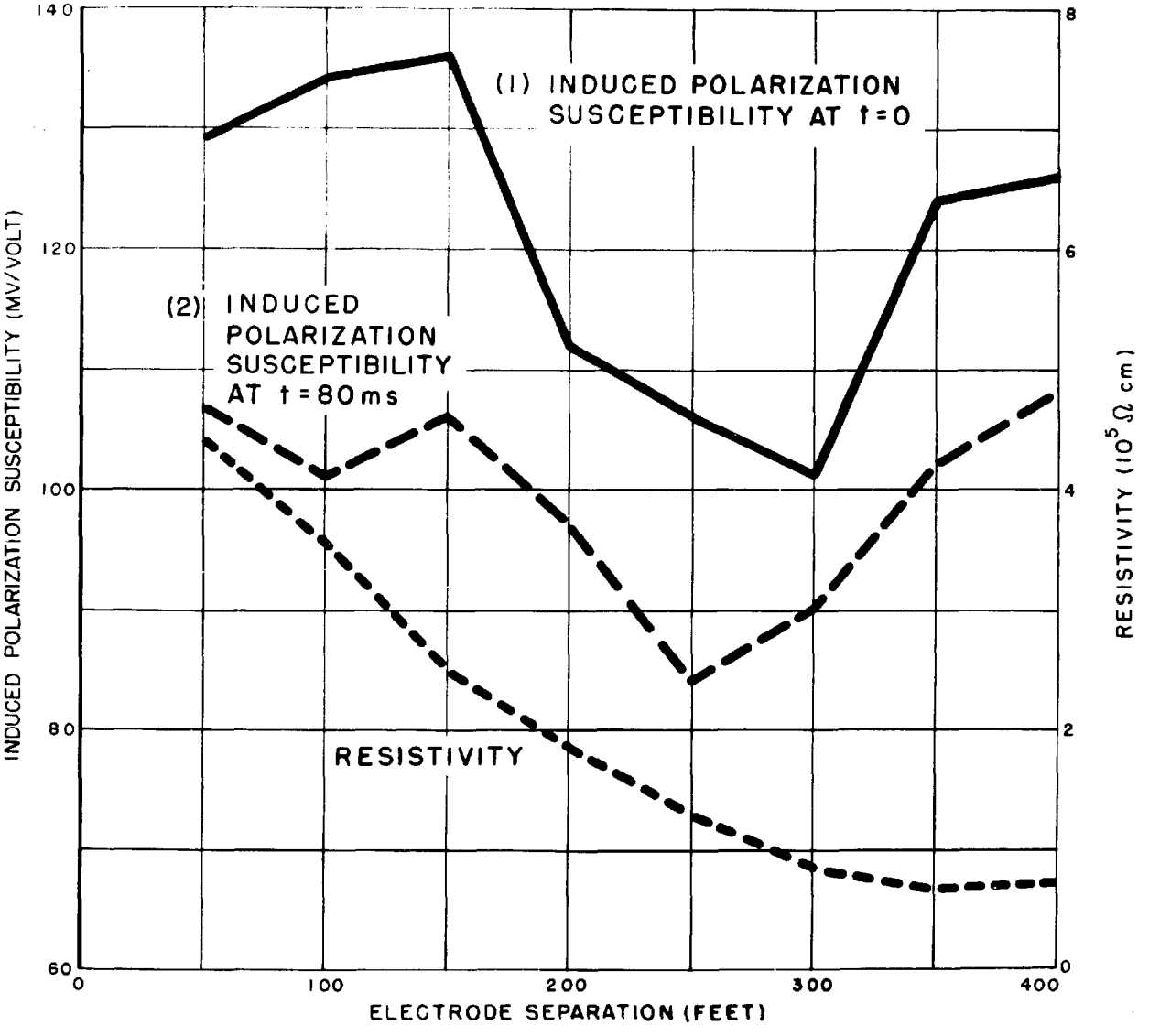

the ore body is shown in Plate 27. Seven traverses were conducted in the area; six of seven were over the probable ore body and the seventh was intentionally removed therefrom. The location and direction of each of the seven traversed may be seen in Plate 27. The information obtained from the six DDH's was used to construct the probable outlines of the ore body and these outlines are shown in Plates 28, 29, 30 and 31. Plate 28 is a vertical section through Traverse 1. Plate 29 shows a vertical section through Traverse 2 which appears to be the thickest part of the ore. Its maximum thickness, about 60 feet, occurs at approximately 50 foot depth. Plates 30 and 31 are vertical sections through Traverses 3 and 5 respectively.

Traverses 1, 2 and 3 were run roughly parallel to one another in the north-south direction and spaced to pass over the existing drill holes. Along Traverse 1, two runs were completed: Run 1 for which "a" was 50 feet and Run 2 for which "a" was 100 feet. The stations for both of these runs were taken at 25 foot intervals. Three runs were completed along Traverses 2 and 3 and the station intervals were again 25 feet. The first two runs corresponded to the first two of Traverse 1 and the third (Run 3) employed an electrode separation of 150 feet. The data from Run 3 of Traverses 2 and 3 have not been reduced.

The induced polarization susceptibility and the resistivity have been plotted in Plate 32 for Run 1 of Traverses 1, 2 and 3. The magnitude of the polarization susceptibility of the limestone appears to be rather small and uniformly about 20 mv/volt. As the magnetite is approached from the limestone the susceptibility constant increases. The largest value occurs along Traverse 2 where the ore shows its thickest section. The double peak observed along Traverse 1 is of interest. The first peak occurs over the top of the ore (at its shallowest depth) and the second is just south of DDH 3 where the ore is thought to be about 131 feet deep. The resistivity shows a small dip at the same place. In addition to the IP susceptibility and resistivity measurements, vertical magnetic field readings were also taken along Traverses 1, 2 and 3 (see Plate 36). An anomaly in the vertical field measurements which is as large as the largest value measured along Traverse 2 occurs at the same location as the second peak in the IP curve. There is certainly a well localized conducting body located just south of DDH 3 which is not revealed by the existing drill holes. It should be noted that the IP susceptibility curves and the vertical magnetic field data both point to Traverse 2 as the location of the largest amount

PROBABLE LIMIT OF ORE BODY

HORIZONTAL PROJECTION

MAGNETITE

LEBANON COUNTY, PENNSYLVANIA

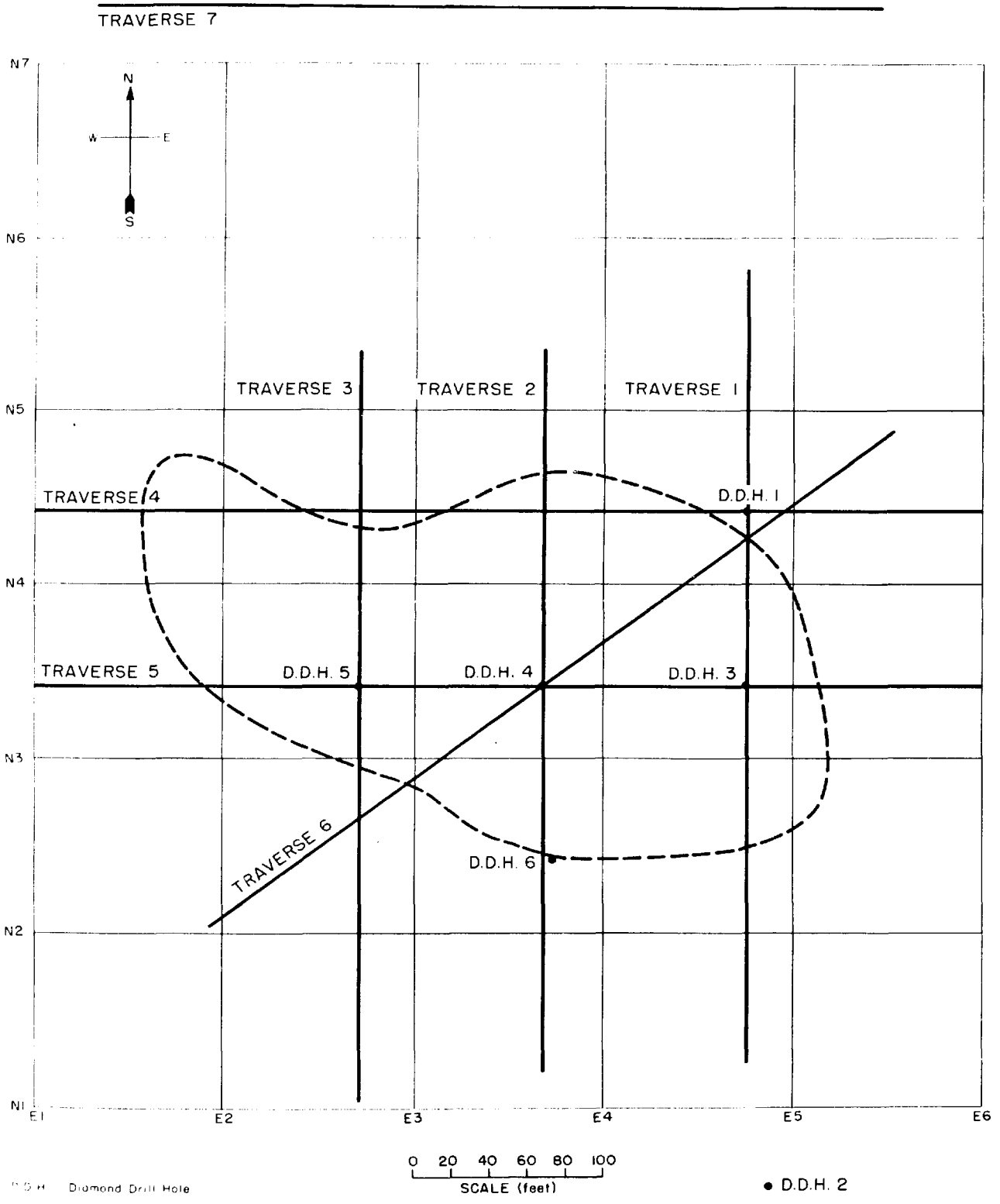

VERTICAL CROSS SECTION
THROUGH MINERALIZED ZONE
ALONG TRAVERSE I

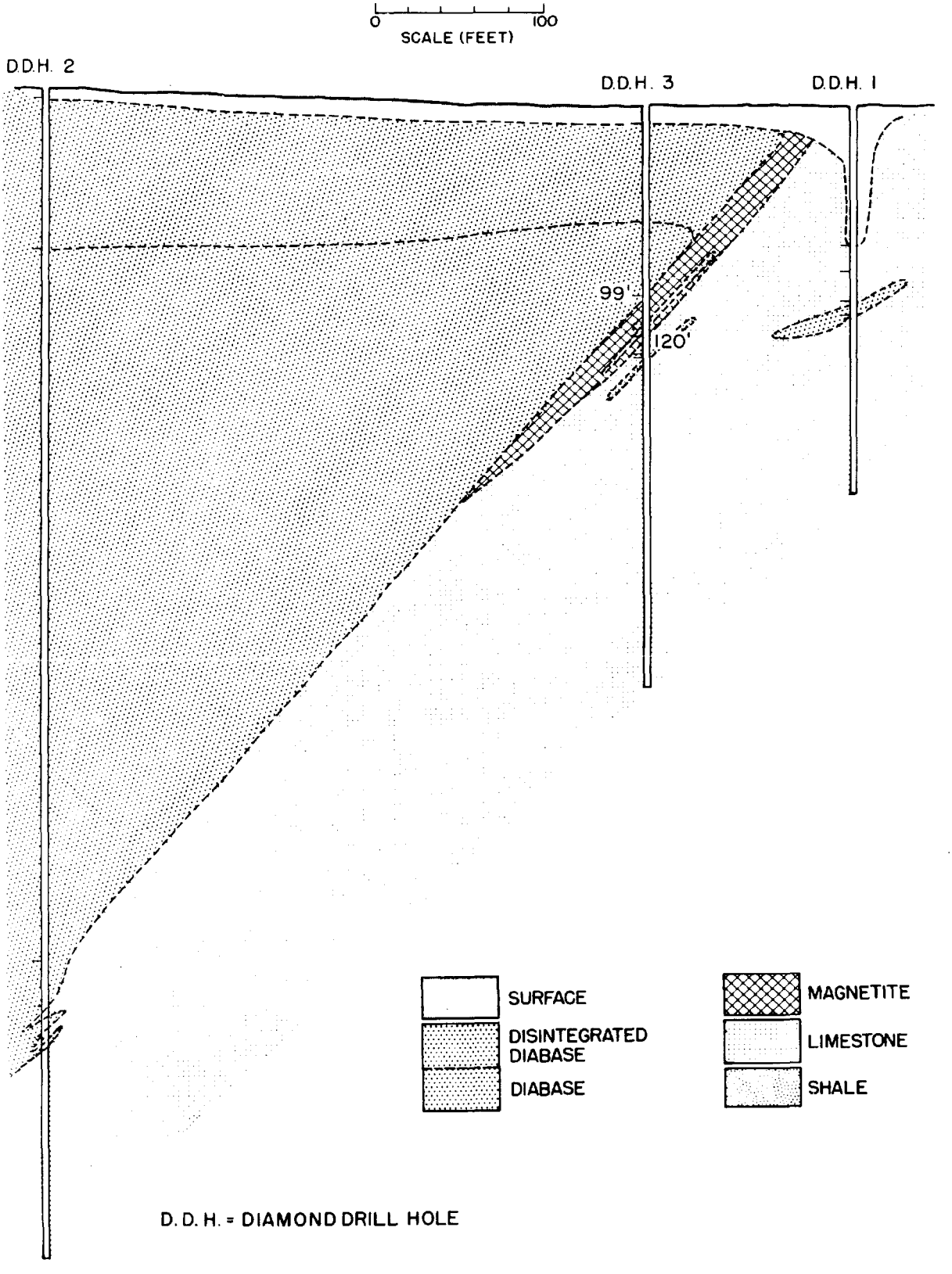

D. D. H. = DIAMOND DRILL HOLE

PLATE 29

VERTICAL CROSS SECTION
THROUGH MINERALIZED ZONE
ALONG TRAVERSE 2

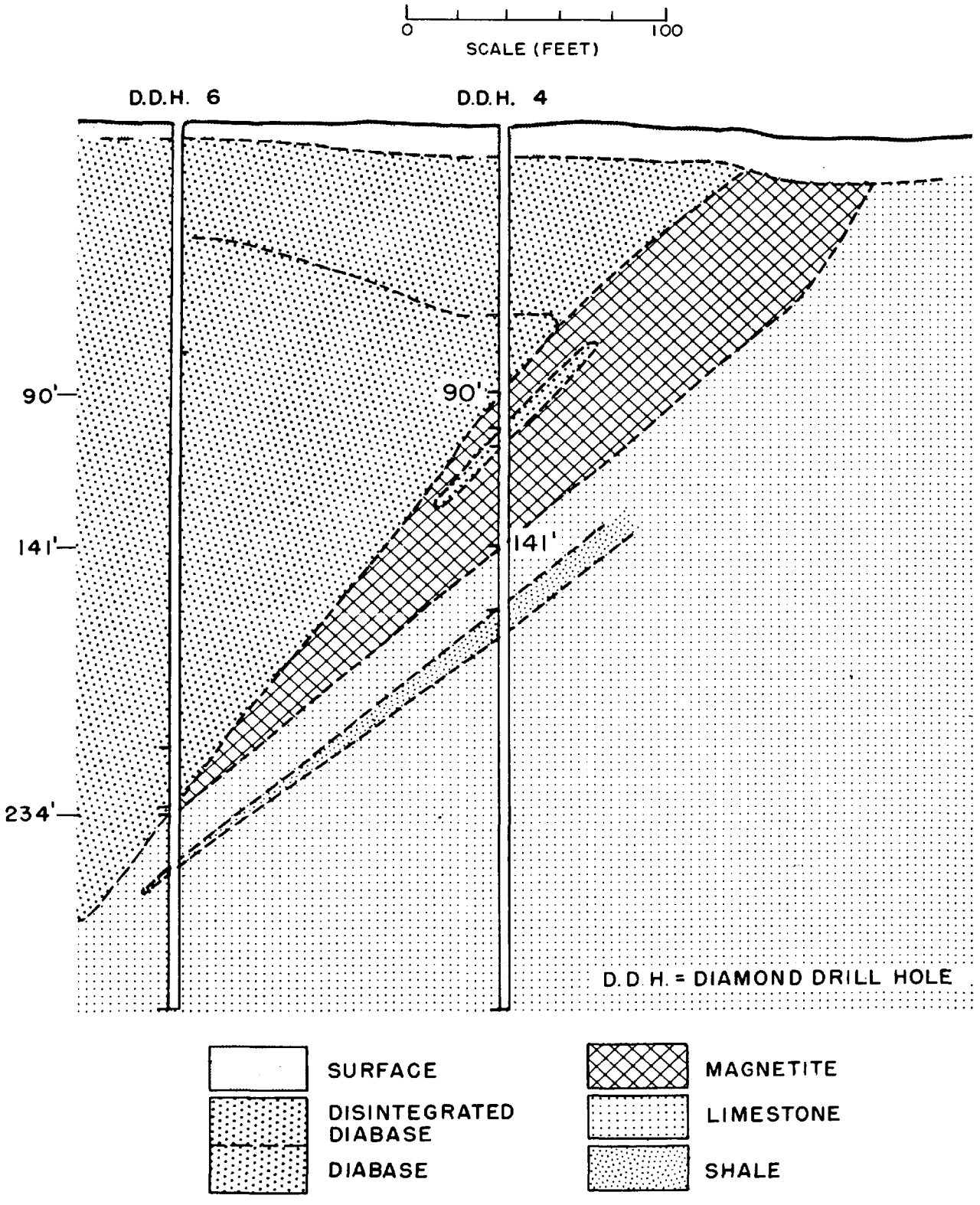

PLATE 30

VERTICAL CROSS SECTION
THROUGH MINERALIZED ZONE
ALONG TRAVERSE 3

0 100
SCALE (FEET)

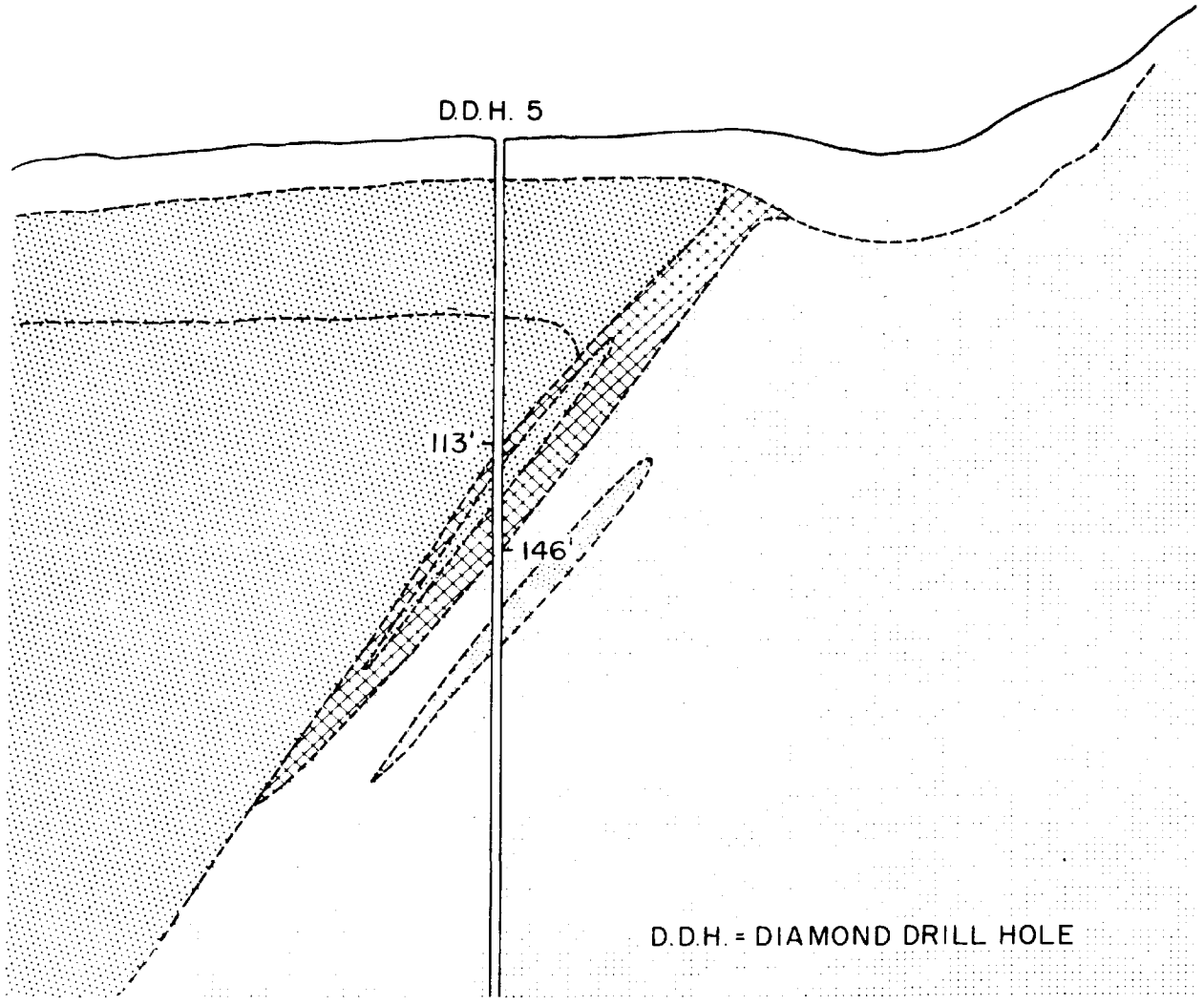

SURFACE
DISINTEGRATED DIABASE
DIABASE
MAGNETITE
LIMESTONE
SHALE

PLATE 31

VERTICAL CROSS SECTION
THROUGH MINERALIZED ZONE
ALONG TRAVERSE 5

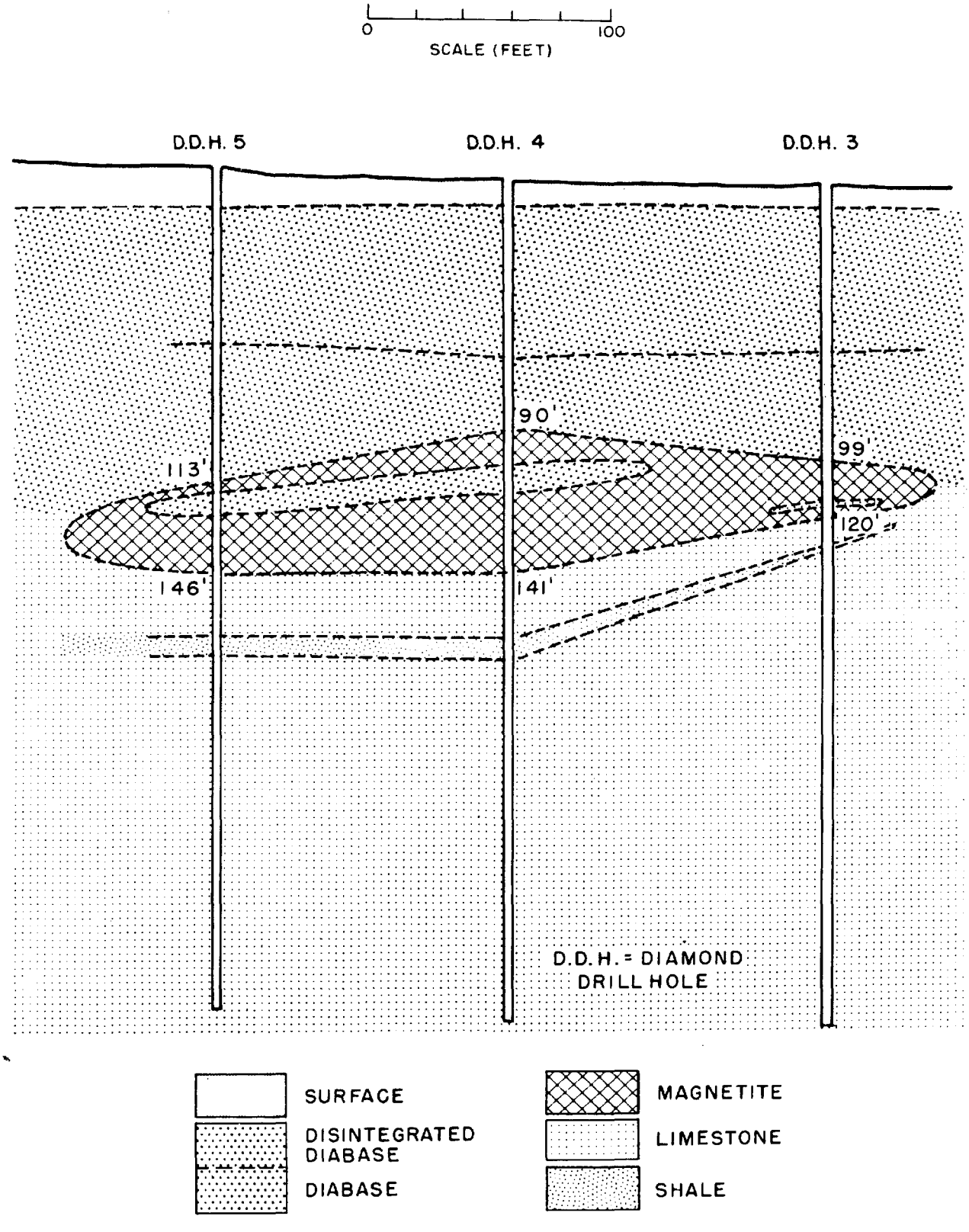

PLATE 32

INDUCED POLARIZATION SURVEY

MAGNETITE

LEBANON COUNTY, PENNSYLVANIA

HORIZONTAL TRAVERSES a = 50 FT

RUN I

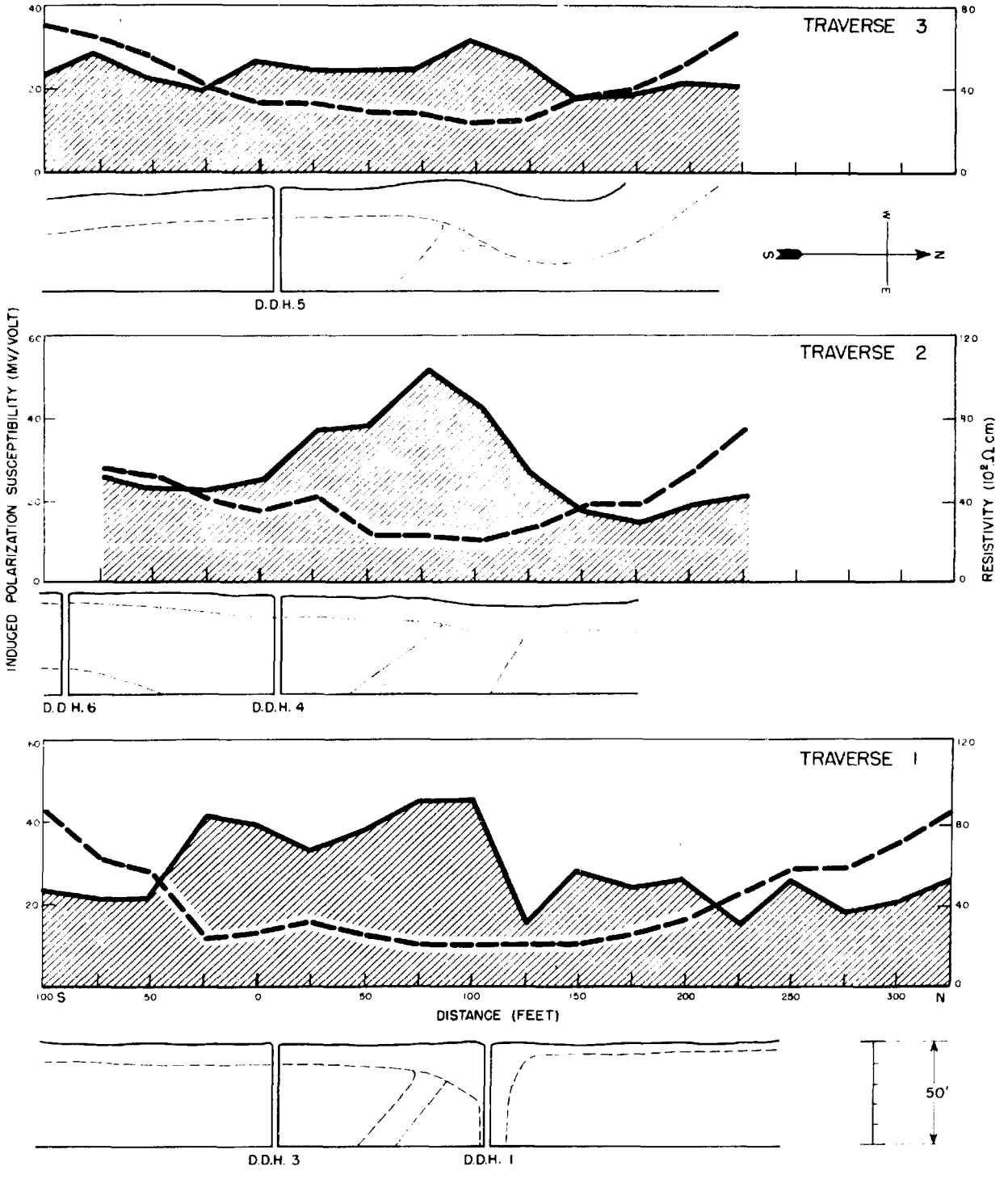

of mineral. On the other hand, there appears to be little difference in the resistivity data from the three traverses. Run 2 of Traverses 1, 2 and 3 show (Plate 33) essentially the same information as is given in Plate 32. The double peak of Traverse 1 has practically disappeared and the peak along Traverse 3 has increased and broadened somewhat. The results, otherwise, appear much the same. The differentiation between the signals obtained over the ore body and those obtained from either side of it is not great. However, the ore is not very thick in this north-south direction. Better contrast can be obtained by plotting areal susceptibility maps. These maps have been plotted such that all signals 50 mv/volt or more are shaded black. The 5 mv/volt contour intervals are shaded such that each interval is lighter as the signal decreases. Two such maps have been plotted. The data of Run 1, Traverses 1, 2 and 3 were used to prepare Plate 34 and the data from Run 2 of the same three traverses were used in the preparation of Plate 35. Both maps show the greatest signals over the leading edge of the ore body and they both indicate the direction of the strike of the ore.

Data from Traverse 4 was obtained with an expanding electrode array which had its center 100 feet north of DDH 4 and its line of electrodes in the east-west direction. Traverses 5 and 6 were vertical profiles with their centers over DDH 4. Traverse 5 was parallel to Traverse 4 and Traverse 6 ran N 52° E. The results obtained from Traverses 4 and 5 are shown in Plate 37 along with fabricated vertical sections of the ore body corresponding to imaginary drill holes directly below the center of each electrode system. The results of these two traverses are to be disregarded for the large electrode separations because it was discovered, after the data had been taken, that the electrodes had been set near some cast iron drainage pipes which were in a horizontal position and along the line of the electrodes. However, neglecting the large separations there appears to be little correlation between depth of influence and electrode separation. The ore is nearer the surface under the electrode line of Traverse 4. The IP susceptibility is much larger for the small electrode separations along Traverse 4 than along Traverse 5 which indicates that the magnetite along Traverse 4 has been polarized. The results obtained along both traverses approach roughly the same value as the electrode separation increases. Traverse 6 was conducted in order to get away from the iron pipes, the effect of topography on the resistivity and still cross over the ore body. Only partial success was realized because the electrodes ended up against a metal fence at each end of the line.

INDUCED POLARIZATION SURVEY

MAGNETITE

LEBANON COUNTY, PENNSYLVANIA

HORIZONTAL TRAVERSES a=100 FT

RUN 2

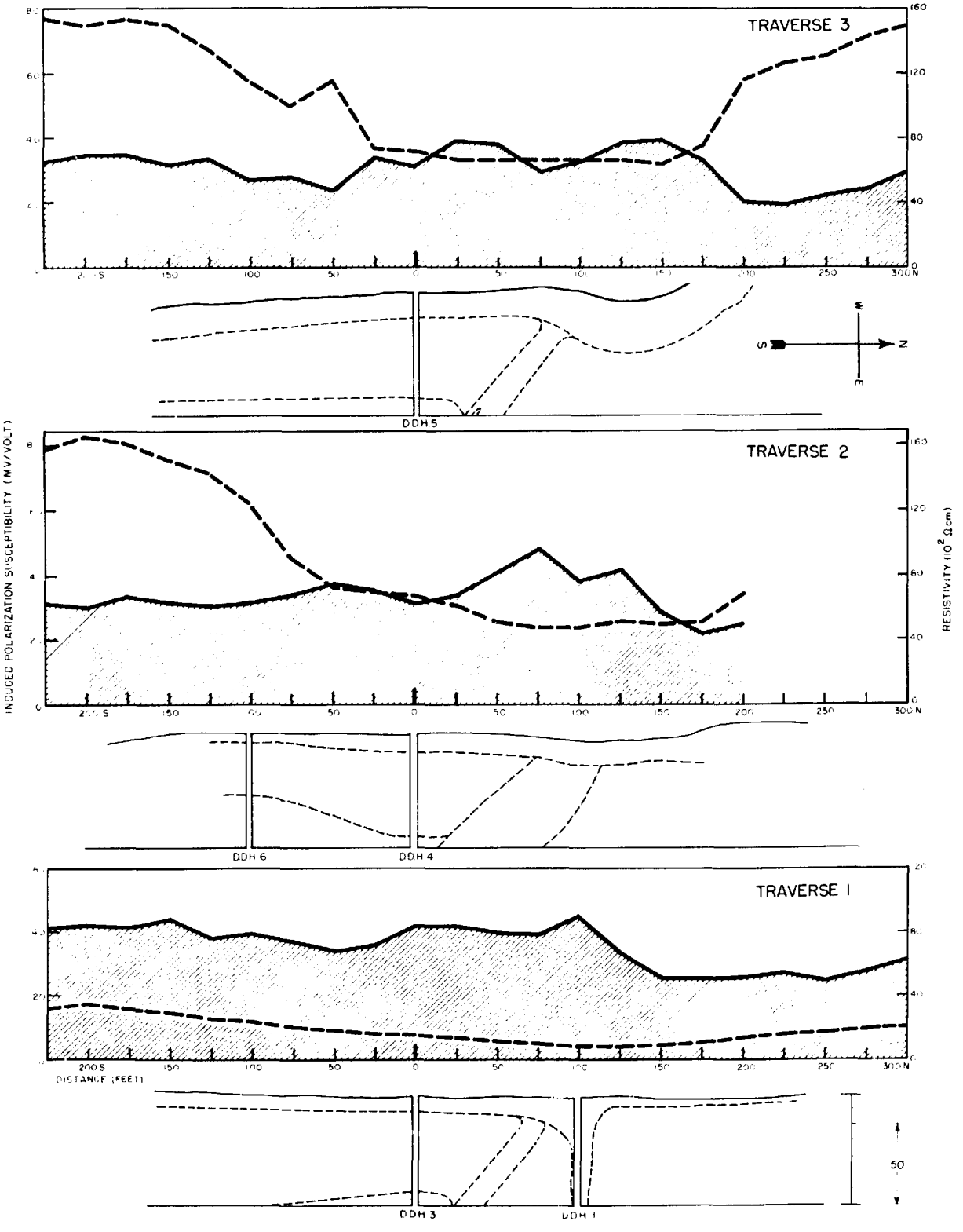

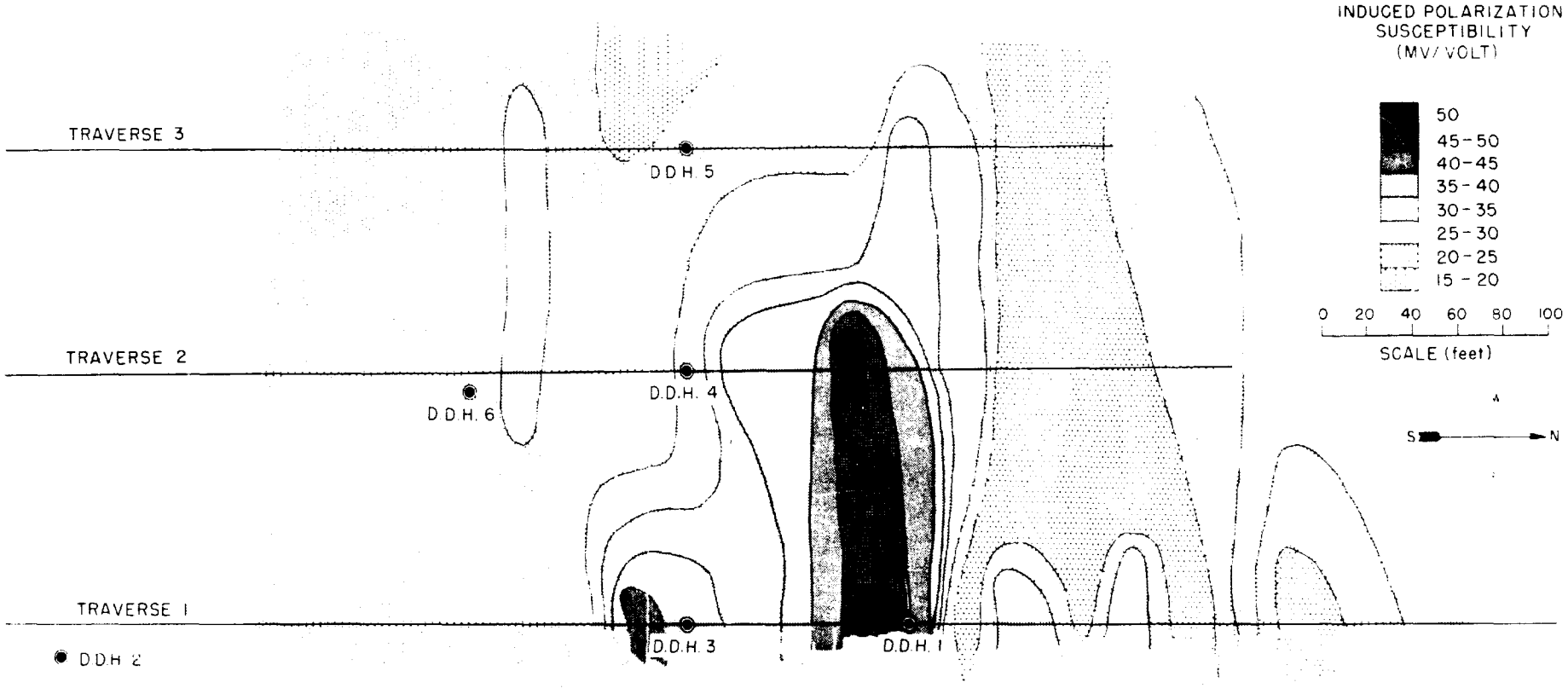

INDUCED POLARIZATION SURVEY

MAGNETITE

LEBANON COUNTY, PENNSYLVANIA

AREAL SUSCEPTIBILITY MAP

a = 50 FT

PLATE 34

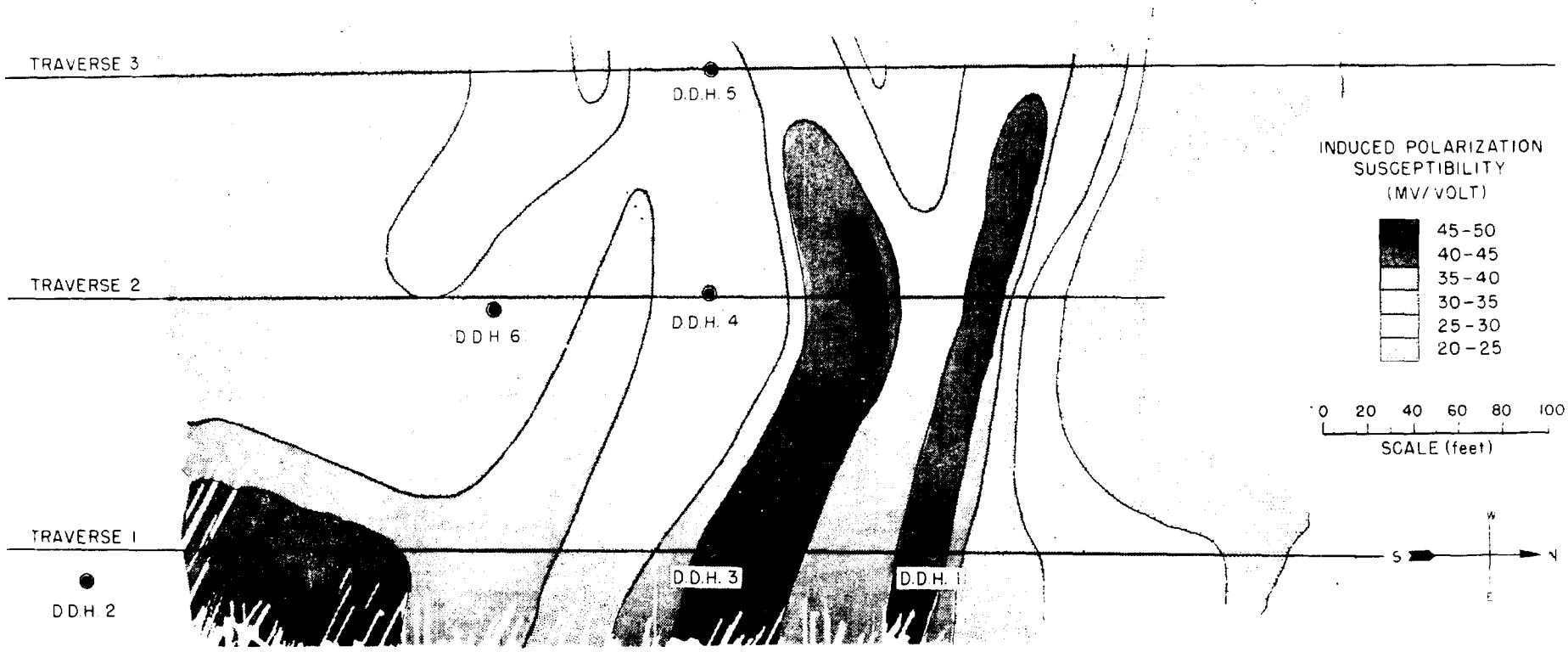

INDUCED POLARIZATION SURVEY

MAGNETITE

LEBANON COUNTY, PENNSYLVANIA

AREAL SUSCEPTIBILITY MAP

a = 100 FT

PLATE 35

VERTICAL MAGNETIC FIELD SURVEY

MAGNETITE

LEBANON COUNTY, PENNSYLVANIA

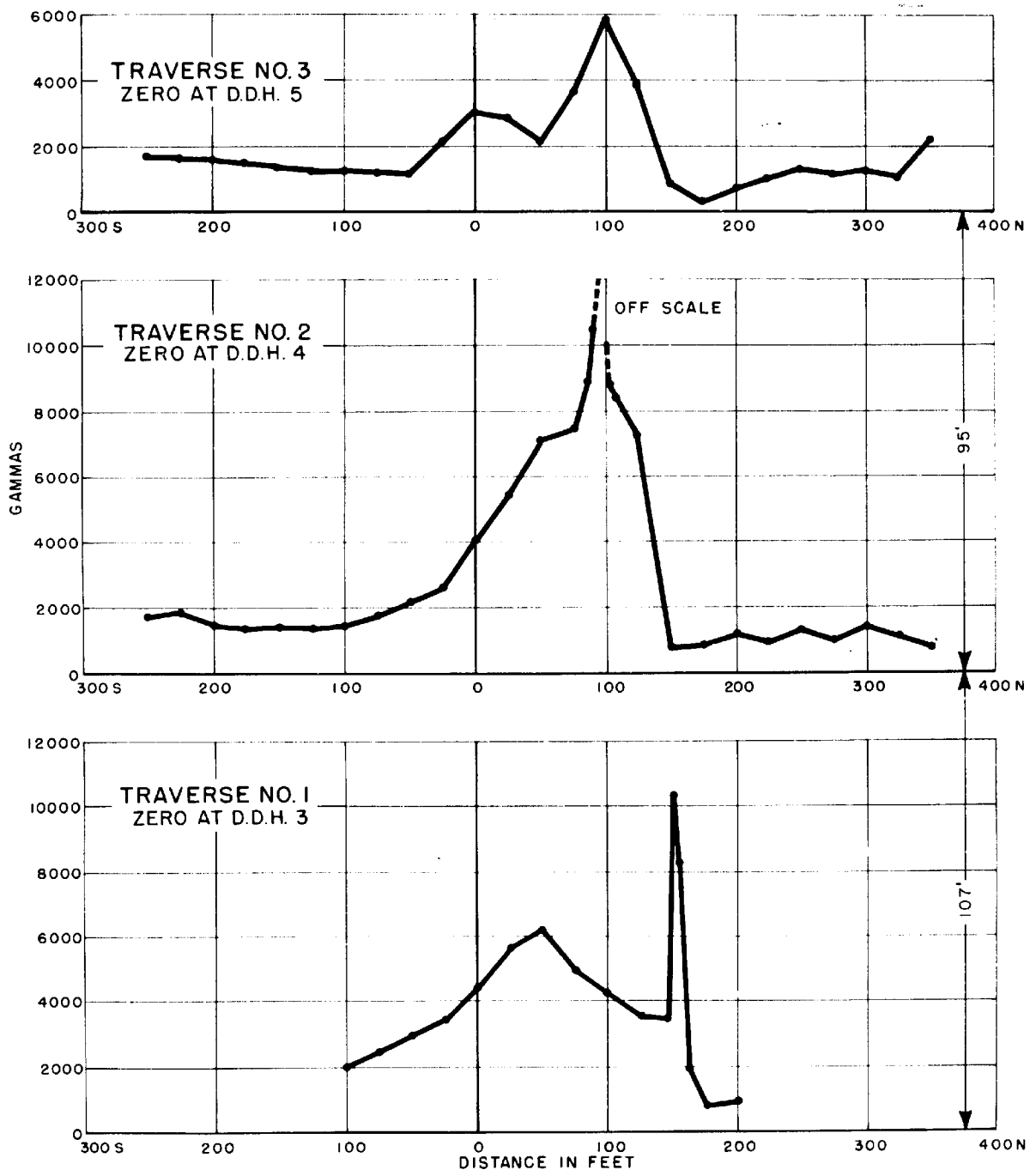

D.D.H. = DIAMOND DRILL HOLE

VERTICAL PROFILE

MAGNETITE

LEBANON COUNTY, PENNSYLVANIA

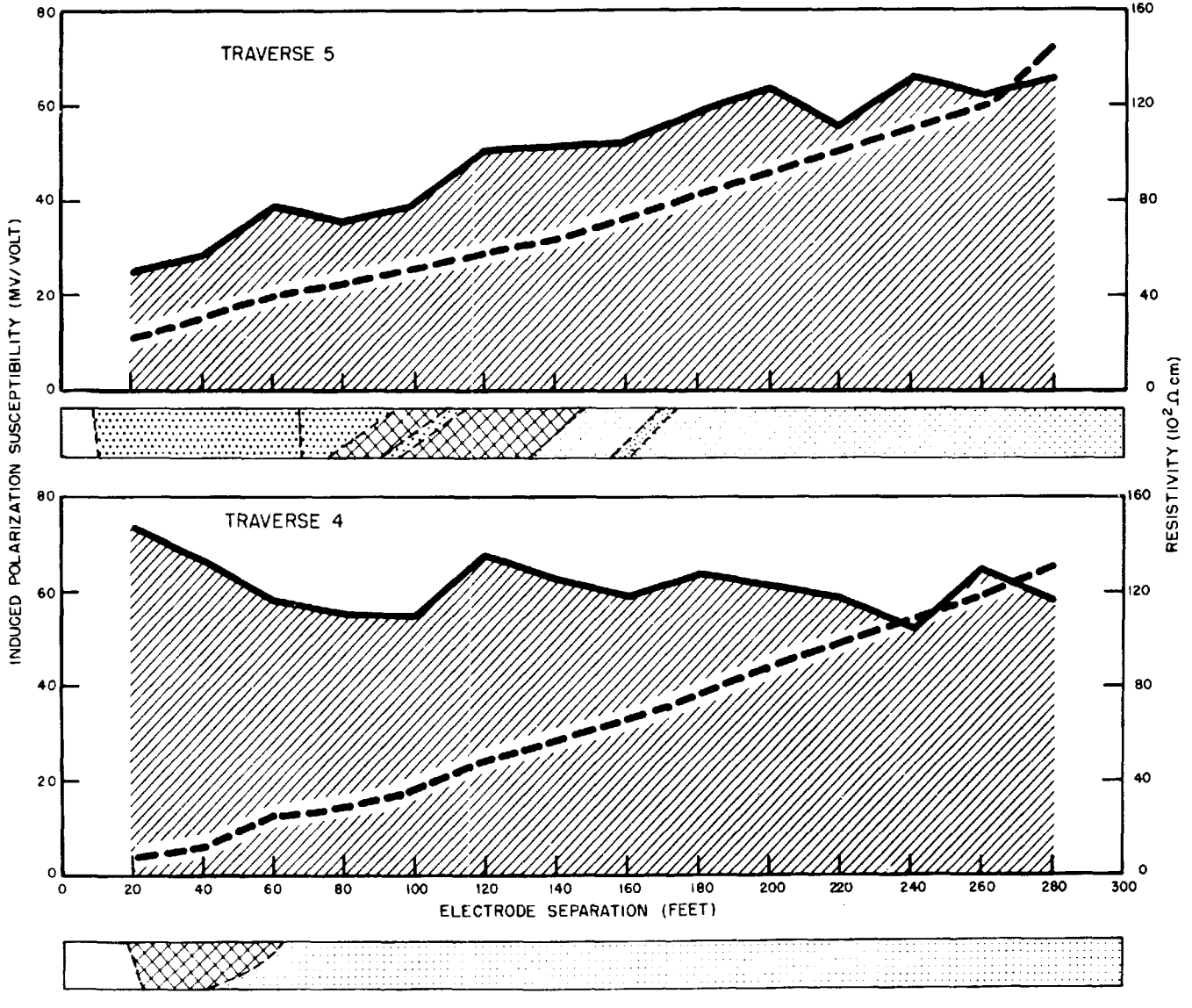

PLATE 37

The results of this traverse are shown in Plate 38. Once again there appears to be little correlation between the depth of influence and the electrode separation. Rather, it appears that, as one of the potential electrodes approaches the ore, the IP signal increases. As a check on the results obtained over the magnetite deposit a vertical profile was run in the east-west direction at a place well into the limestone and removed from the ore. The results (Plate 38) indicate the IP susceptibility to be small and quite uniform. The almost constant response is in agreement with the theory for the uniformly mineralized earth (Part C-1).

The data obtained from the vertical profiles (Traverses 4, 5 and 6) are still useful even though the desired correlation of depth with electrode separation is not apparent. Over DDH 4, at an electrode separation of 100 feet, there are three values of the IP susceptibility; Traverse 2 Run 2 in the north-south direction, Traverse 5 and Traverse 6. When the results from these three stations are compared, it is found that the greatest value came from Traverse 5, the least from Traverse 2 and the value from Traverse 6 was intermediate. The discussion concerning the ellipse of polarization (Part C-3) predicted that the greatest signal would appear in the direction of the strike. For this deposit the strike is in the east-west direction and the largest signal appeared in that direction. The results predicted by the discussion concerning the ellipse of polarization received additional verification from a survey conducted for that purpose.

The results obtained everywhere over the limestone were consistently low and of the same magnitude. Those results obtained over the diabase were larger than the limestone measurements. Three more surveys were run in this area to check the predictions concerning the ellipse of polarization. For each survey a Wenner system was used. The electrodes were separated by 50, 100 and 150 feet for each orientation of the electrode line. The line was oriented first in the north-south direction and then at 30°, 60°, 90°, 120° and 150° to the original direction. The first survey was conducted far removed from the ore and well over the limestone. The second survey had its center or rotation somewhere near DDH 4. The results of these two surveys are plotted in Plate 39. The induced polarization susceptibility for the limestone and the magnetite are plotted in pairs according to the electrode separation used. It should be noted that the values for the limestone are quite uniform, both with respect

VERTICAL PROFILE

LEBANON COUNTY, PENNSYLVANIA

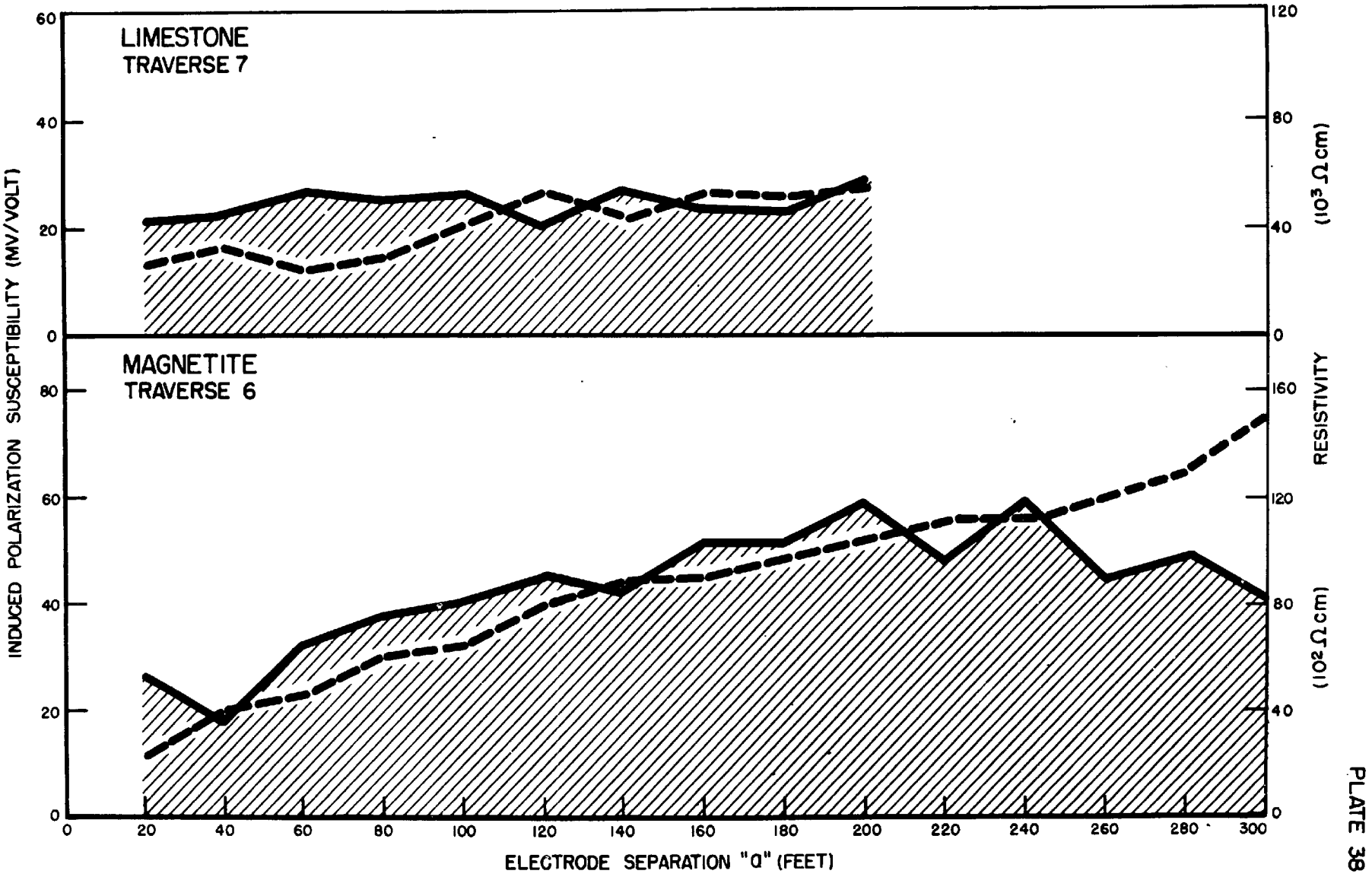

PLATE 38

ELLIPSE OF POLARIZATION

LEBANON COUNTY, PENNSYLVANIA

20 MV/VOLT
SCALE

LIMESTONE

MAGNETITE

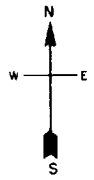

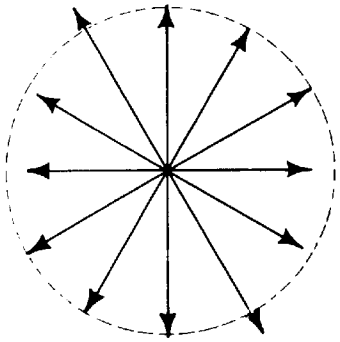

a = 50 FT

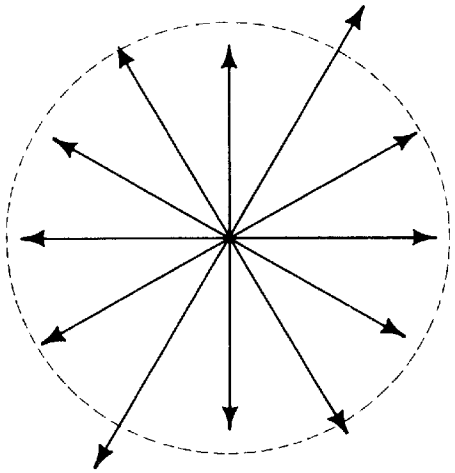

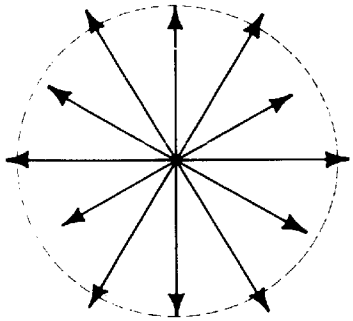

a = 100 FT

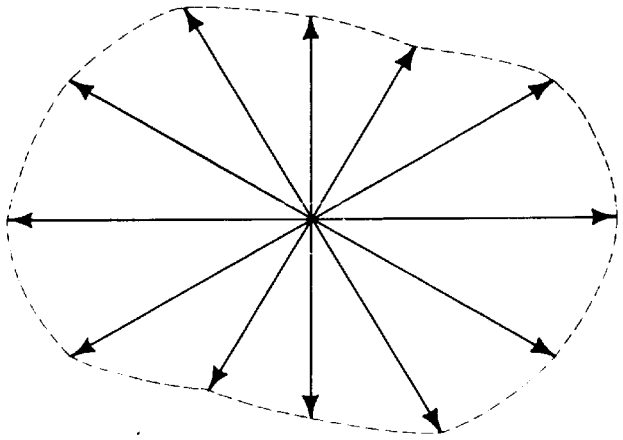

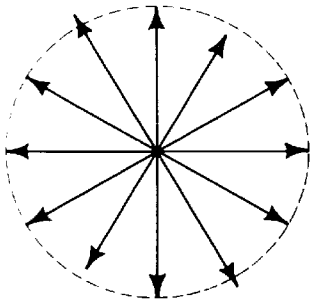

a = 150 FT

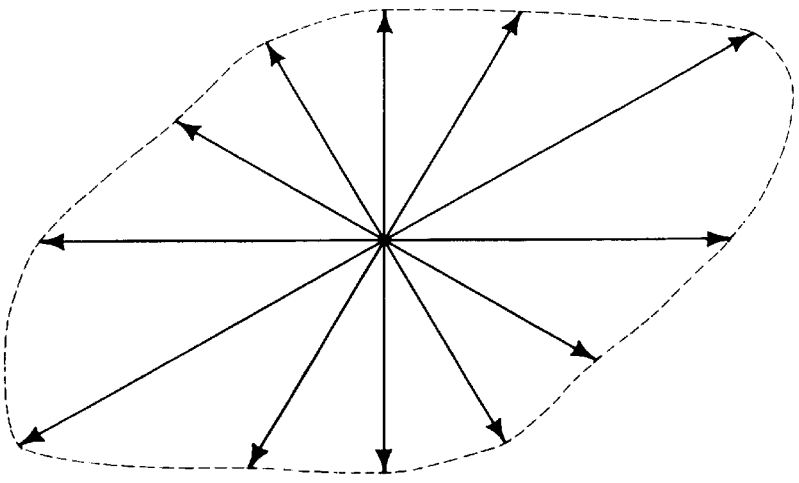

to the orientation of the line and with the electrode separation. The dashed-circle is the average value of all the vectors for the particular electrode separation employed. The limestone has a resistivity of about 50 • 10^3 ohm-cm and, because the polarization susceptibility is low, the limestone must be weakly but uniformly mineralized. The three curves obtained over the magnitite changed considerably with electrode separation. When "a" is 50 feet the susceptibility is nearly constant which results in a circular pattern which is as it should be. The center of the system is over DDH 4 and the ore is more than 50 feet from this point in any direction. Therefore, the ore is outside the influence of current density pattern and it is only the diabase which is polarized. For the 100 feet separation the IP susceptibility signal is 1.5 times as large in the direction of the strike as it is in the direction normal to the strike. The ratio of the largest to the smallest signal for the 150 foot separation has increased to roughly 2 : 1 but the indicated direction of the strike has changed slightly. This rather preliminary investigation is considered to be in good agreement with the predictions of the theory.

The third survey was conducted over the diabase at a place well removed from the ore. It is known that the diabase is more highly mineralized than the limestone but it was expected that it would also be uniformly mineralized. Certainly no one direction was to be preferred over any other. However, an examination of the results, plotted in Plate 40, reveals that the induced polarization susceptibility is greater in the north-south direction than in any other direction. The measured value of the IP susceptibility in the north-south direction is at least twice that measured in the east-west direction. The vectors plotted for the electrode separation of 50 feet show the IP susceptibility to be larger in the neighborhood of the north-south direction than it is in the east-west direction. The figure is more nearly an ellipse than a circle. However, for the electrode separation of 100 feet the vector pattern is more like, except for the north-south direction, a circle than an ellipse and for the 150 foot electrode separation it is essentially a circle except for the north-south direction. The vector in the north-south direction increased as the electrode separation increased. It was concluded that the source of the polarization potential was a long metallic object such as a water pipe or cable oriented in the north-south direction because the side vectors decreased and the north-south vector increased as the electrode array was expanded. A letter was sent to the owner of

ELLIPSE OF POLARIZATION

DIABASE

LEBANON COUNTY, PENNSYLVANIA

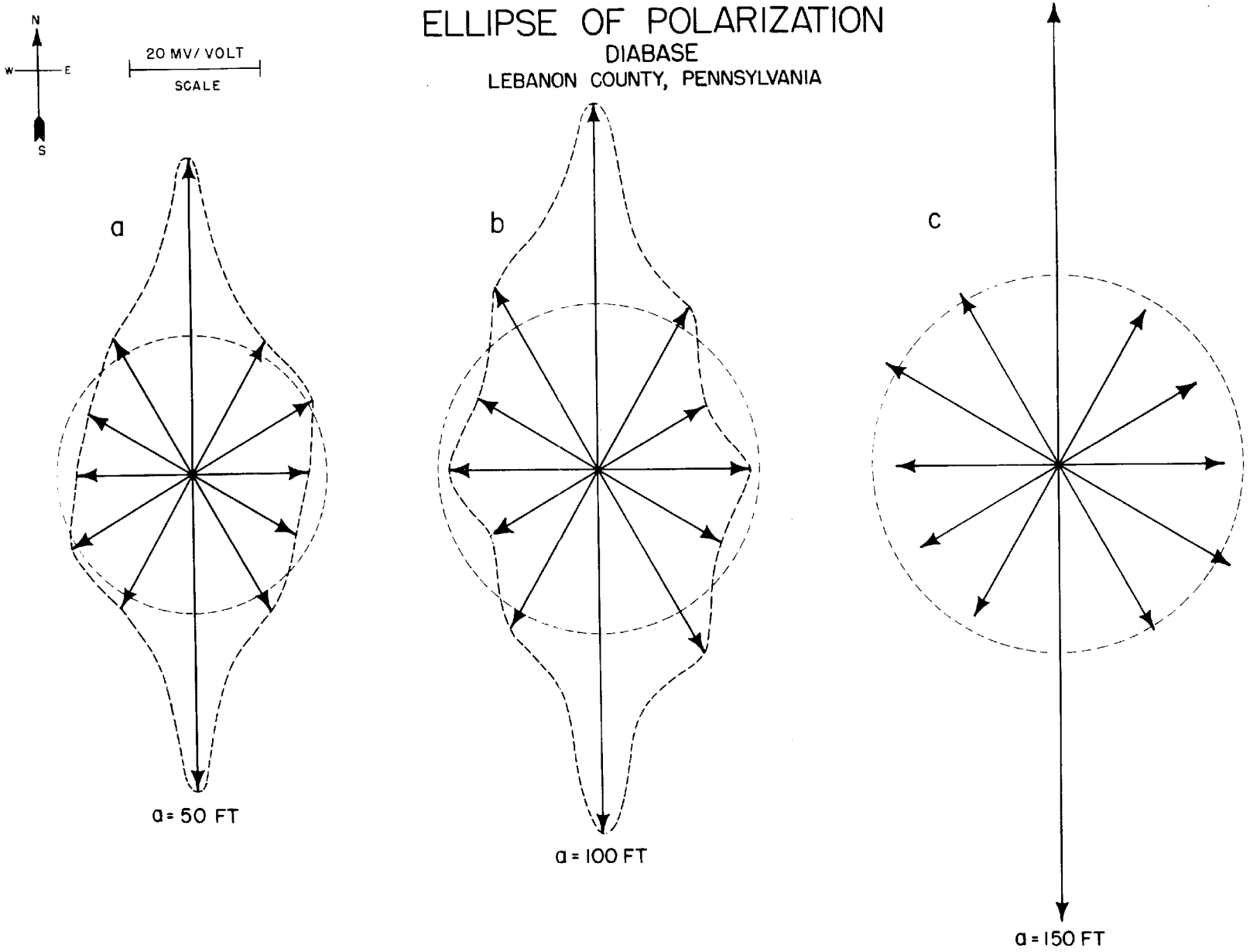

PLATE 40

the land who in turn confirmed the existence of a water pipe in the place indicated by the measurements.

It is concluded that the magnetite deposit was clearly located by the induced polarization susceptibility. Other electrode arrangements or different types of traverses can be arranged such that the contrast between the induced polarization susceptibility measured over the ore and off the ore will be greater than it is now. However, that is a task for the future. The survey over the magnetite deposit concludes the field work.

SUMMARY

It is the intention of this thesis to correct some of the errors which have crept into the literature, to remove some of the existing mystery and to bring out the advantages and limitations of the method of induced polarization with the hope that it will grow into a useful tool for geophysical prospecting. To accomplish this purpose a series of laboratory experiments, designed to reveal the fundamental relations involved, were conducted; a theoretical rerelation, based on the results of the laboratory experimentation, has been developed for the interpretation of field data, and in addition to the preliminary field survey over an amphibolite dike, the method has been applied to three mineralized areas where the detailed geology is quite well known. The results obtained in the field are promising and in keeping with the experimental and theoretical developments. In the light of the results of this work the literature is briefly reviewed.

The conclusions reached by Schlumberger[4] concerning geophysical prospecting by the method of induced polarization have been examined. He apparently understood the elements of the fundamental process involved but he was lead to conclusions, either because of inadequate equipment or insufficient experimentation, which can not be supported by this work. His claims that the self-potentials generated by sulphide ores concealed the induced polarization effect are not supported by the present measurements over the pyrrhotite outcrop as reported in this thesis. At the east edge of the ore the self-potential generated was more than 300 mv. However, no evidence was found to support the contention that the induced polarization potential was concealed by that self potential. As a matter of fact, the largest value of the induced polarization potential was measured at this interface. The energizing current was made to flow in both directions across the boundary and the induced polarization for each direction of the current was measured. Within the limits of experimental error, the measurements were the same in both directions. If, because of chemical action, the interface of an ore body became saturated with electromotively

active material, then additional current forced into the ground would either deposit more material or remove some, all according to whether the energizing current aided or opposed the natural current. The addition of more electromotively active material can not increase the potential of the saturated interface and, therefore, no induced polarization potential can be measured. If, on the other hand, the energizing current opposed the natural current some material would be removed. If the amount of material removed reduces the concentration of the active material below saturation, the return to saturation would be measured. The self potentials required to maintain the surfaces of an ore body in a saturated condition will be difficult to realize under the conditions of natural current flow.

Schlumberger stated that the resistivity of the rock, surrounding the ore body, enters into the induced polarization effect not more than to a secondary measure. This statement is not far from correct if the form of the decay curve alone is considered. However, one of the results obtained in this thesis states that the induced polarization potential is proportional to the potential gradient established. This makes the induced polarization effect directly proportional to the resistivity. Furthermore, the laboratory experiments have failed to bear out Schlumberger's statement that the "residual" polarization potential was due to a transport of ions creating a dissymmetry between the regions surrounding the electrodes. Contrary to this statement, it was found that the only time polarization potentials were observed was when electrically conducting minerals were present. This observation lead to the theoretical development of the polarization potential of a uniformly mineralized earth which has been verified experimentally in the laboratory and in the field during the course of the work reported here.

The publications of Müller[5,7] and Weiss[6] concerning the "Electrochemical Method" contain so many errors that it is unfortunate that they were published at all. The work of Belluigi[8,9] might have succeeded except that he discarded only part and not all of the procedure established by Müller. Although Belluigi improved the method of measurement he retained much of the interpretation given by Müller. Variations in the resistivity alone might well have accounted for the results Belluigi obtained. The present work has shown that polarization is induced only when electrically conducting minerals are present in the structure. Formation boundaries are not polarizable unless a differential exists in the

concentration of electrically conducting mineral across such boundaries. Oil, as a non-electrolyte, should not generate electromotively active material against a boundary even though the boundary is mineralized. Furthermore, the decay time of of the induced polarization potential is of sufficient duration to mask the difference in time required (as reported by Potapenko[13]) to polarize an electrode first in an electrolyte and then in oil. It is concluded that oil cannot be directly located by the induced polarization method nor can oil be indirectly located unless it is very shallow.

The method of induced polarization requires for its operation the existence of electrically conducting minerals in an electrolyte. This requirement confines the method to the location of electrically conducting minerals and other metallic objects. Its best application should be to shallow mineral prospecting. It may, however, be used to locate pipe lines, rails, cables and other buried metallic objects. The method does differentiate between those areas where resistivity is low because of metallic conduction and those where resistivity is low because of good electrolytic conduction. The method is also capable of differentiating between two areas of equal resistivity but unequal mineralizations. It should be of use, therefore, in the location of disseminated minerals, such as the galena in the Missouri-Oklahoma-Kansas "Tri-state" region, where the resistivity change from a mineralized area to an unmineralized one is insufficient to enable detection of the mineralized area by resistivity measurements. The ellipse of polarization principle enhances the use of the method.

This preliminary work has revealed certain disadvantages in the IP method, several of which are inherent in the method itself and others that may be eliminated by further development of the method. To begin with, the induced polarization measurements cannot be divorced from resistivity measurements. This does not mean that separate equipment must be employed nor that the resistivity must be separately measured. However, the two separate measurements will undoubtedly be desirable. A more serious limitation on the method and the one which confines it to shallow work is the "fall-off" of the signal with depth. First, a current density must be established in order to polarize the earth minerals and then the signal must be returned to surface which gives, at best, an inverse fourth power relation. However, the magnitude of the potential increases with the linear dimensions of the body and

thereby improves the relation of the signal vs depth. Another limitation at present is the polarization of disseminated minerals which may mask the deeper lying ore bodies. The effect produced by changes in the concentration of the disseminated mineral is not known. There may be a saturation effect which depends upon the percentage concentration of the mineral particles. Still another limitation, although not serious, is that potentials measured by the induced polarization method are usually one order lower than those measured by the resistivity method.

It is expected that the method of induced polarization will, with improved instrumentation and a larger background of field results, find its place among the existing tools for geophysical prospecting for minerals. It must be remembered that the work reported here is only the initial phase. It is the author's hope that a useful method of geophysical prospecting will be built upon the foundation established by this paper.

ACKNOWLEDGEMENTS

The author is indebted to the Naval Ordnance Laboratory for the use of the equipment and facilities available at the Laboratory which have made this work possible. He is deeply grateful for the continued interest and the many timely suggestions and criticisms of Dr. L. H. Rumbaugh and Dr. W. G. Keck of the Laboratory staff. It is a privilege to acknowledge the assistance of illustrators and photographers at the Naval Ordnance Laboratory in the preparation of the plates and the assistance of Messrs. E. L. Sanderson and S. P. Haddad in the collection of the data.

The author wishes to thank the Geophysics Section of the U. S. Geological Survey for services and facilities which were placed at his disposal and for the assistance given to him in the field work. Dr. J. H. Swartz supplied the vertical magnetic field readings and Mr. H. C. Spicer supplied the Gish-Rooney resistivity measurements over the amphibolite dike. The author is indebted to them for these data and for their assistance in the field work.

He also wishes to thank members of the Michigan State College faculty, particularly Dr. C. D. Hause for his interest and suggestions and Dr. C. P. Wells for the tedious job of checking the mathematics.

REFERENCES

1. C. Schlumberger, German patent #269,928 (6 Nov. 1912)
2. C. A. Heiland, Geophysical Exploration. Prentice-Hall, Inc., New York (1940), p 763
3. C. Schlumberger, Etude Sur La Prospection Electrique Du Sous Sol. Gauthier-Villars et C's. Paris (1920) Ch. 8
4. C. Schlumberger, loc. cit. revised (1930)
5. M. Müller, Zeits. f. Geophysik. 8, 423 (1932)
6. O. Weiss, World Pet. Congr. (London) Proc. 1 (1932)
7. M. Müller, Gerlands Beitr. z. Geophysik. 4, 302 (1934); Zeits. f. Geophysik 4, 330 (1934); ibid 16, 274 (1940)
8. A. Belluigi, Beitr. z. Angew. Geophysik. 5, 169 (1934)
9. A. Belluigi, Riv. Geominer 2, 56 (1941)
10. L. W. Blau U. S. patent # 1,911,137 (1933)
11. C. and M. Schlumberger, A.I.M.E. Geophys. Prosp. 32 (1932); T. M. Pearson, ibid 34 (1934)
12. P. F. Hawley, Geophys. 3, 247 (1938)
13. G. Potapenko, U. S. patents # 2,190,320, #2,190,321, #2,190,322, #2,190,323 (1940)
14. G. Peterson, U. S. patent #2,190,324 (1940)
15. A. Matsubara, U. S. patent #2,153,636 (1939)
16. H. M. Evjen, U. S. patent # 2,375,776, #2,375,777, #2,375,778 (1945)
17. F. P. Bowden and E. R. Rideal, Roy. Soc. Proc., 'A 120, 59 (1928)
18. J. A. Stratton, Electromagnetic Theory, McGraw-Hill, New York (1941) p 15
19. G. Prasad, Spherical Harmonics, Part I, Mahamandal Press, Benares City, India (1930) p 104
20. J. P. Webb, Phys. Rev. 37, 292 (1931)
21. This work was done at the NOL by Mr. C. Lufcy
22. C. Milton, Geologist at USGS, Personal communication
23. R. J. Wright and N. D. Raman, USGS Reports - Open File Series, The Gossan Lead, Carrol County, Virginia, Released 19 February 1948

APPENDIX

I

Since there exists an unresolved difference between the work of Webb[20] and the calculations in this paper the derivation of the constants employed is given here. This derivation is not intended to be completed in itself but must be read in conjunction with Webb's paper. Wherever they fit, Webb's calculations are used but there is an interchange in the summation indicies. When reading Webb's formulas read m in place of n and vice versa.

(1)

$$U_e = \frac{\rho_1 I}{4\pi r_2} = \frac{D}{r_2}$$

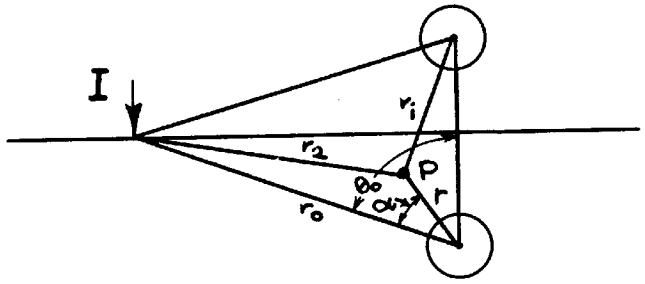

Now $1/r_2$ can be expanded in terms of the polar coordinates of the origin at the center of the sphere by the relation

(2) $$\frac{1}{r_2} = \frac{1}{r_0}\sum_{n=0}^{\infty}\left(\frac{r}{r_0}\right)^n P_n(\cos\alpha)$$

which can be further expanded by the biaxial expansion

(3) $$P_n(\cos\alpha) = \sum_{m=0}^{m=n}(2-\delta_m^0)\frac{(n-m)!}{(n+m)!}P_n^m(\cos\theta_0)P_n^m(\mu) \times \cos m(\varphi-\varphi_0).$$

Substituting (2) and (3) in (1) the potential due to the electrode becomes

(4) $$U_e = \frac{\rho_1 I}{4\pi r_0}\sum_{n=0}^{\infty}\sum_{m=0}^{m=n}\left(\frac{r}{r_0}\right)^n\left(2-\delta_m^0\right)\frac{(n-m)!}{(n+m)!}P_n^m(\mu_0)P_n^m(\mu)\cos m(\varphi-\varphi_0)$$

$$= \frac{D}{r_0}\sum_{n=0}^{\infty}\sum_{m=0}^{m=n}\left(\frac{r}{r_0}\right)^n\left(2-\delta_m^0\right)\frac{(n-m)!}{(n+m)!}P_n^m(\mu_0)P_n^m(\mu)\left(\cos m\varphi\cos m\varphi_0+\sin m\varphi\sin m\varphi_0\right)$$

The potential due to the real sphere is

$$(5)\quad U_s = \sum_{n=0}^{\infty}\sum_{m=0}^{\infty}\left(\frac{a}{r}\right)^{n+1}\left(A_{mn}\cos m\varphi + B_{mn}\sin m\varphi\right)P_n^m(\mu).$$

and that due to the image sphere is

$$(6)\quad U_i = \sum_{n=0}^{\infty}\sum_{m=0}^{\infty}\left(\frac{a}{r_i}\right)^{n+1}\left(A_{mn}\cos m\varphi_i + B_{mn}\sin m\varphi_i\right)P_n^m(\mu_i).$$

The subscript i refers to the coordinates of the point $P(r,\theta,\varphi)$ measured with respect to the center of the image sphere instead of the origin in the real sphere.

The potential anywhere outside the sphere is the sum of these three potentials; i.e.,

$$\Phi_e^o = U_e + U_s + U_i$$

$$= \sum\sum\left(\frac{r}{r_o}\right)^n\left({}^1K_{mn}\cos m\varphi + {}^2K_{mn}\sin m\varphi\right)P_n^m(\mu)$$

$$+\sum\sum\left(\frac{a}{r}\right)^{n+1}\left(A_{mn}\cos m\varphi + B_{mn}\sin m\varphi\right)P_n^m(\mu)$$

$$+\sum\sum\left(\frac{a}{r_i}\right)^{n+1}\left(A_{mn}\cos m\varphi_i + B_{mn}\sin m\varphi_i\right)P_n^m(\mu_i).$$

Hobb has given an expression for

$$\frac{P_n^m(\mu_i)}{r_i^{n+1}} = \sum_{k=m}^{\infty}\frac{(n+k)!}{(n-m)!\,(m+k)!}\,\frac{r'^k}{h^{n+k+1}}\,P_k^m(\mu')$$

where r' and μ' are coordinates of the point P_i in terms a center at the image sphere. An interchange of the indicies n and k gives

$$\sum\sum\left(\frac{a}{r_i}\right)^{n+1}\left(A_{mn}\cos m\varphi + B_{mn}\sin m\varphi\right)P_n^m(\mu_i)$$

$$= \sum_{n=0}^{\infty}\sum_{m=0}^{\infty}\sum_{k=m}^{\infty}\left(A_{mk}\cos m\varphi + B_{mk}\sin m\varphi\right)\frac{a_{mkn}}{a^n}r'^n P_n^m(\mu')$$

where (depth of sphere = h/2).

$$a_{mkn} = \frac{(n+k)!}{(n+m)!(k-m)!}\left(\frac{a}{h}\right)^{n+k+1}$$

Now since this is the potential at P_i (the image of P) due to S, it is also the potential at P due to S_i. We need only to interchange r' and r and μ' and μ.

The potential inside the sphere is obviously

$$\Phi_E^I = \sum_{n=0}^{\infty}\sum_{m=0}^{\infty}\left(\frac{r}{a}\right)^n\left(C_{mn}\cos m\varphi + D_{mn}\sin m\varphi\right)P_n^m(\mu).$$

The boundary conditions require that

$$\Phi_E^o = \Phi_E^I \quad \text{at } r=a$$

which gives

$$\sum\sum\left(\frac{a}{r_o}\right)^n\left({}^1K_{mn}\cos m\varphi + {}^2K_{mn}\sin m\varphi\right)P_n^m(\mu)$$

$$+\sum\sum\left(A_{mn}\cos m\varphi + B_{mn}\sin m\varphi\right)P_n^m(\mu)$$

$$+\sum_n\sum_m\sum_k\left(A_{mk}\cos m\varphi + B_{mk}\sin m\varphi\right)a_{mkn}P_n^m(\mu)$$

$$=\sum\sum\left(C_{mn}\cos m\varphi + D_{mn}\sin m\varphi\right)P_n^m(\mu),$$

and

$$\frac{1}{\rho_1}\left(\frac{\partial\Phi_E^o}{\partial r}\right) = \frac{1}{\rho_2}\left(\frac{\partial\Phi_E^I}{\partial r}\right) \qquad r=a$$

which gives

$$\frac{1}{\rho_1}\Big[\sum\sum \frac{n}{a}\left(\frac{a}{r_o}\right)^n \left({}^1K_{mn}\cos m\varphi + {}^2K_{mn}\sin m\varphi\right) P_n^m(\mu)$$
$$+ \sum\sum -\frac{(n+1)}{a}\left(A_{mn}\cos m\varphi + B_{mn}\sin m\varphi\right)$$
$$+ \sum\sum\sum \frac{n}{a} a_{mkn}\left(A_{mk}\cos m\varphi + B_{mk}\sin m\varphi\right) P_n^m(\mu)\Big]$$
$$= \frac{1}{\rho_2}\Big[n\left(C_{mn}\cos m\varphi + D_{mn}\sin m\varphi\right) P_n^m(\mu)\Big].$$

Now set

$$\beta = \frac{\rho_1}{\rho_2}$$

and equate similar tesseral harmonics.

Then

(1)

$$\left(\frac{a}{r_o}\right)^n {}^1K_{mn} + A_{mn} + \sum_k A_{mk} a_{mkn} = C_{mn}$$

and

(1'

$$\left(\frac{a}{r_o}\right)^n {}^2K_{mn} + B_{mn} + \sum_k B_{mk} a_{mkn} = D_{mn}.$$

Also

(2)

$$n\left(\frac{a}{r_o}\right)^n {}^1K_{mn} - (n+1) A_{mn} + n\sum_k A_{mk} a_{mkn} = n\beta C_{mn}$$

and

(2')

$$n\left(\frac{a}{r_o}\right)^n {}^2K_{mn} - (n+1) B_{mn} + n\sum_k B_{mk} a_{mkn} = n\beta D_{mn}$$

from which

$$n\left(\frac{a}{r_o}\right)^n {}'K_{mn} - (n+1)A_{mn} + n\sum_k A_{mk}a_{mkn} = n\beta\left[\left(\frac{a}{r_o}\right)^n {}'K_{mn} + A_{mn} + \sum_k A_{mk}a_{mkn}\right] - (n+1)A_{mn} - n\beta A_{mn} = n\beta\,{}'K_{mn}\left(\frac{a}{r_o}\right)^n - n\,{}'K_{mn} \times \left(\frac{a}{r_o}\right)^n + n\beta\sum A_{mk}a_{mkn} - n\sum A_{mk}a_{mkn} - \left[n((\beta+1)+1\right]A_{mn} = n(\beta-1)\,{}'K_{mn}\left(\frac{a}{r_o}\right)^n + n(\beta-1)\sum_k A_{mk}a_{mkn}$$

Now dividing by n $(\beta - 1)$

$$-\left[\frac{(\beta+1)}{(\beta-1)} + \frac{1}{n(\beta-1)}\right]A_{mn} = {}'K_{mn}\left(\frac{a}{r_o}\right)^n + \sum_k A_{mk}a_{mkn}$$

$$\alpha_n A_{mn} = -{}'K_{mn}\left(\frac{a}{r_o}\right)^n - \sum_k A_{mk}a_{mkn}$$

and a similar expression for B_{mn}

$$\alpha_n B_{mn} = -{}^2K_{mn}\left(\frac{a}{r_o}\right)^n - \sum_k A_{mk}a_{mkn}$$

where

$${}'_2K_{mn} = \frac{D}{r_o}(2-\delta^o_m)\frac{(n-m)!}{(n+m)!}P_n^m(\mu_o)\begin{Bmatrix}\cos m\varphi_o \\ \sin m\varphi_o\end{Bmatrix}.$$

The value of K_{mn} given by Webb

$$K_{mn} = \frac{2D}{r_o}\left(\frac{a}{r_o}\right)^n\frac{(n-m)!}{(n+m)!}P_n^m(\mu_o)\cos m\varphi_o$$

differs from that obtained above in the following points:

1) it includes the term $\left(\frac{a}{r_o}\right)^n$ (This is the most serious discrepancy.)

2) there is a difference of sign between the value of K_{mn} given here and that given by Webb

3) the Kronecker δ^o_m is missing which reduces

coefficient of D in this paper to 1 when m = 0. For values of m ≠ 0 the coefficient in Webb's formula is in agreement.

4) although Webb has specifically given only cos mφ for the value of K_{mn} it appears that the sin mφ was taken care of by mental reservation.

II

The Induced Polarization Potential of a Sphere In an Infinitely Extended Uniform Medium.

The problem of the buried sphere in a uniform half-space was complicated by the air-earth boundary. As a first approximation to the problem consider the sphere to be at distance h below a horizontal plane in an infinitely extended uniform full-space. The radius of the sphere is a, its resistivity is ρ_2 and it is completely surrounded by a medium of resistivity ρ_1. Take the origin of the coordinate system at the center of the sphere and the z axis to be the line joining the center of the sphere

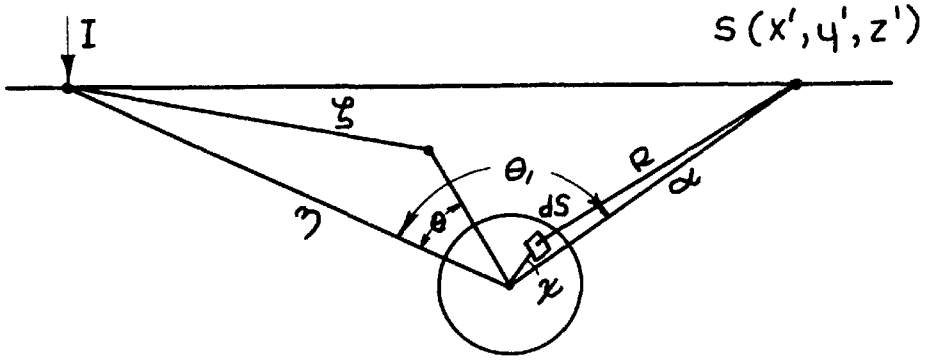

and the current electrode.

The energizing current I produces a polarization charge density σ on the surface of the sphere which according to the laboratory experiments is given by the relation

(1) $$\alpha = -\chi i_a$$

where i_a is the normal component of the current density on the surface of the sphere.

The potential at the point P(x'y'z') whose radius vector is α and whose colatitude angle is θ_1 is given by

(2)

$$\phi(x',y',z') = \int_S \frac{\sigma dS}{R}$$

The charge density σ can be found from relation above and Ohm's law. In order to find the current density at the surface of the sphere and normal to it the potential inside and outside the sphere due to the energizing current must be calculated. The potential outside is due in the first part to the ohmic drop in the medium produced by the energizing current and in the second part to the distortion of the field introduced by the sphere. The potential at some point P outside the sphere is

$$\phi^+ = \frac{\rho_1 I}{4\pi r} + \sum_{n=0}^{\infty} \frac{B_n P_n(\cos\theta)}{r^{n+1}}$$

The potential on the inside of the sphere must be finite at r = 0 and, therefore, must have the form

$$\phi^- = \sum_{n=0}^{\infty} A_n r^n P_n(\cos\theta)$$

At the surface of the sphere the boundary conditions are:

$$\phi^+ = \phi^-(r=a)$$

and

$$\frac{1}{\rho_1}\frac{\partial\phi^+}{\partial r} = \frac{1}{\rho_2}\frac{\partial\phi^-}{\partial r}(r=a)$$

Substituting the expression for the potential into the boundary value equations and equating coefficients gives

$$A_n = \left[\frac{\rho_1 I}{4\pi\eta^{n+1}} + \frac{n\rho_1 I}{4\pi\eta^{n+1}}\beta_n\right]$$

$$B_n = \frac{n\rho_1 I a^{2n+1}}{4\pi\eta^{n+1}}\beta_n$$

where

$$\beta_n = \frac{\rho_2 - \rho_1}{n\rho_1 + (n+1)\rho_2}$$

Now the potential at any point P outside the sphere becomes

$$\phi^+ = \frac{\rho_1 I}{4\pi}\sum_{n=0}^{\infty}\left[\frac{r^n}{\eta^{n+1}} + \frac{na^{2n+1}}{\eta^{n+1}r^{n+1}}\beta_n\right]P_n(\cos\theta).$$

The radial component of the current density can now be computed from Ohm's law which gives

$$i_r = -\frac{1}{\rho_1}\frac{\partial\phi^+}{\partial r} = -\frac{I}{4\pi}\sum_{n=0}^{\infty}\left[\frac{nr^{n-1}}{\eta^{n+1}} + \frac{na^{2n+1}(-n-1)}{\eta^{n+1}r^{n+2}}\beta_n\right]P_n(\cos\theta)$$

$$r=a;\ i_a = -\frac{I}{4\pi}\sum K_n P_n(\cos\theta) \text{ where } K_n = \frac{na^{n-1}}{\eta^{n+1}}\left[1-(n+1)\beta_n\right].$$

Now from Equation 1 the charge density becomes

$$\sigma = \frac{kI}{4\pi}\sum_{n=0}^{\infty} K_n P_n(\cos\theta)$$

and the potential from Equation 2 is

$$(3)\qquad \phi(x',y',z') = \frac{kI}{4\pi}\int_S\sum\frac{K_n P_n(\cos\theta)}{R}\,dS$$

Now write

$$\frac{1}{R} = \frac{1}{\alpha}\sum_{s=0}^{\infty}\left(\frac{a}{\alpha}\right)^s P_s(\cos\psi)$$

and apply the biaxial expansion which gives

$$\frac{1}{R} = \frac{1}{\alpha}\left[\sum\left(\frac{a}{\alpha}\right)^s\sum_{m=0}^{m=s}(2-\delta^o_m)\frac{(s-m)!}{(s+m)!}P_s^m(\cos\theta_1)P_s^m(\cos\theta)\cos m\varphi\right]$$

Substituting for 1/R into Equation 3 gives

$$\phi(x',y',z') = \frac{kI}{4\pi\alpha}\int_S\sum_{n=0}^{\infty}K_n P_n\cos\theta\,dS\left[\sum_{n=0}^{\infty}\left(\frac{a}{\alpha}\right)^s\sum_{m=0}^{m=s}(2-\delta^o_m)\frac{(s-m)!}{(s+m)!}\times P_s^m(\cos\theta_1)P_s^m(\cos\theta)\cos m\varphi\right]$$

However, because of the orthogonal properties of the Legendre polynomials, m = 0 and s = n, which gives for the potential after integration over the sphere

$$\phi(x',y',z') = \frac{kIa^2}{\alpha}\sum K_n\left(\frac{a}{\alpha}\right)^n\frac{P_n(\cos\theta_1)}{2n+1}.$$

Writing $\rho_1 = p\rho_2$ and assume that $p \geq 100$ then the potential becomes

(4)
$$\phi(x',y',z') = kI\Sigma \frac{a^{2n+1}}{(\eta\alpha)^{n+1}} P_n(\cos\theta).$$

Equation 4 has been developed on the assumption that the surrounding medium was a complete uniform space. If it were a half space the value of the potential at any point on the air-earth boundary would be increased because of the infinite number of images generated. If the sphere is buried to a depth $h = 10a$, the effect of the multiplicity of images is greatly reduced and the potential is approximately twice the value given by Equation 4.